ARPA ORDER NO.: 189-1

R-760/1-ARPA

September 1971

EFFECTS OF STRONG EXPLOSIONS - II
(Soviet Literature Translations)

Compiled by Simon Kassel

A Report prepared for

ADVANCED RESEARCH PROJECTS AGENCY

Rand
SANTA MONICA, CA. 90406

)CUMENT CONTROL DATA

ORIGINATING ACTIVITY	2a. REPORT SECURITY CLASSIFICATION
The Rand Corporation	UNCLASSIFIED
	2b. GROUP

. REPORT TITLE

EFFECTS OF STRONG EXPLOSIONS - II (Soviet Literature Translations)

. AUTHOR(S) (Last name, first name, initial)

Compiled by, Kassel, Simon

REPORT DATE	6a. TOTAL NO. OF PAGES	6b. NO. OF REFS.
~~August~~ September 1971	119	—
CONTRACT OR GRANT NO.	8. ORIGINATOR'S REPORT NO.	
DAHC15 67 C 0141	R-760/1-ARPA	

a. AVAILABILITY/LIMITATION NOTICES	9b. SPONSORING AGENCY
DDC-A	Advanced Research Projects Agency

10. ABSTRACT

English-language abstracts of 143 articles and 3 conferences from the open Soviet technical literature of 1969, 1970, and early 1971, relevant to the interactions of explosions and shock waves with the ground, the atmosphere, and materials. They are grouped under these 20 headings: shock waves in solids; interaction of shock waves with solids; shock waves and explosions in gases; laser interaction with plasma; gas breakdown due to lasers; radiation effects of laser-induced breakdown; laser interaction with solids; deformation; radiation damage; static high pressure research of solids; soil mechanics; electron beams; hypersonic flow past bodies; hypersonic trails; equations of state for gas; exploding wires; atmospheric physics; instrumentation and measurement; conferences; and miscellaneous. The conferences reported are (1) the Second All-Union Symposium on Combustion and Explosions; (2) the Fifth All-Union Conference on Strength and Plasticity: The Mechanics and Physics of Destruction; and (3) the Thirteenth Scientific and Technical Conference of the All-Union Scientific Research Institute of Electrical Machine Building.

11. KEY WORDS

Physics
Lasers
USSR-Science
Gas Dynamics
Thermodynamics
Nuclear Explosions
Aerodynamics
Bibliography
Fluid Dynamics

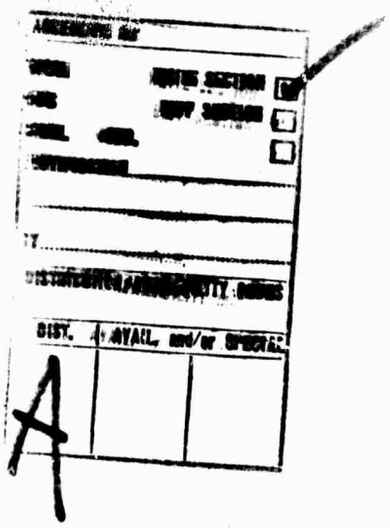

This research is supported by the Advanced Research Projects Agency under Contract No. DAHC15 67 C 0141. Views or conclusions contained in this study should not be interpreted as representing the official opinion or policy of Rand or of ARPA.

ARPA ORDER NO.: 189-1

R-760/1-ARPA

September 1971

EFFECTS OF STRONG EXPLOSIONS - II
(Soviet Literature Translations)

Compiled by Simon Kassel

A Report prepared for

ADVANCED RESEARCH PROJECTS AGENCY

Rand
SANTA MONICA, CA. 90406

PREFACE

This structured collection of abstracts has been prepared as part of a continuing study of selected areas of Soviet science and technology within the Rand project -- Soviet Literature Exploitation -- sponsored by the Advanced Research Projects Agency of the Department of Defense.

The material in this report is based exclusively on Soviet open-source technical literature published in 1969, 1970, and the early part of 1971.

The English language abstracts have been prepared by Informatics, Inc.

CONTENTS

INTRODUCTION

This report is one of a series intended to provide a preliminary overview of current Soviet research activities on the effects of explosions. Interaction of explosions with the ground, the atmosphere, and materials have broad research ramifications and significance, especially in the case of nuclear explosions. The pertinent topics include simulation studies, effects of high pressures and temperatures on materials, reentry problems, radiation effects, electromagnetic phenomena, etc. It is expected that in the course of this series most of these topics will be covered in this and future reports based on the current Soviet scientific and technical literature.

The abstracts in this report are arranged according to fairly general subject areas and vary in length depending on the degree of pertinence and significance of the individual papers. Their purpose is primarily to call attention to the work being done in the USSR on the given subject.

I. SHOCK WAVES IN SOLIDS

1. Gryaznov, I. M., K. I. Kozorezov, L. I. Mirkin, and N. F. Skugorova. Carbon impregnation of steel by the action of shock waves. Doklady AN SSSR, v. 194, no. 1, 1970, 70-72.

Experiments in impregnating annealed low carbon steel (St. 20) with carbon, using shock waves, are described. For this purpose, a steel plate was covered with an even layer of graphite powder and a pulsed load was applied by impelling another steel plate at a velocity 1975 m/sec, using an explosion. A plastic explosive in a sheet form, with a detonation velocity of 7500 m/sec and density 1.65 g/cm^3, was used. At the impact point, a pressure of 425 kbar was produced by the shock.

Several structural zones along the shock wave propagation path were discovered. A sharply defined, case-hardened layer is 0.05 mm thick and has a high hardness (from 580 to 935 kg/mm^2). Three other subsequent zones are defined and described in detail.

On the basis of structural investigations, the following physical mechanism is assumed. The shock wave compresses the porous layer of the graphite powder. Combined with the effect of high pressure, the graphite is heated to a temperature exceeding the melting temperature of iron. A layer of the carbon diluted in the liquid iron emerges, which then solidifies, precipitating the excess carbon in the form of cementite needles.

2. Funtikov, A. I. Method of studying phase transitions at high pressures using the shock compression of porous materials. Fizika goreniya i vzryva, v. 5, no. 4, 1969, 510-512.

The behavior of shock adiabats during the change of the phase state of a substance is utilized to study the phase transition (melting) by means of shock compression of porous materials. The method is based on measuring the relationship of the shock wave velocity to the initial density of the substance based on the curve of a single detonation. As a single parameter relationship, it may be measured with relatively high accuracy in simple experiments. The difference in the equations of state for liquid and solid

phases leads to a break in the single detonation curve. The comparative measurements of the shock wave velocity in samples of various density permit determination of the break points, from which the porosity limit M_{li} (defined as the ratio of normal density to initial density) can be determined. The melting temperature is then determined by the equation of the solid phase state. Some data obtained are given in the table below.

Substance	M_{li}	P, Mbar	T x 10^3, °K
KCl	1.32	0.170	3.62
NaCl	1.85	0.132	3.70

The suggested method does not have restrictions for the investigation of other phase transitions at high pressures.

3. Pavloskiy, M. N. Shock compression of diamond. Fizika tverdogo tela, v. 13, no. 3, 1971, 893-895. (1)

Pavloskiy, M. N. Shock compressibility of very hard materials. Fizika tverdogo tela, v. 12, 1970, 2175-2178. (2)

Shock compressibility of natural diamond monocrystals with an initial density $\rho_o = 3.51$ g/cm^3, and of porous diamond samples (density $\rho_{oo} = 1.90$ g/cm^3 and the grain size 10 — 14μ) has been investigated experimentally (1). The "reflection" method was used, with the propagation velocity of the shock waves recorded by means of electric contacts (L. V. Al'tshuler, Uspekhi fizicheskikh nauk, v. 85, 1965, 197). The obtained relationship, i.e., the wave velocity (D) as a function of mass velocity (U) in (1) monocrystalline (the scale at left) and (2) porous (the scale at right) diamond, is presented in Figure 1.

Fig. 1

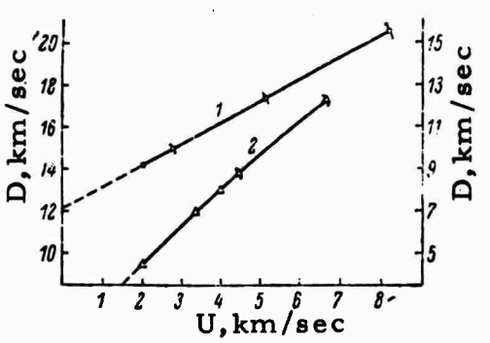

The shock pressure (P) as a function of the relative compression ($\delta=\rho/\rho_o$) is presented in Figure 2.

Fig. 2

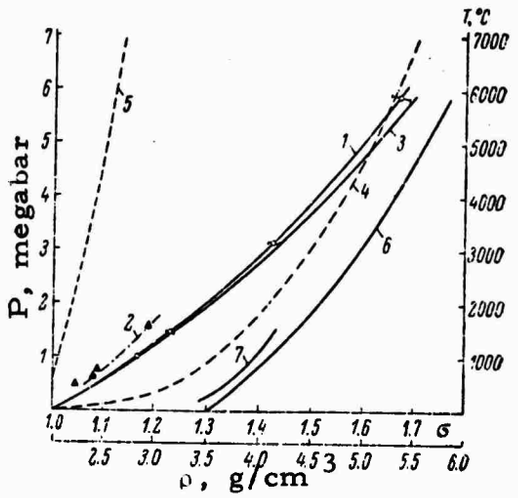

The numbered curves are: 1 and 2 -- calculated shock adiabats with experimental points for monocrystalline and porous diamond, respectively; 3 -- calculated "0 °K" isotherm of diamond; 4 and 5 -- temperature as functions of shock adiabats; 6 and 7 -- final densities of shock-compressed diamond (both types and in the same order as 1 and 2) as functions of applied pressure. From measurement data, the value of the Gruneisen factor for the upper point of the porous diamond adiabat is estimated as 0.48, while its initial value is about 0.9.

Shock compressibility of other hard materials, e.g., monocrystalline ruby and polycrystalline corundum (Al_2O_3), beryllium oxide (BeO), boron carbide (B_4C), tungsten carbide (WC), and tantalum carbide (TaC), were measured earlier (2) using the same method. Results are presented in Figure 3

Fig. 3

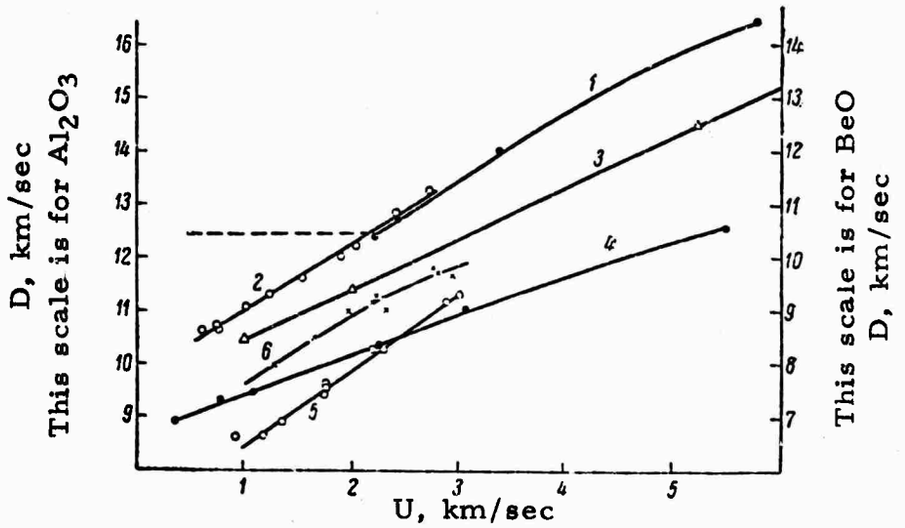

and 4. The numbered curves in Figure 3 are: 1 -- ceramic BeO; 3 -- monocrystalline ruby; and 4 -- ceramic corundum. For comparison 2, 5, and 6 present the same data taken from Compendium of Shock Wave Data, University of California, Livermore, 1966.

Curves 1, 2, and 3 in Figure 4 are for B_4C, TaC, and WC respectively. The scale at left is for B_4C and WC and at right for TaC.

Fig. 4

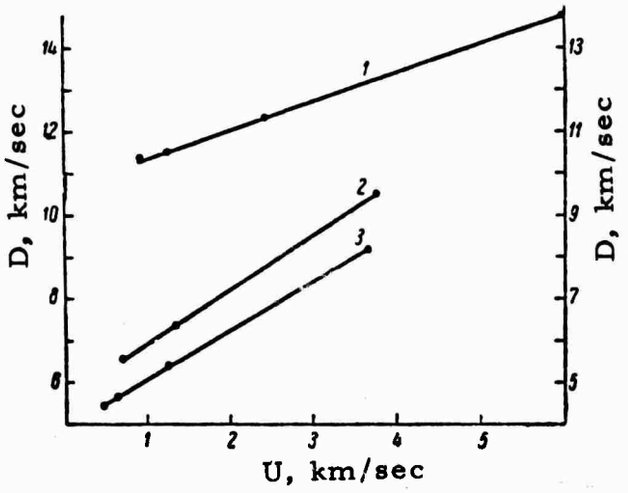

4. Zubarev, V. N., T. N. Ignatovich, A. N. Shuykin, and P. A. Yampol'skiy. Conductivity of acrylamide and polyacrylamide behind the front of a shock wave. Fizika goreniya i vzryva, v. 5, no. 4, 1969, 524-528.

The conductivity of acrylamide (AA) and polyacrylamide (PAA) at shock pressures 80 and 160 kbar is measured. A schematic drawing of the experiment setup is shown below.

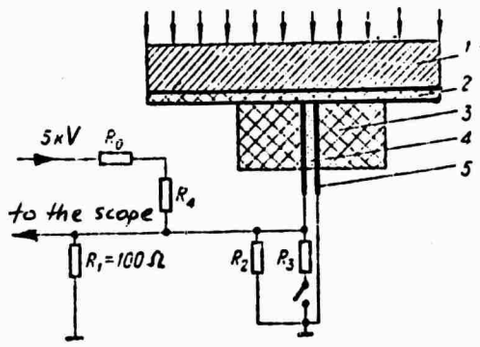

Plane shock waves were generated in Al or Cu shields 1 by the explosions. Samples 4 (height $\sim$ 20 mm and thickness $\sim$ 2 mm) were separated from the shields by paraffin spacers 2 (3 mm thick). On the sides, the samples were also surrounded by paraffin blocks 3. Electrodes 5 are made from copper foil 0.1 mm thick and 20 mm wide. The measurement technique was identical to the one described by L. V. Al'tshuler, et al., (ZhETF, v. 39, 1960, 16). Typical oscillograms are shown in the original article, and numerical data derived from them are presented in the table below.

Substance	P, kbar	
	80	150
Acrylamide	$< 10^{-2}$	80
Polyacrylamide	8	30
50/50 mixture (by weight of both materials)	$< 10^{-2}$	50

5. Addurov, G. A., L. A. Matveyeva, and V. Sh. Shekhtman. Structural changes in a single crystal caused by a shock wave. Fizika metallov i metallovedeniye, v. 31, no. 1, 1971, 122-127.

The authors describe the X-ray investigation of copper and molybdenum single crystals, recovered after an explosion experiment which provided a single shock wave compression ($\sim$500 kbar) and a small residual deformation ($\sim$ 5 —6%). Molybdenum and copper samples of cylindrical shape were cut from single-crystal rods. They were oriented to correspond to the shock wave passage from a direction of 100° ($\pm$10°) and 110° ($\pm$2°) for molybdenum samples, and from a direction of 110° ($\pm$4-5°) for copper samples. A schematic drawing of the experiment setup is shown in the figure below. Here 1 is the generatrix of a plane detonation wave; 2 is the TNT charge (100 mm diameter, 10 mm thick): 3 is a steel disk (2mm thick); 4 is the air gap; 5 is the aluminum impactor (70 mm diameter, 1 mm thick); 6 is the copper cup; 7 is the investigated sample; and 8 is the steel yoke. In special experiments with polycrystal copper, the shock wave parameters are: velocity of the shock wave front D, mass velocity U behind

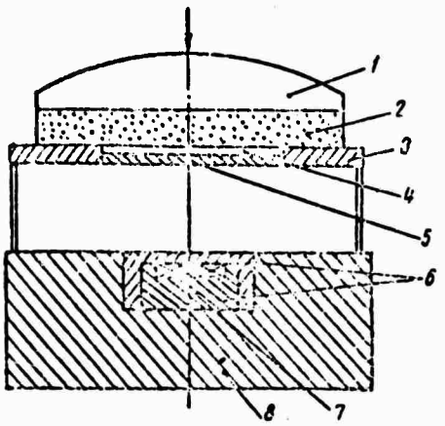

the front, and pressure of the shock compression p. They are presented in Table 1.

Table 1

Shock wave parameters	Depth, mm	
	4	8
D, km/sec	5.38	5.0
U, km/sec	0.95	0.69
p, kbar	455	307

Parameters of the shock wave on the sample surface are presented in Table 2.

Table 2

Material	τ μsec	P kbar	T_s °K	T_r, °K	T_m, °K
Copper	1.5	455	650	450	1356
Molybdenum	2	517	530	430	2883

Here, τ is the duration of high pressure, T_s is the temperature of the shock compression, T_r is the temperature upon pressure release (these temperatures

are taken from McQueen, R. G., and S. P. Marsh (J. Appl. Phys., v. 31, 1960, 1253), and T_m is the melting temperature.

X-ray diffraction patterns of samples before and after shock wave passage are presented in the original article, and the conclusion is made that, under conditions of a single shock wave compression, transition from the single-crystal into the polycrystal state may occur. The state of the samples after the experiment is analogous to the one which may be obtained in a single crystal by its deformation with subsequent annealing, assuming recrystallization processes.

6. Mineyev, V. N., A. G. Ivanov, Yu. V. Lisitsyn, Ye. Z. Noviskiy, and Yu. N. Tyunyayev. Electric signals produced by the shock compression of doped silicon. Zhurnal eksperimental'noy i teoreticheskoy fiziki, v. 59, no. 10, 1970, 1091-1102.

Electric signals produced by the shock compression of p- and n-type silicon single crystals containing various amounts of impurities are investigated. A schematic drawing of the experiment setup is shown below, where 1 is the measuring electrode, 2 is the silicon sample, and 3 is the shield. Arrows indicate the propagation direction of the shock wave front. Experiments were conducted at pressures of 20, 40 and 200 kbar. It is shown that the emf observed during the shock compression of silicon is not associated with surface phenomena, and therefore, is caused by the volume redistribution of the ionized impurity atoms during shock compression, i.e., by shock polarization. In contrast to dielectrics, the recorded polarization current during shock compression of semiconductors is determined only by time varying polarization.

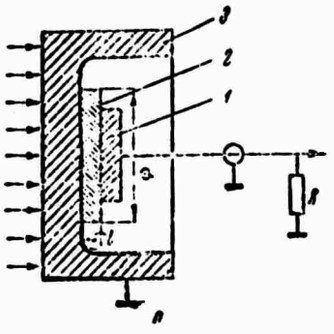

7. Podurets, A. M., and R. F. Trunin. A certain peculiarity of the shock compressibility of quartzite. Doklady AN SSSR, v. 195, no. 4, 1970, 811-813.

In the 100- to 300-kbar range of pressures at the shock wave front, silica undergoes a combination of crystalline phases. The velocity of the shock wave as a function of the pressure stays constant; however, the wave remains single, indicating the absence of equilibrium between the phases. A mechanism of the kinetics which explains phase transitions is offered. The transition from a light to a dense phase occurs in the shock wave front, while behind the front, in a smooth wave, the phase composition remains practically fixed. If a strong shock wave is broken into several waves of smaller amplitude which successively compress the substance (limit case being a smooth compression wave), then the content of the denser phase decreases. Experimental data supporting this explanation are included.

8. Trunin, R. F., G. V. Sikakov, M. A. Podurets, B. N. Moiseyev, and L. V. Popov. The dynamic compressibility of quartz and quartzite at high pressures. AN SSSR. Izvestiya. Fizika zemli, no. 1, 1971, 13-20.

New experiments were conducted to study the dynamic compressibility in absolute measurements of quartz at pressures up to 3.5 Mbar and of quartzite at pressures of up to 7 Mbar. In addition, results are presented for studies of the comparative compressibility of quartzite and aluminum at pressures of up to approximately 20 Mbar. A shock wave, formed by the explosion of a high explosive, passes through a metal shield and the samples. Special sensors placed in the wave path are then activated and the signal obtained is recorded using two-beam cathode oscillographs with driven sweep. Having determined from preliminary experiments the dynamic adiabat of the shield, the recorded wave velocity in it uniquely determines all the remaining compression parameters, i.e., mass velocity, pressure and density of shock compression. The results of the experiments are presented in the table and figure below. The figure is presented in D — U and P — ρ coordinates. (D - wave propagation velocity, U - mass velocity of motion of the substance behind the shock wave front, P - pressure, and ρ - density.) The maximum density attained under these conditions exceeds the original values by 2.65 times. In order to explain the problem of possible relaxation phenomena connected with short-term dynamic loads, the action time for the shock waves in the experiments was considerably increased for the samples. Extrapolations are presented for the dynamic adiabat

Table

Shield material (standard)	U km/sec	Sample thickness Δ, mm	Substance studied	Parameters of dynamics compressib. D km/sec	U km/sec	P kbar	ρ g/cm³	Form of experiments
Copper	1,71	4 ÷ 8	Quartz	6,27	2,52	418	4,43	
Aluminum	2,82	4 ÷ 8	"	7,18	3,13	595	4,69	
Iron	2,82	4 ÷ 8	"	8,54	3,92	887	4,90	
"	4,56	4 ÷ 8	"	12,01	6,20	1974	5,48	Method of
"	6,51	4 ÷ 8	"	15,42	8,79	3590	6,16	reflection
Copper	0,17	4 ÷ 8	Quartz-	5,06	0,25	33,5	2,79	
"	0,21	4 ÷ 8	ite	5,03	0,31	41,3	2,82	
"	0,37	4 ÷ 8	"	5,45	0,54	78,0	2,94	
Aluminum	0,69	4 ÷ 8	"	5,67	0,79	118	3,08	
"	1,14	4 ÷ 8	"	5,70	1,25	188	3,39	
"	1,50	4 ÷ 8	"	5,72	1,68	255	3,75	
"	1,80	4 ÷ 8	"	5,75	2,05	312	4,12	
Copper	1,71	4 ÷ 8	"	6,10	2,54	410	4,54	"Reverse"
Iron	2,82	4 ÷ 8	"	8,56	3,91	878	4,88	method of
Iron	4,56	4 ÷ 8	Quartz-	12,12	6,18	1985	5,41	reflection
Aluminum	12,24	160	ite	19,92	12,37	6530	6,99	
"	7,22	300 ÷ 500	"	13,60	7,38	2660	5,80	
"	8,57	300 ÷ 500	"	15,28	8,72	3530	6,15	
"	11,10	300 ÷ 500	"	18,43	11,24	5500	6,78	

Note: The state of impact compression in the shields was determined according to the D — U relationships of copper, iron and aluminum which practically agreed with values published earlier.

Figure

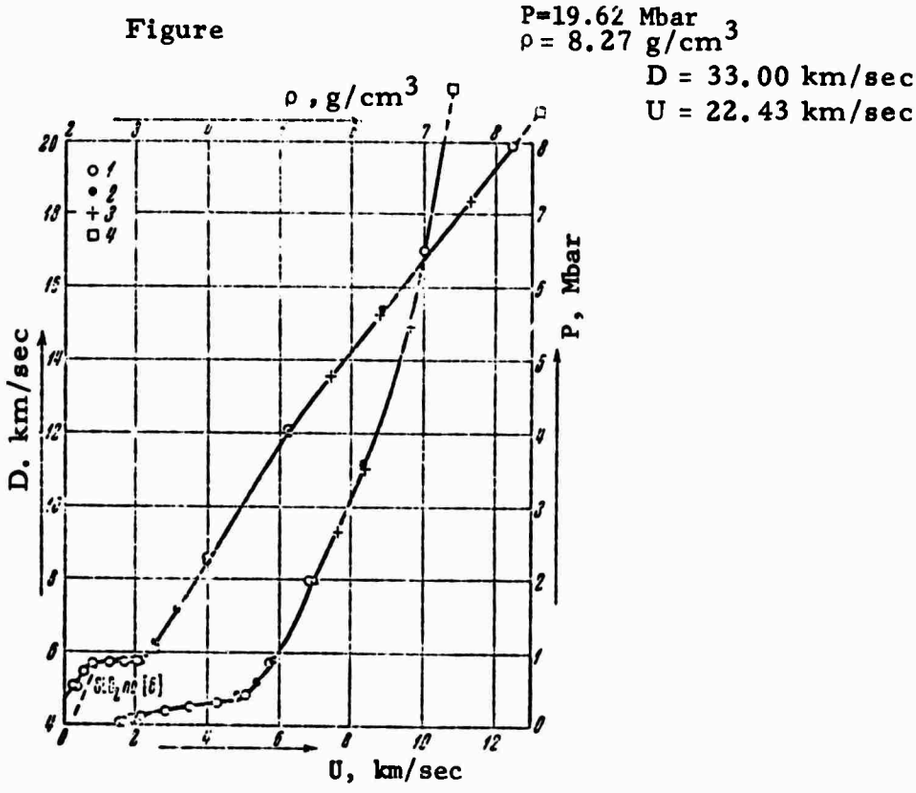

Experimental D — U and P — ρ relationships.
1 - absolute measurements in quartzite (method of reflection); 2 - the same for crystalline quartz; 3 - absolute measurements in quartzite ("reverse" method of reflection); 4 - data from comparative measurements.

of quartzite in the range of pressures determined by computation. The dynamic experiment attests to the absence of density discontinuities, which are related to the metallization of quartz.

9. Chernyshov, A. D. Propagation of shock waves in an elastic space in the case of finite deformations. Prikladnaya matematika i mekhanika, v. 34, no. 5, 1970, 885-890.

The subject of this theoretical study is how the propagation of shock waves in a three-dimensional elastic medium is affected by finite deformations and by existence of convective terms in the expression for the velocity of the medium through displacements. Correspondingly the initial equations are written to contain the respective terms. It is then shown that the number of shock waves and their properties are strongly dependent on the deformation of the medium in front of the surface of strong discontinuity, and on the fact of whether or not the nonlinear terms in the rheological equations are taken into account. Thus, precise equations for the case of small deformations indicate the possibility of propagation for three different shock waves. In a special case, when in front of the shock wave the medium is in a nondeformed state, all qualitative results coincide with the results of the similar linear problem. In particular cases, expressions are obtained for the velocities of shock waves in the explicit form.

10. Belinskiy, I. V., and B. D. Khristoforov. Dynamic compressibility of porous NaCl at low pressures. Zhurnal prikladnoy mekhaniki i tekhnicheskoy fiziki, no. 2, 1970, 134-139.

Dynamic compressibility of porous NaCl in the range of pressures from 1 to 200 kbars is experimentally investigated. Experiments were conducted with cylindrical samples (34 mm dia and 2 to 25 mm thick) compressed from NaCl powder (0.3 mm grain size) to a density of 1.87 to 1.90 g/cm^3. Plane shock waves were generated by explosion or impact by thin aluminum plates. The wave and mass velocities of the shock waves were measured using the electromagnetic and/or capacitive methods. In order to determine the elastic characteristics of the samples under normal conditions, the longitudinal (C_1) and transverse (C_2) velocities of sound were measured at 1.67 MHz with a UZIS LETI - 4 ultrasonic apparatus. The C_1 and C_2 values served to calculate the hydrodynamic velocity of sound $C_3 = (K/\rho_{oo})^{1/2}$, Poisson's ratio ν,

Young modulus E, the bulk modulus K, and shear coefficient G.

Results of the experiments indicate that the hydrodynamic model is not suitable for the description of porous NaCl behavior in dynamic loading in the range of stresses comparable to the strength of the material.

11. Doronin, G. S., and V. P. Stupnikov. Calculation of shock adiabats for mixtures and porous materials. Izvestiya SO AN SSSR, Seriya tekhnicheskikh nauk, no. 3, vyp. 1, 1970, 102-105.

A formula is offered to calculate the shock adiabat of a mixture when the shock adiabats and concentrations of the mixture components are known. Calculations made for a mixture of marble and paraffin coincide very well with experimental data published elsewhere. In addition, a formula is derived for the shock adiabat of porous material, and it is shown that this formula can be obtained also from the first formula, by considering the porous material as a mixture of a compact material with air. Finally, a formula is given for a porous mixture of two materials and more calculated data are compared with experimental data. The following conclusions are made:

1. the energy in a porous body during shock compression is made up of the compression energy of a solid body and the energy of pure collapse and

2. the formation of the shock-wave front in a mixture or in a porous substance depends not on separate particles, but on average density if the thickness of the front is at least several times larger than the dimensions of the separate particles.

12. Vakhrameyev, Yu. S. Certain relationships of similarity for the motion of loose consolidating media. Prikladnaya matematika i mekhanika, v. 34, no. 5, 1970, 930-934.

A solution is given for a class of one-dimensional self-similar problems of the convergence of shock waves and the expansion of a gas-filled cavity. The corollaries connected with self-similarity are examined. The condition of unlimited cumulation is obtained and two modes of cavity expansion are revealed. The similarity relationship is established for cratering explosion in a loose uniformly consolidating medium and in highly fissured rock.

13. Novikov, S. A., and L. M. Sinitsyna. Effect of shock compression on the critical shear stresses in metals. Zhurnal prikladnoy matematiki i tekhnicheskoy fiziki, no. 6, 1970, 107-110.

Critical shear stresses σ_* behind the shock wave front in explosion experiments with aluminum, copper and lead are investigated. The desired quantities were obtained from the comparison of calculated and experimental relations, which characterize the pressure decrease on the shock wave front in these metals caused by the overtaking elastic unloading wave. The experiment setup and technique are described in detail. Calculations are made on the basis of well-known equations of state for the metals investigated, described earlier by L. V. Al'tshuler et al (ZhETF, v. 38, no. 4, 1960). The σ_* values obtained and their corresponding pressure amplitudes P-(in kbars) in the elastic unloading wave under a shock compression pressure of P (in kbars) are given in the table below:

Metals	P-	σ_*	P
Al	300-680	17-29	60-100
Cu	340-860	25-41	90-150
Pb	460	0	0

II. INTERACTION OF SHOCK WAVES WITH SOLIDS

14. Dremin, A. N., and G. I. Kanel'. Refraction of an oblique shock wave at an interface with a less rigid medium. Zhurnal prikladnoy matematiki i tekhnicheskoy fiziki, no. 3, 1970, 140-144.

An approximate method for calculating the unloading polar and the velocity of sound behind the shock-wave front in solid condensed media is offered. The substitution of the isentrope by a broken curve with a constant sound velocity for each section of the curve, was used for this purpose. An elaborate explosion experiment to determine the calculated refraction parameters is described in detail, and good agreement between the calculated and experimental parameters is demonstrated in Figures 1 and 2. Formulas are derived to calculate

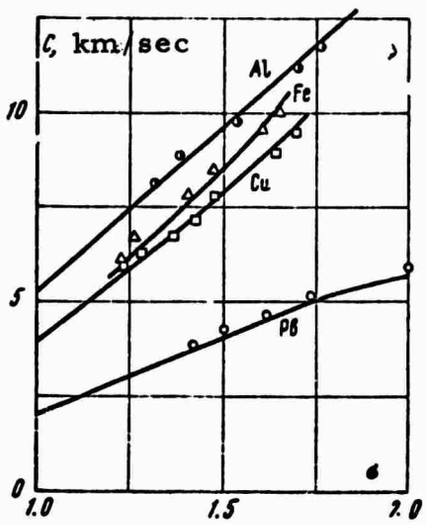

Fig. 1 - Calculated (solid lines) and experimental dependencies of sound velocity on the shock adiabat from the degree of metal compression.

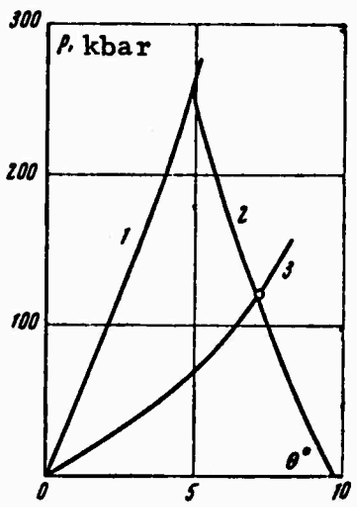

Fig. 2 - 1 and 3 - shock polars of aluminum and plexiglas for v_o = 14.2 km/sec;
2 - unloading polar of aluminum.

the magnitude of the critical angle for the ordinary reflection of an oblique shock wave at the interface with a less rigid medium and the angle of the maximum flow deviation. It is stated that problems of this type are typical for the calculation of shock-compression parameters for explosion welding conditions, and shock-compression for other conditions.

15. Trunin, R. F., G. V. Simakov, and M. A. Podurets. The compression of quartz by high-intensity shock waves. AN SSSR. Izvestiya. Fizika zemli, no. 2, 1971, 33-39.

Results are presented for the experimental determination of the dynamic compressibility of quartz with varying initial densities (ρ_{00} = 1.15, 1.35, 1.55, 1.75, and 2.2 g/cm^3) over a wide range of pressures and densities. The position of the experimental curves in the P — ρ plane (shown in Figure 1) attest to the transformation of quartz (under the effect of shock waves) into the high-density

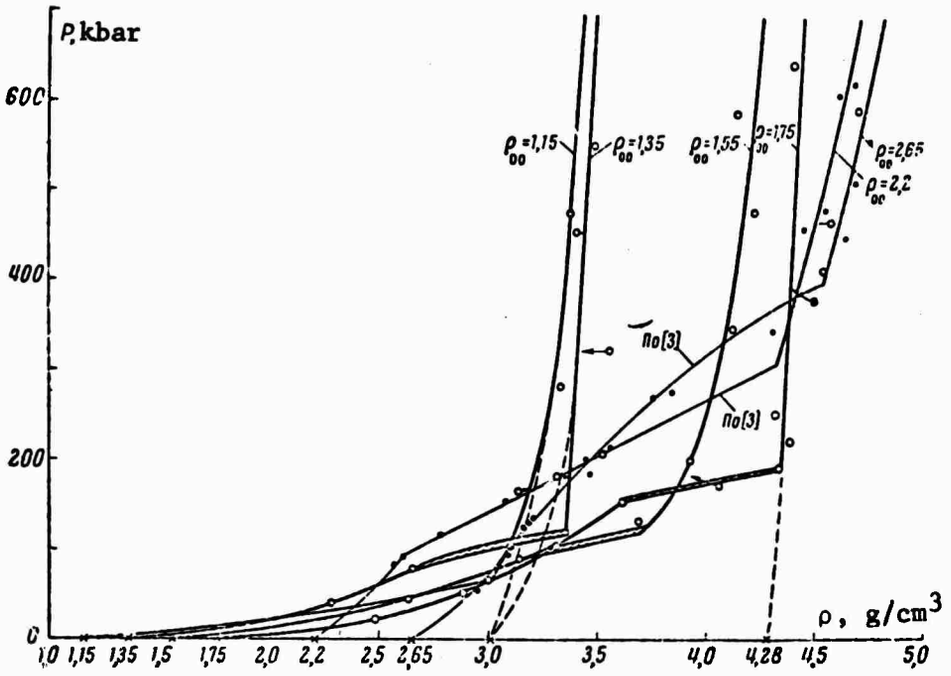

Fig. 1 - Diagram of pressure P - density ρ.

1 - ----^{0}----, the experimental data from the present work;

2 - ----.----, results obtained from Wackerle, I. Shock-wave compression of quartz, Journal of Applied Physics, v. 33, no. 3, 1962, 922.

The shaded part shows the possible boundaries of phase transitions.

modifications - coesite and stipoverite. The position of the phase equilibrium curve (see Figure 2) is evaluated for pressures up to 600 kbar, i.e., pressures and temperatures which substantially exceed the data from static measurements. The experimental results, which are related to the range of pressures for phase transitions, indicate that thermodynamic equilibrium is absent during the compression of quartz and they attest to the complex kinetic processes which occur in the shock wave front.

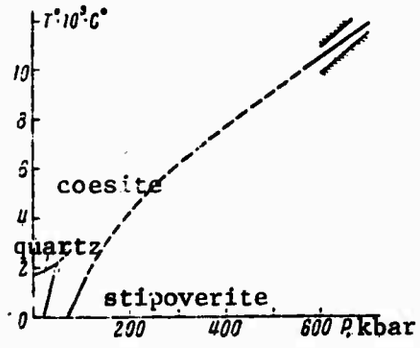

Fig. 2 - Interpolation relationships of the phase equilibrium line between coesite - stipoverite. The hatched part shows the range of temperature variation of shock compression.

16. Mogilevskiy, M. A. Structural changes in pure copper under shock loading. Fizika goreniya i vzryva, v. 6, no. 2, 1970, 229.

An experimental investigation was made of changes in the crystalline structure of pure (99.996%) copper, e.g., dislocations due to the application of a plane shock wave. The types and magnitudes of defects produced by the shock wave are judged by the change in the structure-sensitive properties and particularly in electrical resistivity of the samples during their isochronous annealing, when structural changes are gradually removed. For this purpose, the shock wave was applied to the samples at the temperature of liquid nitrogen and the electrical resistance of the samples was measured during their isochronous warm-up. The experimental explosion setup and measurement technique are described in detail. Results are illustrated and discussed under headings: spectrum of lattice defects, density of dislocations and possible changes in the mechanism of deformation at high pressures.

17. Filippov, M. A., and V. N. Kodess. Variation in the fine structure of manganese steels under the effect of high-pressure shock waves. Fizika metallov i metallovedeniye, v. 31, no. 1, 1971, 172-176.

Variations in the fine structure of manganese austenitic steels were studied for the case when they are subjected to a pulsed load. Forged austenitic steels 40G13 (0.41% C; 13.62% Mn; 0.69% Si; 0.42% Cr; 0.15% Ni; 0.006% S; 0.02% P) and 125G13 (1.25% C; 12.80% Mn; 0.69% Si; 0.51% Cr; 0.03% P; 0.09% S) were studied. These steels were quenched in water at 1100° C. The pulsed load was applied by means of exploding 1.5 g cylindrical charges of high explosive in the center of the surface of samples which had dimensions of 20 x 20 x 9 mm at room temperature. Th pressure pulse, created in the metal under the explosive charge in this method, was equal to approximately 500 kbar. The surface of samples with an area of 3 x 3 mm^2, placed directly under the bottom of the crater, was studied after series etching of the layers of definite thickness down to the lower surface of the specimens. X-ray diffraction patterns were obtained with a URS-50IM diffractometer in filtered Fe and Mo radiation. Quantitative phase analysis was conducted by means of measuring the relative integral intensity of the $(111)_\alpha$ lines of austenite, and the lines of the $(100)_\alpha$ of the ε-phase and the $(110)_\alpha$ of the ε-phase. A relationship is established between the characteristics of the fine structure and a variation in microhardness. It is shown that the low value for the packing defect energy plays a basic role in the processes of the interaction of dislocations and the creation of a high level of strengthening of manganese austenite under the influence of pulsed loads. The especially high strengthening capacity of unstable manganese austenitic steels under pulsed loads is caused by the formation of martensite complexes from the α- and the ε-phases, since high-intensity shock waves generate the flow of the $\gamma \rightarrow \varepsilon$ transformation, while the weaker ones initiate the $\gamma \rightarrow \alpha$ transformation. Unstable steels also possers (within the limits of load under study) a higher level of plastic properties, which is connected with the occurrence of the martensite transformation under the effect of the shock waves.

18. Donukis, T. L., V. A. Lobodyuk, G. I. Savvakin, P. V. Titov, N. P. Fedas, and L. G. Khandros. Investigating the structure and properties of ferronickel alloys after shock loading. Fizika metallov i metallovedeniye, v. 31, no. 1, 1971, 183-189.

Using electron miscroscope and x-ray methods, the structure of ferronickel alloys (Fe - 30% Ni and Fe - 32% Ni) was studied following shock loading.

The loading of the sample, placed in a yoke, was produced by the impact of a steel plate which was accelerated by a plane detonation wave generator. The size of the charge and the thickness of the plate were selected in such a manner that the required initial parameters of the shock wave could be ensured. The average velocity of the plate's motion at a distance from 6 to 10 mm from the specimen surface was taken to be equal to its velocity at the moment of impact. The initial pressure on the contact boundary at the moment of impact was 100 or 300 kbar, the time in which the high pressure acted on the contact boundary was approximately 1.4 μsec, and the residual deformation of samples in the yoke was less than 5%. The shock wave attenuates in proportion to its distance from the load surface, which leads to variations in the phase composition, structure, and hardness. In the figure below, results are presented for the layer-by-layer investigation of

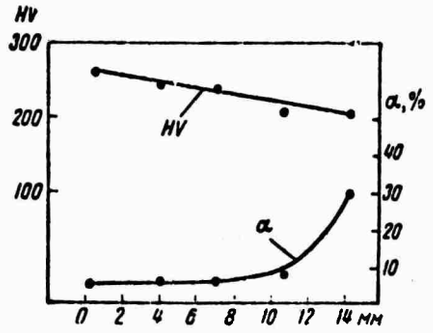

Fig. 1 - Change in the hardness and amount of martensite in alloy Fe - 30% Ni in relation to the distance from the surface of the impact.

samples of the Fe - 30% Ni alloy, strengthened by a 300 kbar shock wave after cooling in liquified nitrogen. When removed from the surface, which receives the impact, the hardness uniformly decreases from 270 to 230 HV (Vicker's hardness scale) down to a depth of 14 mm. The impact loading was responsible for considerable strengthening. The hardness of annealed samples when a shock wave was passed through them with a pressure of 300 kbar increased approximately by 120 HV and reached a value of 220 HV. The shock wave causes the $\alpha \rightarrow \gamma$ transformation. In the γ-phase which is formed, the following are observed: a needle-like structure which is unusual for austenite, twin bonds, and a cellular dislocation structure. Weakening of the γ-phase occurs 200°C below the weakening temperature of statically deformed austenite.

19. German, V. N., M. P. Speranskaya, L. V. Al'tshuler, and L. A. Tarasova. Investigating the structure of iron silicide monocrystals deformed by high-intensity shock waves. Fizika metallov i metallovedeniye, v. 30, no. 5, 1970, 1018-1026.

X-ray and metallographic studies are conducted on monocrystals of iron silicide and samples of Armco iron, subject to the effects of shock waves which create phase transformations. A relationship is established between the magnitude of sample microhardness and the applied pressure (shown in Figure 1). It is established that within the range of pressures being studied (from 90 to 500 kbar) in the monocrystals the preferred orientation of the crystal blocks is maintained which is close to the initial orientation of the monocrystal. The effect which is observed is explained by the incompleteness of the phase transitions and by the localization of the phase transformations along the twinning planes.

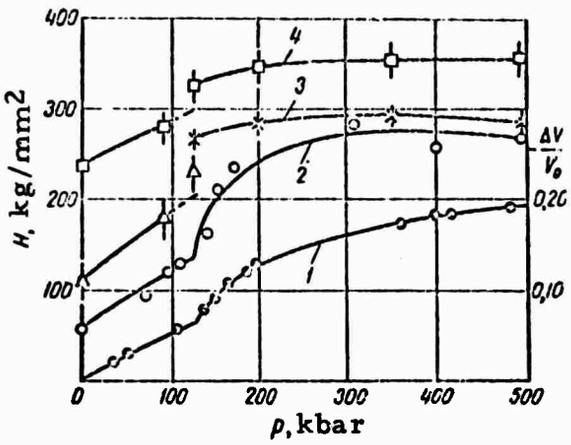

Fig. 1 - Volumetric deformation ($\Delta V/V_0$) and hardness (H) of iron by shock pressure. 1 - volumetric deformation behind the shock wavefront computed earlier; 2 - hardness of iron samples after shock compression computed earlier; 3 - microhardness of Armco iron; 4 - microchardness of shock-deformed monocrystals of iron silicide; x - data for needle-shaped grains and Δ - for weakly deformed grains.

20. Zubarev, V. N., N. V. Panov, and G. S. Telegin. The width of the stationary zone in detonation waves. Fizika goreniya i vzryva, v. 6, no. 1, 1970, 107-113.

Experiments were conducted to determine the width of the stationary zones in detonation waves, using both a mixture of trotyl-hexogene TG 50/50 (ρ_0 = 1.67 g/cm^3) and pressed TNT (ρ_0 = 1.63 g/cm^3). In distinction to previous works, in which the width of the stationary zone was established by a break in the velocity profile for a fixed length of explosive charge, in this report the dimensions of the "chemical peak" were determined on the basis of comparing the attenuation curves which were obtained for charges with varying lengths. The TNT charges were 20, 40, and 200 mm long and 90 mm in diameter. The thickness of the obstacle varied between 1.5 and 10 mm. The length of the TG 50/50 charges, 120 mm in diameter, varied within wider limits, from 10 to 440 mm, as did the thickness of the obstacle made of aluminum (from 0.2 to 18 mm). Results of the measurements, expressed in the form of functions of $u_{Al}(\Delta)$ (u_{Al} - the mass velocity in Al, Δ - the thickness of the obstacle) are presented in Figures 1 and 2.

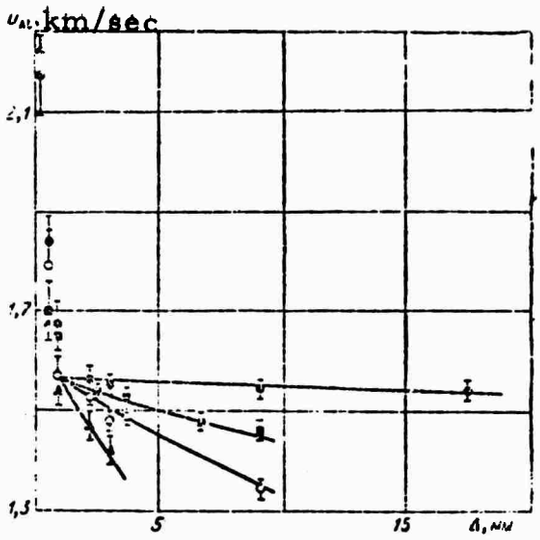

Fig. 1 - for TG 50/50

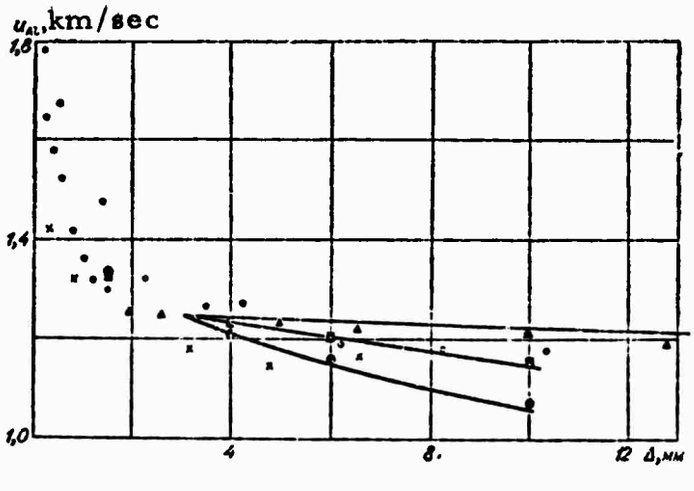

Fig. 2 - for TNT

21. Kiselevskiy, L. I., and V. A. Morozov. The interaction mechanism of pulsed hypersonic jets with solid obstacles. Voprosy fiziki nizkotemperaturnoy plazmy. Minsk, Izd-vo "Nauka i tekhnika", 1970. (Reports of the Second All-Union Conference on Low-Temperature Plasma), 624-626.

This is an experimental study of the effects produced by pulsed hypersonic flow on a fixed metal target covered by transparent cellophane film (Figure 1), which absorbs radiation only for the wavelengths $\lambda < 2200$ Å. In front of the film, a shock compressed layer of plasma is created, which is optically dense (in A-A direction) with the luminance temperature 19000°K. Only radiant thermal flux (4×10^9 w/m^2) reaches the metal target. Absorption of radiant flux leads to the warmup and destruction of the target (fusion and subsequent evaporation). Spectral investigations in the B-B direction indicated that radiation has a continous nature in the and ultra-violet regions.

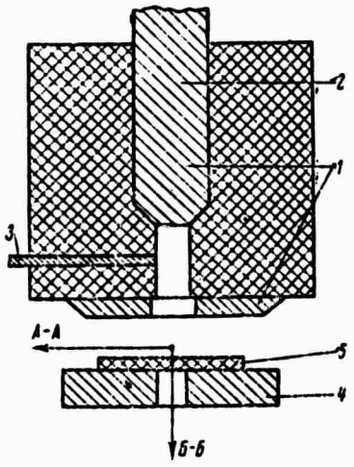

Fig. 1 - 1 - basic electrodes;
2 - dielectric discharge gap (plastic);
3 - igniting electrode;
4 - target; 5 - transparent film;
A-A and B-B - observation lines.

22. Chelyshev, V. P., B. I. Shekhter, and L. A. Shushko. Pressure variation on an obstacle surface during the contact detonation of an explosive charge. Fizika goreniya i vzryva, v. 6, no. 2, 1970, 217-223.

This paper offers an approximate analytic solution for the pressure variation (in time) in the interface boundary between the explosion front and the obstacle. This is done for a one-dimensional flow of detonation products, and it is stated that conditions close to one-dimensional exist in the explosion of a cylindrical charge inside an nondestructible casing. As a generalized

characteristic for the shock compressibility of the obstacle material, a parameter β is offered. It is expressed approximately as

$$\beta = 1 + 0.02\ (\overline{\rho}_o,\ \overline{c}_o)^{0.24}$$

where $\overline{\rho}_o$ - initial density of the obstacle material
$\overline{c}_o$ - initial velocity of sound in the obstacle material.

III. SHOCK WAVES AND EXPLOSIONS IN GASES

23. Bronshten, V. A. Propagation of a strong cylindrical wave in a nonuniform atmosphere. Izv AN SSSR. Mekhanika zhidkosti i gaza, no. 6, 1970, 108-111.

An approximate solution of the indicated problem was given, applicable to any given angle formed by the wave axis with a vertical. The solution, based on the method developed by Laumbach and Probstein (J. Fluid Mech., 1969, v. 35, pt. 1, 53-75), may be used to calculate the waves generated by the passage of large meteorites through the atmosphere. The method used to calculate the velocity D of a shock wave is applicable only with the following assumptions: the ratio of pressures in the shock wave is > 40, i.e.; the ratio of velocities $D/a > 6$, where a is the acoustic velocity; the gas is ideal with a given adiabatic exponent γ; the atmosphere is cold with density given by $\rho=\rho_0 e^{-H/H^*}$, where H* is the scale of heights at a given level H and ρ_0 is the density at the level H=O; and all other effects, e.g. gravitational, magnetic, etc., are negligible. Under these conditions, propagation of a cylindrical wave from a section of its trajectory around a point C in the perpendicular plane can be described by $\phi\eta\eta'' + \psi\eta\eta'^2 = \pm 1$, where η is the dimensionless velocity of the shock wave and η' and η'' are time derivatives of η. The solution of this equation for η' indicates that the velocity of an ascending ($\eta>o$) cylindrical wave, as with that of a spherical wave, decreases to a minimum at $\eta=3$ and then increases, while the velocity of a descending wave decreases progressively.

24. Galiyev, Sh. U., M. A. Il'gamov, and A. V. Sadykov. Periodic shock waves in gases. Izv AN SSSR. Mekhanika zhidkosti i gaza, no. 2, 1970, 57-66.

Longitudinal, nonlinear oscillations were studied in an 82 mm diameter shock tube closed at one end. Harmonic oscillations were generated by a motor-driven piston moving in the tube at its open end, with the excitation frequency ω being controlled by the current in the motor. Shock wave pressure p was measured accurately to 10^{-3} bar at various points along the tube within a wide range of ω. Pressure pick-up signals were transmitted to a PM-1 measuring device and an oscilloscope for observation and photographing. Photographs of the pressure oscillations were shown at $\omega=\Omega=\pi a_0 L$ (L=340 cm) and $\omega=\frac{1}{2}\Omega$ (L=170 cm)

where Ω is the first eigenfrequency of the gas column, a_0 is sound velocity in an unperturbed gas, and L is tube length. In both cases, the profiles of the shock waves show harmonic or near-harmonic oscillations of the gas column at pre-resonance frequencies. Breaks in the profiles appear near the approach to resonance, and increase to a maximum at resonance. A graphical presentation of shock wave trajectories shows that gas oscillations sufficiently remote from resonance can be described by a linear acoustics formula. The shock waves were described by nonlinear gas dynamics equations in the case of $\omega = \frac{1}{2}\Omega$, using the method of successive approximations. The calculated amplitudes of pressure curves differed by 10% at most from the experimental values. A general formula is included for calculating pressure at $\omega = N\Omega$ (2N=1, 3, 5, ---).

25. Ivanov, M. Ya. Calculation of gas flow through a shock tube of variable cross section. Izv AN SSSR. Mekhanika zhidkosti i gaza, no. 3, 1970, 162-166.

Gas flow was analyzed in an axisymmetrical shock tube for the case of instantaneous removal of an infinitely thin diaphragm separating a compression chamber from a low-pressure chamber. The latter is assumed to be connected to a terminal nozzle whose contour consists of line segments and arcs. A modified differential method proposed by Godunov et al (ZhVMMF, v. 1, no. 6, 1961, 1020-1050) was used to calculate the velocity component along the x-axis, density, and pressure p in a nonstationary gas flow, without separating out sharp breaks, i.e. the regions of sharp gradients. Pressure distribution is given along the wall of the shock tube at its cross section at different times t and along the nozzle at a given t. A comparison was made between identically calculated p data for one-dimensional and two-dimensional flow. The discrepancy between the two sets of local p characteristics of the flow was greater than between the two sets of summary characteristics, i.e. gas mass versus time characteristics. The differential method used is applicable to p gradients $>>$ 100 at the diaphragm. Calculations of p distribution along the axis of a cylindrical shock tube showed that the differential method used resulted in only insignificant diffusion of compression shock, as compared to the exact solution and to the Lax method.

26. Mozzhilkin, V. V. Propagation of shock waves through a gas of nonuniform density. Izv AN SSSR. Mekhanika zhidkosti i gaza, no. 5, 1970, 68-72.

The method of successive approximations was used to solve the problem of a plane shock wave propagating through a polytropic gas of variable pressure

and density. Special independent variables R_1 and R_2 were introduced into the system of basic gas dynamic equations. A discontinuous motion law was derived from the transformed basic equations, and the correlations of R_1 and R_2 with the originally selected x and t coordinates were determined. This solution, based on the method of G. B. Whitham (J. Fluid. Mech., 1958, v. 4) did not satisfy the boundary condition $R_1 = R_1(R_2)$. Solving the system of equations obtained by the Whitham method jointly with the Rankine-Hugoniot and boundary conditions produced the discontinuous motion law in a null approximation. The same law in the first, second, and following approximations was derived in an analogous manner.

The above method of successive approximations was applied to the self-similarity problem of propagation of a powerful shock wave through a gas of density $\rho_0 = bx^{\delta}$ ($\delta > 0$, b=const.). An expression for self-similarity index α was derived from a system of equations of discontinuity; here α_1 was calculated for the values of adiabatic exponent $\gamma = 1.2$, 1.4, 5/3 and for $\delta = 2.0$, 1.0, and 0.5. The tabulated α values were found to be in good agreement with data from the literature.

27. Mozzhilkin, V. V., and S. V. Fal'kovich. Propagation of shock waves in a medium with exponentially-varying density. Izv AN SSSR. Mekhanika zhidkosti i gaza, no. 6, 1970, 48-54.

Propagation was analyzed of a shock wave through a channel whose cross section obeys the formula $A = A_0 e^{\lambda \beta x}$, where A_0 and β^{-1} are constants with the dimensions of area and length respectively, and λ is a dimensionless constant. The gas was assumed to be polytropic with adiabatic exponent γ. A self-similar solution ($p = p_0 = \text{const} \neq 0$) was presented on the basis of the equation of gas motion in a hydraulic approximation and the boundary conditions for the shock wave were set by introducing a set of self-similarity variables. Two possible cases of self-similar solutions were analyzed: $0 \leq \alpha \leq 2$ and $\alpha = 2$, where α is the self-similarity index. The analysis revealed that at $\alpha = 2$, self-similar motion of a shock wave of constant intensity exists, when $\frac{1}{2} \leq \lambda \leq \lambda^0$, and that the Mach number M varies from 1 to $+\infty$ with increase in λ. There exists only the self-similar motion of the second type in a strong shock, when $\lambda \geq \lambda^0$. A law of shock damping was formulated within the limits of linear theory, assuming the existence of non-self-similar flow with weak shock waves at $\lambda < \frac{1}{2}$. It was shown that in this case the intensity of shock decreases simultaneously with increase in velocity of the shock wave.

28. Gorelova, M. A., and V. A. Gorelov. Electrode method for measuring electron temperature, ion density and electrical conductivity behind a shock wavefront. IN: Teplofizicheskiye svoystva nizkotemperaturnoy plazmy. Moskva, Izd-vo nauka, 1970, 95-100.

Experimental results are described for measuring electron temperature T_e, ion density n_i and electrical conductivity σ in a plasma region behind a shock wavefront. The tests were done in an electrically discharged shock tube with an initial downstream air pressure of 0.3—2.0 torr, shock wave velocities in the 4 to 9 km/sec range, a plasma temperature of $4-8 \times 10^3$°K, and density $\sim 10^{-5}$ g/cm^3. Measurements were made with two tungsten probes inserted into the plasma; probe dimensions were 0.1 mm diameter and 5 mm long, oriented parallel to the plasma flow. In addition, the probes were modulated with a sinusoidal voltage of 3.5 v peak at 150 and 200 KHz. The theoretical basis and experimental results for T_e, n_i and σ measurements are presented over the cited range of test parameters. The dual probe technique is recommended as a simple method with good spatial resolution for diagnostics of low-temperature, short duration plasmas. Furthermore, this technique for measuring σ requires no calibration and is accurate to within 20—25%.

29. Belova, A. V., and V. F. Turishcheva. Shock wave in a binary mixture of monatomic gases. IN: Sbornik. Aerodinamika razrezhennykh gazov. Vallander, S. V. (ed). Leningrad University, 1969, 125-132.

A theoretical analysis is given of shock wave structure in a binary mixture of monatomic gases. The work is an extension of a cited previous study in which an approximate solution of the problem based on the Mott-Smith method was presented. The present work uses the method of successive approximations set forth by Vallander et al (Vestnik LGU, no. 7, 1961), in which a system of integral kinetic equations was employed. A mixture of gases a and b is assumed to flow with a general velocity v along the x-axis, with initial parameters known (ρ_1, v_1, T_1). The object is to determine the variation of these three parameters for the mixture as well as for the individual gas components. It is shown that the problem reduces to finding the distribution functions $f_a(x)$ and $f_b(x)$ of the component parameters. The solution given for the binary case can also be extended to larger numbers of component gases.

30 . Kazandzhan, E. P., and V. S. Sukhorukikh. Interference variations in gas dynamics. DAN, v. 194, no. 5, 1970, 1045-1048.

The authors propose a single-exposure monochromatic light beam method for obtaining an interference pattern in gas dynamic studies. This is claimed as an improvement over the standard technique, which requires both monochromatic and achromatic exposures to get a complete interference pattern. Theoretical and experimental results are presented in support of the proposed method, showing a near equivalence to the two-step procedure for the observation of hypersonic gas flow about a blunt body. The technique is evidently a variant of the usual holographic method, with the exception that the illumination is monochromatic only, without being coherent as well.

31 . Savrov, S. D., and A. N. Dremin. A new method for generating powerful shock waves in gas. DAN, v. 194, no. 4, 1970, 811-814.

A modified shock tube using an explosive charge to generate a high velocity plane shock wave is described. The design combines several advantages of various conventional types of shock tubes, in that it develops plane shock waves in the 15—20 km/sec range, while still maintaining a sufficiently transparent plasma region behind the shock wave so that optical probe methods can be used for diagnostics. A diagram of the device is shown in Figure 1.

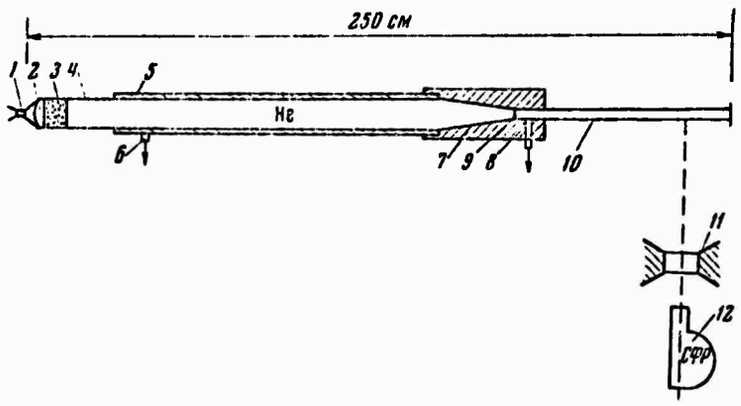

Fig. 1 - Explosive-charge shock tube. 1 - percussion cap; 2 - shaping lens; 3 - charge (hexogen, 0.5 g); 4 - glass tube, 100 mm dia. x 250 mm long; 5 - steel tube, 110 mm dia. x 1.5 mm long; 6, 8 - evacuation ports; 7 - matching conical section; 9 - Mylar diaphragm; 10 - glass tube, 35 mm dia. x 1 m long, filled with the driven gas; 11 - illuminator; 12 - camera.

The operation is in two stages, as follows: the driver gas (He or H_2) is compressed and heated by the charge detonation, forming a shock wave which ruptures the mylar diaphragm (9) and in turn generates a shock wave in section (10), containing the driven gas at a static pressure of 0.5 to 30 torr. The success of this design depends greatly on the design of the driver stage and pressure of the driver gas, so that the shock wave propagates well ahead of the explosive detonation products in order to retain the necessary transparency in the working section (10). In a cited example, He at atmospheric pressure was found optimal as a driver gas. Test results for three working gases are summarized in Table 1, in which temperature and pressure values behind the shock wave are taken from several other authors.

	Air		He	Ar
Initial pressure torr	10,0	1,0	10,0	3,0
Shock wave vel., km/sec	13,8	18,3	18,0	15,0
Temp. behind incident wave, °K	18 000	19 500	20 000	28 000
Press. behind incident wave, atm	65	8	10	—
Drop in velocity at tube end, %	—	8	3	10

Table 1 - Shock wave parameters for tested glass.

32. Zheleznyak, M. B. Ionization relaxation behind shock waves of 17—25 km/sec velocities in nitrogen. PMTF, no. 6, 1970, 126-130.

A theoretical study is reported on plasma parameters of high-speed shock wave propagation in nitrogen. This is based on similar previous studies in air, where a non-monotonic relationship between ionization rate and shock wave velocity v_s begins to appear at v_s = 9.5 km/sec. The author extends the treatment to propagation in nitrogen, at sufficiently high v_s that the gas may be considered completely ionized. Computer solutions of parameter profiles were obtained for this model under assumed realistic conditions. A typical example showing computed temperature and density profiles behind the shock wave is given for v_s = 21 km/sec.

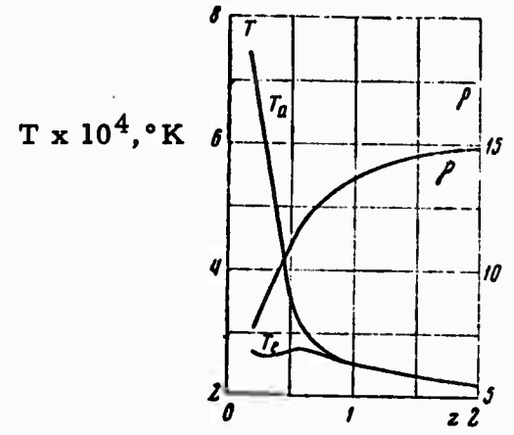

Fig. 1 - T and ρ profiles in nitrogen plasma for v_s = 21 km/sec.

33. Barenblat, G. I., and G. I. Sivashinskiy. Self-similar solutions of the second type for the problem of the propagation of strong shock waves. Prikladnaya matematika i mekhanika, v. 34, no. 4, 1970, 685-692.

The authors analyze the problem of the propagation of strong shock waves, with the provision that the adiabatic exponent γ_1, under shock wave conditions, differs from the value of the adiabatic exponent γ in differential equations describing continuous motion behind the wave. This provision for $\gamma_1 < \gamma$ offers the possibility of a qualitative estimate of the energy losses for dissociation, ionization, and excitation of oscillatory degrees of freedom of the molecules. The solution of the problem is reduced to the construction of a self-similar solution of the second type. For completeness, the case $\gamma_1 > \gamma$ is also analyzed. The family of solutions obtained describes continuous set of motions, including an ordinary strong explosion and the propagation of strong detonation waves.

IV. LASER: INTERACTION WITH PLASMA

34. Generalov, N. A., G. I. Kozlov, and Yu. P. Rayzer. Nonequilibrium states and variation in absorptive capabilities of a plasma from the effect of powerful optical pulses. PMTF, no. 3, 1970, 27-37.

This paper gives an extended analysis of test results reported previously by the authors on laser absorption in plasma (ZhETF Pis'ma, v. 8, no. 3, 1968; ZhETF, v. 56, no. 3, 1969; PMTF, no. 1, 1970). Their experiments have shown that absorptive capacity of a plasma depends on incident beam intensity, and generally will vary in a non-monotonic manner. The analysis investigates the kinetics of heating, ionization and absorption of optical energy for a variety of plasma and laser parameters. A treatment of this sort is considered essential for explaining certain phenomena of interest such as the self-shielding effect of a laser-generated plasma on the solid surface beneath it. The theoretical results agree adequately with the cited experimental findings.

35. Goncharov, V. K., L. Ya. Min'ko, and Ye. S. Tyunina. Modeling of hypersonic flow in a partially-expanded plasma by means of laser interaction with absorptive materials. ZhPS, v. 13, no. 4, 1970, 707-711.

An experiment is described in which plasma dynamics were observed from interaction of powerful laser radiation with absorptive solids. The description indicates that local hypersonic flows in the generated plasma were monitored by passing the plasma through a nozzle, but the manner of doing this is not specified in any detail. A neodymium laser was used developing energies in the 50—150 j range; the laser was operated in random, controlled and quasistationary modes to give a variety of local plasma flow conditions. Target materials mentioned are brass and a tin-lead alloy; the tests were run at atmospheric pressure. Spectral and high-speed photo data are given for different plasma conditions, and plasma parameters are tabulated for the two general cases of plasma jets with a periodic structure and jets with a shock wave. This technique is cited as very promising for the study of plasma jets generated by beam-target interactions.

V. LASER: GAS BREAKDOWN

36. Askar'yan, G. A., and V. K. Stepanov. Simultaneous extended action of a powerful optical flux on matter. ZhETF, v. 59, no. 2, 1970, 366-367.

In optical beam-target or gas breakdown tests the laser beam is typically focused by spherical lenses to the desired spot size. A departure from this is considered here by Askar'yan and Stepanov, where they briefly describe beam-target experiments using a two-dimensional or slit-shaped incident beam, formed by cylindrical rather than spherical lenses. In the tests cited a Q-switched neodymium laser with a 6 cm cylindrical lens was used to produce an extended optical breakdown in argon and other gases at pressures up to 20 atm; an unswitched laser was also used to form slits in metal targets. An inherent advantage of this method is that the focused beam area attainable with a cylindrical lens is substantially greater than that for a spherical lens -- by a factor of 100 in the cited case. This paper mostly emphasizes the practical arguments for line-focused beams in material processing; however, in the case of line breakdown in gas or on a dielectric surface, it is also pointed out that plasma propagation velocity can exceed light velocity, which suggests a number of interesting theoretical and practical possibilities.

37. Korneyev, N. Ye., and Yu. I. Pavlov. Generating a plasma by means of focused single-mode laser radiation. IN: Voprosy fiziki nizkotemperaturnoy plazmy. Minsk, Izd-vo Nauka, 1970, 477-478.

A brief discussion is given of spectral studies made of a plasma generated by single-mode laser breakdown in air. This produces some unique plasma effects not typical of the usual multimode laser experiments reported to date. An example cited is the appearance of a bright center region in the spark, whose generation is otherwise not accounted for. The authors used a ruby laser generating single longitudinal and transverse modes, at 40 Mw and 10 nsec duration. The beam was focused for air breakdown by a 30 mm lens to a 0.2 mm radius spot size. The spark region was recorded by photographs using narrow-band ($\Delta\lambda = 20$ Å) filters, and by spectrography. The

spectrograms included distinct lines of singly-ionized nitrogen. Plasma temperature was determined by a relative intensity method to be 55,000°K; this result was repeatable within ±2000° K, which was within the measurement uncertainty range.

38. Korneyev, N. Ye., and Yu. I. Pavlov. Study of plasma jets formed by focused single-mode laser radiation. IN: Teplofizicheskiye svoystva nizkotemperaturnoy plazmy. Moskva, Izd-vo nauka, 1970. 164-166.

Air breakdown studies from focused single-mode laser radiation are briefly described, in which the configuration of Figure 1 was used. The authors compare their results to several previous articles, particularly those of Mandel'shtam et al (ZhETF, v. 47, 1964, 2003). Several phenomena

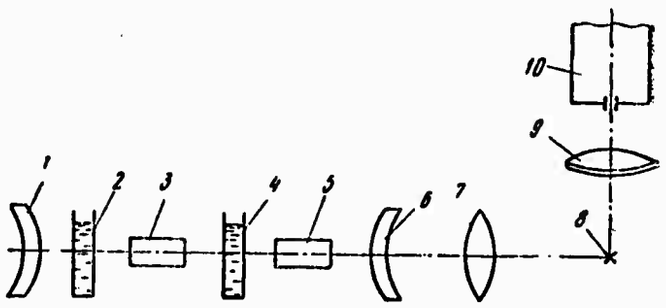

Fig. 1 - Single-mode laser air spark experiment. 1 - convex mirror; 2, 4 - phthalocyanine filter, $\lambda = 6943$ Å; 3, 5 - ruby laser; 6 - output mirror; 7 - lens; 8 - spark; 9 - condenser; 10 - spectrograph. Pulse width = 20 ns, power = 6 mw.

in spark generation associated with jet formation are considered poorly understood by the authors; the main object in the present tests, therefore, was to determine electron density N_e and plasma temperature T_e as functions of test variables. Based on observation of N II lines, T_e was determined to be 32,000° K; N_e was on the order of $6 \times 10^{18}/cm^3$, agreeing well with Mandel'shtam's figure. In comparison to the latter's wide spread in temperature values, however, Korneyev and Pavlov report good repeatability of their T_e data.

VI. LASER: RADIATION EFFECTS OF LASER-INDUCED BREAKDOWN

39. Askar'yan, G. A., M. M. Savchenko, and V. K. Stepanov. Diamagnetic moment of a strong shock wave from high temperature optical explosions in gases. ZhETF, v. 59, no. 4, 1970, 113-1145.

This is an extensive experimental and theoretical investigation of the diamagnetic moment phenomenon produced in a laser explosion, which has been the subject of several previous papers by Askar'yan and coworkers. In the present tests, pulsed laser radiation was focused in various gases within a pressure vessel, while the resulting plasma generation and magnetic field behavior were monitored. A high-power Q-switched laser was focused through a chamber window into a wide variety of gases, including air, N_2, O_2, H_2, D_2, CO_2, SF_6, and the noble gases, at a wide range of initial static pressures. External fields up to 10^4oe were simultaneously applied in the region of the focal point, with an inductive pickoff coil placed around the focal region to register local suppression of the applied field following an explosion. The main object of this experiment was to find the dependence of the generated diamagnetic moment M on incident energy E absorbed in the spark at various densities ρ, for each of the tested gases. Tests showed a nearly linear dependence of $M(E/\rho)$ for all gases, irrespective of the wide range of laser energies and gas densities (more exactly, $M\ (E/\rho)^{1.2}$. Furthermore, M was directly proportional to the mass of the ion or atom in question. The behavior of M was also investigated as a function of the dimensions of the spark region and of the geometry of the incident laser beam; however, it was again confirmed that M was dependent only on E, regardless of the variations in these parameters.

From these experiments, Askar'yan postulates the following model for the diamagnetic phenomenon in high temperature shock waves. The diamagnetic perturbation is caused by eddy currents generated by motion of conducting layers in the medium behind the expanding shock wave. Initially, the dimensions of the perturbation region may approach those of the shock wave; with expansion and decreasing temperature at the shock wave front, the eddy current region becomes confined to the interior higher temperature region, in accordance with the assumed inverse temperature gradient from the shock wave front back to the energy release point. The question is then to relate the lifetime of the perturbation region to penetration of the external magnetic field and to shock wave radius r_{sh}. Askar'yan does this rigorously, showing that the magnetic parameters

have an almost negligible dependence on r_{sh}, i.e. on time, for a sufficiently hot spark. He goes on to show that the external field can, in fact, be made the dominant factor in determining diamagnetic lifetime in the plasma, regardless of the stage of plasma development.

40. Bunkin, F. V., and A. Ye. Kazakov. Electron heating and noncoherent hard radiation generated by interaction of ultrashort powerful laser pulses with matter. ZhETF, v. 59, no. 6, 1970, 2233-2243.

A theoretical study is described on electron heating mechanisms in laser-generated plasmas. The analysis is principally concerned with the case of pulse widths on the order of a picosecond, at a wide range of intensities. For intensities I substantially above critical I_{cr}, it is assumed that beam interaction is entirely with the plasma electrons and nuclei, with ionization occurring "instantaneously", i.e. within the first one or two periods of the exciting radiation. Continued irradiation at this level can result in hard, noncoherent bremsstrahlung generation from the plasma, conditions for which are discussed. It is pointed out, however, that bremsstrahlung can also occur at appreciably lower electron temperatures ε_e, owing to electron vibratory energy ε_{vib}. For the sake of analysis, therefore, the conditions governing bremsstrahlung are defined in terms of two general conditions, namely $\varepsilon_{e>\varepsilon_{vibr}}$ ("heated" electrons) and $\varepsilon_{e<\varepsilon_{vibr}}$ ("unheated" electrons). Practical limits for obtaining the critical temperature and plasma density are also discussed.

VII. LASER: INTERACTION WITH SOLIDS

41. Kondrat'yev, V. N., I. V. Nemchinov, and V. M. Khazins. Calculating the expansion of a heated surface layer of matter on the basis of its phase composition. PMTF, no. 4, 1970, 79-90.

The authors consider various combinations of physical effects which govern the evaporation and ejection of solid matter under high-power laser radiation. Several theoretical cases are assumed which include one or more of the phenomena associated with laser explosions, i.e. vaporization, ionization, and solid particle ejection of surface layer material. The evaporation behavior is also shown to depend on target material parameters such as optical transparency and thermal conductivity, as well as on laser pulse energy and duration. For released energy $f \gg$ heat of evaporation Q, a self-similar model is assumed to be satisfactory in defining the kinetics of the exploded mass; however, in cases where $f \leq Q$ a more complex situation occurs which requires numerical solutions based on experimental data. Examples are given for metals with typical thermal constants, showing that for applied pulse intervals on the order of 1 ns or less, the increase in depth of the affected surface layer during exposure may be considered negligible.

42. Vilenskaya, G. G., and I. V. Nemchinov. Numerical calculation of motion and heating of a laser-generated plasma formed by absorption bursts in vapors of solids. PMTF, no. 6, 1969, 3-19.

A detailed theoretical study is given of time-variable parameters in plasmas generated by laser irradiation of solids. The analysis takes into account the pulsating or "burst" variations in plasma pressure which are shown to occur in the typical beam-target interaction. In such cases the initially evaporated surface layer expands outward and begins to cool, as long as it remains relatively transparent to the laser beam, which continues to evaporate fresh surface layers. This continues until a critical point occurs when the net evaporated mass becomes optically thick enough to absorb the incident beam, causing a rapid local plasma heating, ionization, and detonation, while the target surface is temporarily shielded. When this initial

surface mass is then sufficiently dispersed, it again becomes transparent and surface evaporation resumes in the same manner. Pressure pulsations thus will occur thoughout the radiation interval, and the process is nonmonotonic except for the initial shielding phase. The authors derive expressions for various parameters based on this model, together with boundary conditions. Figure 1 illustrates the repeated pressure burst effect measured in

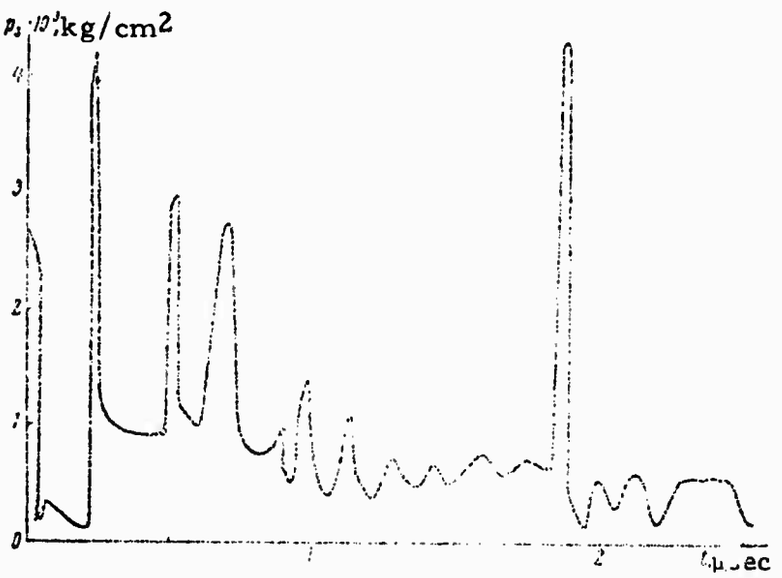

Fig. 1 - Pressure at the boundary surface vs. exposure time.

experimental tests, indicated by the text to be from free-running laser irradiation of a carbon target at a density of 300 mw/cm^2.

Essentially the same treatment of the pressure pulsation phenomenon is given by the authors elsewhere (ZhPS, v. 11, no. 4, 1969, 637-643). Here they also relate the time τ required for developing a pressure burst to the incident optical flux q as follows: $q \sim \tau^{1/\alpha 1}$, where α is an empirical constant on the order of unity.

43. Grevtsev, N. V., V. G. Karabutov, A. S. Skripnichenko, and A. A. Uglov. Calculated and experimental values for depth of the evaporated layer in silicon from the effect of a Q-switched laser. FiKhOM, no. 3, 1970, 8-13.

Laser parameters are studied which become the critical factors in controlled beam-target applications such as crater formation and spectroscopy of surface materials. The mode, power and pulse duration must be chosen to produce the desired amount of material evaporation, ionization, etc., thus a free-running laser will produce a desired degree of vaporization, but its relatively long pulsewidth does not provide the energy densities needed for surface ionization in spectral studies. Hence for the latter purpose a Q-switched mode is preferable, which causes evaporation only to depths of 1 — 2 μ. Experiments in controlled cratering are described in which a Q-switched ruby was used on silicon specimens, operating at 40 nsec pulses with intensities on the order of 10^{11} w/cm^2 in a 20 μ diameter spot. Theory indicates this should yield craters several microns deep in Si, which proved to be the case. Photos are included showing a crater directly after formation, and then with ejecta cleared away.

44. Rykalin, N. N., and A. A. Uglov. Effect of internal vaporization on laser heating of metals. FiKhOM, no. 2, 1970, 30-33.

In laser heating for welding purposes a solid bond may be prevented by spatter outside the liquid-phase fusion zone, principally when beam temperature exceeds some critical value for the particular metal. The present paper examines several factors that, along with beam focusing, can lead to spattering. A common method of combatting this phenomenon is to increase the duration of the laser pulse (i.e., reduce beam power density), which in turn retards heating and lowers the critical temperature of the liquid metal. One of the probable spatter mechanisms is intense boiling of the liquid phase as a result of superheating within a short time (relative to pulse duration). It is noted that even at beam intensities over 10^6 w/cm^2 internal vaporization plays no significant role in metal breakdown. If the material contains considerable amounts of evolved gases, or if the metal has gas cavities or microscopic pores, the volume of gas can during rapid heating form hundreds of spaces in the basic metal. Under intense heating the gases are liberated, which can lead to partial spattering. Another factor promoting boiling in heterogeneous materials is the presence of an interface area, whose contact is usually imperfect. If the melting point of the lower material is higher than that of the

upper, the surface of the solid phase can initiate formation of nuclei in microcracks of the solid surface. Gas bubbles are facilitated by spike laser pulses in free-running modes, which can lead to surface temperature pulsations and consequently to internal compression waves and damage of a degree equivalent to that experienced with ultrasonic waves. This spike structure can also increase the probability of bubble formation through amplification of local density fluctuation in nucleus-formation areas. A qualitative analysis of the dynamics of spatter development in the presence of gas vapor bubbles thus concludes that bubble growth is determined by the degree of superheating at the end of the pulse, and that a substantial increase in the volume of internal gas and vapor phases can cause spatter.

45. Bykovskiy, Yu. A., N. N. Degtyarenko, V. G. Yelesin, Yu. P. Kozyrev, and S. M. Sil'nov. Energy spectra of ions formed by the interaction of laser radiation with a solid target. ZhTF, no. 12, 1970, 2578-2580.

Energy distributions of multiply charged Co_{59}^{27}, Ta_{181}^{47}, and W_{184}^{48} ions formed during laser irradiation of a solid target were determined by a time-of-flight mass spectrometer with a magnetic analyzer. A three-stage laser with a maximum power W= 2 Gw and a beam density of up to $q_{max}=10^{13} w/cm^2$ was employed. Ion energies for z = 1—25 are plotted for Co at $q = q_{max}$. The number of ions decreases consistently during a single laser pulse, and E_z increases monotonically with an increase in z. With a decrease in q the ions exhibited lower z maxima, and E_z exhibited weak dependence on q. The interpretation of these results is based on the assumption of thermodynamic equilibrium in the plasma, and establishment of steady-state vaporization and heating during the period of interaction. Theoretical threshold q values for the formation of Co ions are shown to be in good agreement with experimental values. Analysis of the latter shows that ion groups with corresponding T and z(T) exhibit independent accelerations. It is noted that analysis of energy spectra supplies information on the physics of laser beam interactions with solids and on the kinetics of plasma flare dispersion. This offers the possibility of determining the ionization potentials of elements and the recombination time of multiply charged ions.

46. Korunchikov, A. I., V. V. Panteleyev, O. I. Putrenko, and A. A. Yankovskiy. Relationships governing the ejection of metallic material from laser irradiation. ZhPS, v. 12, no. 5, 1970, 819-823.

The magnitude of optical ejection of metals depends primarily on their

melting point. Another important contributor is the amount of light energy reflected by them; the amount of laser energy absorbed by the metals in fact constitutes a small part of the total incident light energy. The major ejection can be considered to occur in the form of the molten phase, and not in the form of vapors. This explains the absence of a relation between atomic weight and the magnitude of ejection, as well as the distance of the condensation zone from the surface of the metal. These relationships are illustrated in the enclosed table. These data for a pulse energy of 10 j, at λ = 1060 nm, pulse duration of $7 \cdot 10^{-4}$ sec, focal length of 200 mm, spot diameter of 0.1 mm, and a random generation mode. The amount of ejecta also proved to be independent of ambient pressure, but dependent on the density of the laser energy around the sample, the degree of "moderate" damage being a function of a melting point and coefficient of reflection: the lower the latter, the less intense the energy density required for moderate damage. These two properties also determine ejection distance and direction. The phase behavior, condensation zone, and the effects of single-pulse and spike laser modes on the ejected material are also discussed.

47. Putrenko, O. I., and A. A. Yankovskiy. Characteristics of material ejected as a result of laser irradiation. ZhPS, v. 11, no. 4, 1969, 617-622.

Explosive ejection of target material under laser irradiation at 10^8—10^9 w/cm is known to occur primarily in the condensation phase. The present paper deals with relationships governing the spatial distribution of this phase, for the case of free-running laser generation. Experiments were run with a GSI-1 laser at an energy of about 7 j; focal distance was 200 mm. A 5-mm long carbon cylindrical tube with an interior diameter of 4 mm was affixed to the target surface, and the laser beam was aimed down its axis, so that material ejected by the laser beam adhered to its interior walls. After the tube was removed, metallic beads formed from the ejecta were found on the surface of several metals. The density of the beads decreased markedly with height, and they became progressively more jagged. The most pronounced jagged effect occurred with copper, followed by zinc and iron; lead and tin samples produced no bead formations, although they experienced much greater mass ejections. A glass plate in front of the sample and normal to the beam was used to study angular ejection. An annular distribution, with its center at the point of beam incidence, was observed, maximum material density occurring within the inner circle of the ring. In the region next to this circle ejecta density and particle size were small. Density maxima for the craters of various metals are discussed, along with the relationship of crater characteristics to ejecta and beam duration. A crater-formation process is suggested

Element	Atomic Weight	M. p., °C	Fraction of Absorbed Light Energy	Plasma jet velocity (km/sec), 5 mm from surface	Max velocity of plasma cloud (km/sec)	Distance from melting zone (mm)	Ejection (mg)
Tin	119	232	0,46	12	0,18	13	10
Lead	207	327	0,46	11,5	0,24	9	13
Zinc	65	419	0,33	9	0,12	8	4,4
Magnesium	24	650	—	11	0,14	7	1,0
Aluminum	27	660	0,26	10,5	0,16	5	1,4
Copper	63	1083	0,09	6,5	0,12	3,5	0,8
Nickel	58	1455	0,28	9	0,13	5	1,3
Iron	56	1530	0,40	8	0,18	4,5	0,7
Molybdenum	95	2622	—	5,5	—	2	0,5
Tungsten	184	3390	0,40	5,5	0,16	1,5	0,8
Carbon	12	4000	0,73	8,5	0,20	5	0,2

Table 1 - Effect of laser radiation on metals
(cf Korunchikov et al, previous page)

on the basis of these observations. The relationship of ejecta angular distribution to beam density is described. The experiments also investigated, for purposes of spectral analysis, the extent to which the chemical composition of the ejecta corresponded to that of the irradiated material. Copper-zinc alloys and silicon-brass samples were used. In both cases the results indicated that these materials behaved like single metals with respect to ejecta.

48. Alekseyev, N. I., N. V. Volkova, T. V. Stepanova, and L. M. Shestopalov. Surface damage to lithium fluoride single crystals from laser irradiation. FTT, no. 10, 1969, 2720-2723.

It is shown that centers of surface damage in laser-irradiated LiF single crystals are not related to mechanical surface defects. Their number and nature depend largely on the structural state of the crystal as a whole. This conclusion is based on experiments using varied structures of LiF samples, i.e. diverse production methods, dopant contents, and color centers. The samples had a thickness of 3 — 5 mm, were cut along the cleavage planes, and exhibited some surface shear. The crystals were irradiated by an Nd spiked-beam laser, at a distance of 96 cm, (f = 100 cm), and the irradiated samples were then photographed. During the experiments attention was centered on the threshold of surface damage, the threshold of surface luminescence, the nature of damage in different samples at identical energies, and the size and number of damage centers. The main conclusion drawn from these experiments is that the limit of interior optical strength correlates with the threshold of interior optical damage and is a function of the structural state of the crystal as a whole. Photographs at 400 X magnification are included, showing details of damage centers in several LiF specimens at pulse energies from 3 to 10 j.

49. Volkova, N. V., Yu. A. Yershov, V. A. Likhachev, V. P. Osachev, A. A. Patrin, A. P. Fedotov, L. M. Shestopalov, and I. D. Yaroshetskiy. Effect of optical inhomogeneities on damage processes from laser irradiation of polymethylmethacrylate. FTT, no. 2, 1970, 2672-2675.

A systematic approach to determining the optical strength of transparent bodies should include comparative analyses of the stability/strength threshold and of the nature of damage for a wide variation in densities of initial structural

deficiencies. A previously reported method for producing samples with varying inhomogeneity densities is employed here for nine PMMA specimens subjected to spike and single-pulse laser beams, to derive numerical characteristics for structural and strength parameters. The main observations were the following: (1) samples subjected to spike modes exhibited a damage threshold at least an order of magnitude lower than those under single-pulse radiation. At equal pulse energies the specimens differed in the extent of the damage area and the density of damage centers; (2) the density of the initial opaque inclusions correlates with the frequency of damage centers: the higher the density, the greater the number. (It is noted, however, that one sample with no inhomogeneities experienced damage of a nature similar to that of the remainder.); (3) with a Q-switched laser the damage zone comprised two parts: a continuous threadlike track in the focal region and a set of microcenters whose density diminished with their distance from the main focal point; (4) at high beam intensities damage can occur in material without inhomogeneities.

50. Afanas'yev, Yu. V., E. M. Belenov, O. N. Krokhin, and I. A. Poluektov. Self-consistent heating of matter by a laser pulse under conditions of nonequilibrium ionization. ZhETF, v. 60, no. 1, 1971, 73-82.

This theoretical paper deals with the one-dimensional plane problem of forming a multiply ionized plasma by a high-power laser pulse ($q > 10^{12} w/cm^2$) striking the surface of a solid target consisting of heavy elements, and occupying a half-space $x \leq 0$ under conditions of nonequilibrium ionization. Analytic expressions are derived for the hydrodynamic parameters, electron temperature, and ionization level of the plasma as functions of time, beam flux density, and target properties. Under conditions of thermodynamic equilibrium, the ionization energy is the basic component of the intrinsic energy in the partially ionized plasma. This being the case, at large flux densities the presence of nonequilibrium conditions causes plasma behavior to resemble more closely that of an ideal gas, the pressure and internal energy of which are determined by electrons, and the inert properties, by its ions. This nonequilibrium implies also that the plasma produced by heating has a comparatively high temperature, a fact that can be used in those cases where it is desirable to raise plasma temperature. However, this implication holds only in those cases in which energy losses arising from radiation or thermal conductivity do not play an essential part.

51. Karasev, I. G., V. M. Kirillov, V. E. Norskiy, V. I. Samoylov, and P. I. Ulyakov. Kinetics of metal damage by a laser operating in a free-running mode. ZhTF, no. 9, 1970, 1954-1959.

The development of laser cratering in metals was studied experimentally with x-ray and high-speed photography, the latter also being used to study the dispersion of ejecta outside the crater. Laser wavelength was 1.06μ, focal length was 100 mm, and pulse duration was 2—2.5 msec at an average density of 10^7 w/cm^2 and pulse energy of 70—400 j. The x-ray system, which is explained in a diagram and in the text, made it possible to obtain three shadowgraphs within a crater at any moment of beam—target interaction without interfering with the processes taking place. The metals studied were aluminum, copper, molybdenum, tin, nickel, zinc, iron, and hardened 30KhGSA steel. The basic experimental results showed the following: (1) variation in crater depth L(t) was qualitatively the same for all metals; (2) the initial rates of intensive crater-depth development were considerably higher than the mean rates with respect to light flux reduction at the bottom of the pit; (3) in all metals intense cratering began not at the beginning of irradiation but after a certain delay that diminished with an increase in flux density; (4) crater formation ceased before the end of the laser pulse. An increase in mean flux density $\overline{q}$ did not always produce an increase in L(t): beyond a limiting $\overline{q}$ value, increased density did not increase pit depth; (5) crater diameter during the pulse increased at all sections, this growth diminishing toward the end of irradiation. For the heavy metals the angle of ejecta dispersion decreased at the same time. The results of high-speed photography for various periods in the ejection process are presented in a table that gives, for each metal, the $\overline{q}$ value, frontal and lateral flare velocity, and shock wave velocity.

52. Kirillov, V. M., and P. I. Ulyakov. Ratio of the liquid and gas phases in metals irradiated by a focused laser. FiKhOM, no. 1, 1971, 8-12.

Two experimental methods were employed in laser irradiation of metals to determine approximately the postpulse phase ratios of vapors and melts and their variation in the course of the damage process. Pulses with 100—140 j and a duration of $\sim 10^{-3}$ sec were focused on a metal surface ($S \approx 4 \cdot 10^{-3}$ cm^2), producing deep cratering. Fusion products were expelled beyond the radiation zone. Crater depth and ejecta phase composition at various radiation energies were investigated for tin, copper, iron, and aluminum. The first method cited utilized the energy balance of the breakdown process to derive numerical values

for metallic vapors from breakdown energy losses, determined by means described previously by the authors. The range of error was estimated to be 15 – 35%, depending on the metal. The other method measured ejecta impulse magnitudes by means of ballistic pendula; the measurement error range was 15 – 20%. Results with the two methods varied over a range of 50%, which is considered good agreement. Gaseous ejecta composed approximately an order of magnitude less material than those of the melt. The experimental data were used to plot the ratio of the gas component over the duration of the pulse. These curves were confirmed experimentally by irradiating a rotating target: the vapor phase could be discriminated because the vapor dispersion velocity was much greater than the velocity of the liquid phase.

53. Alekseyevskiy, N. Ye., V. M. Zakhosarenko, and V. I. Tsebro. Superconductivity in Au–Ge films obtained by vaporization with a laser pulse. ZhETF PvR, v. 12, 1970, 228-231.

A paper by Luo, Merriam, and Hamilton in 1964 showed that rapid cooling of Au–Ge alloys with a Ge content of 30 – 66% was accompanied by superconductivity, the critical temperature varying from 1 to 1.63° K. In the present paper measurements are reported that were made in films obtained from a 1:1 Au–Ge alloy condensed from alloy vaporization products of a pulsed Nd laser onto a substrate at liquid nitrogen or helium temperatures. The alloy was produced in a high-frequency furnace in quartz ampule in a helium atmosphere. This alloy in liquid helium displayed no superconductivity down to 1.4°K. Films were obtained by two methods that are described in detail. Films produced by either method exhibited a transition to superconductivity at 2.7°K; a sharp drop in voltage with temperature began at 2.75° K and ended at 2.25° K. After the helium vaporized and the film reached room temperature, the transition to superconductivity occurred at a temperature close to that reported in the cited 1964 study. The experimental data show that in laser vaporization onto a supercooled substrate a modification is established in the Au–Ge system which, after heating, is converted to the modification produced by Luo et al. The new modification can perhaps be explained by the fact that the condensation rate during laser vaporization was much greater than in the 1964 study.

54. Anisimov, S. I. Effect of ultrashort laser pulses on absorptive substances. ZhETF, v. 58, no. 1, 1970, 337-340.

An analysis is given of the dynamics of material evaporation by laser pulses on the order of a picosecond, and significant differences are pointed out between these results and those obtained with the usual longer duration pulses. The specific differences occur in the mechanisms of condensed matter evaporation and in the kinetics of expansion of the resulting plasma. The author assumes a laser pulse duration well below the characteristic time for hydrodynamic motion, τ_0, thus mass motion during the pulse interval may be neglected and the hydrodynamic and optical portions of the problem can be treated separately. The analysis shows that determination of specific vaporization energy and of vaporized mass can be obtained from knowledge of shock wave parameters in the target material. It is found that for sufficiently short pulses, the evaporated mass M is related to absorbed energy Q by $M \sim Q^{1-\alpha}$ where $\alpha < 1/6$. This is contrasted with the normally longer applied pulse, in which case the specific energy of evaporation rises rapidly with increased Q.

55. Askar'yan, G. A., and N. M. Tarasova. Initial stage of the optical explosion of a particle of matter in a powerful light beam. ZhETF, v. 60, no. 2, 1971, 617-620.

This theoretical paper is concerned with the very early stages of plasma generation from powerful laser impact on a solid, i.e. the period during which the size of the exploded volume of matter has not yet exceeded the dimensions of the incident laser beam. For their analysis the authors assume a simplified physical model in which total energy absorption occurs in the initially dense plasma, which is justified on the basis of known strongly nonlinear absorptive behavior to very powerful ultrashort laser pulses. In view of the resultant high electron thermal conductivity and small initial plasma dimensions, one may also safely assume an even temperature distribution throughout the plasma at this stage; furthermore, the short time interval involved permits the assumption of no radiant heat loss from the plasma. With these qualifications the authors use energy balance methods to arrive at a characteristic initial expansion velocity v_0 which depends only on incident flux density and initial material density.

For example, for a laser power of 10^{12} W and a focused spot diameter of 10^{-2} cm, flux density is 10^{23} erg/cm^{2}x sec and $v_0 = 10^8$ cm/sec, corresponding to a divergence energy on the order of 10 kev. It follows that in this interval the thermal energy is far greater than the kinetic energy of dispersion. Askar'yan also arrives at an interesting conclusion, namely that during a subsequent interval the plasma radius and velocity increase at an exponential rate, which is untypical of exothermic gas dynamics. From these analytical results, Askar'yan concludes that the described initial interval is the most significant in plasma development from laser pulses on the order of a picosecond; in fact, he characterizes the later stages of plasma expansion in such cases as trivial.

56. Batanov, V. A., F. V. Bunkin, A. M. Prokhorov, and V. B. Fedorov. Motionless shock wave generated by stationary vaporization of metal by laser irradiation. ZhETF, PvR, v. 11, 1970, 113-118.

The dynamics of metal vapor dispersion were studied by high-speed photography with a long laser pulse duration in comparison with typical vapor movement time, i.e., the vapor is assumed quasistationary. Attention was first directed to the motionless (relative to the target) shock wave, at whose front occurred the transition from ultrasonic to subsonic vapor flow. The experiments used bismuth as a target in a helium atmosphere. Laser parameters were typical for such experiments. The shock wave was spherical with a transparent surface, only the contour being visible; the growth and motionless part of the wave are illustrated. Conditions under which a jet develops behind the wave are described, its characteristics are noted, and its velocities before and behind the front are computed. It is shown that $v_1/v_2 > 3.7$, i.e., the shock wave is powerful. This ratio is used to derive an equation for the relationship between shock wave dimension R and helium pressure. In experimental confirmation of this equation, R was observed to increase with an increase in the diameter of the irradiated spot, as predicted by the equation. The same gas dynamic behavior was observed in experiments with aluminum, and is predicted for other metals. Determination of motionless shock wave characteristics makes it possible to find values for particle density and the temperature behind the wave front and thereby to explain the phenomena associated with laser absorption in metal vapors, including plasma flares. Finally, the results can be used to determine the initial conditions of movement on the target surface.

57. Bonch-Bruyevich, A. M., Ya. A. Imas, M. P. Libenson, and B. N. Spiridonov. Damage threshold in thin laser-irradiated metal layers. ZhTF, no. 3, 1970, 658-659.

In a previous paper by Libenson the thermal model of laser--metal interaction, when applied to thin layers, including films, showed that the rates of heating and vaporization are functions of the relationship between the specific internal heat of the layer and the heated area of the substrate.

In the present paper the boiling point is taken to be the damage threshold for a thin metal layer in air. At this temperature thin films are completely destroyed, while thick mirror layers suffer irreversible loss of reflective properties. An approximate calculation of optical flux threshold density q_* is made by extrapolating a temperature-time function to the temperature range $T_{melt}-T_{boil}$. This extrapolation, which is based on the fact that while absorptive capacity exhibits stepwise growth during metal fusion, additional heat losses occur at the same time in the phase transition during melting, indicates that with an increase in pulse duration the threshold of layer damage drops in proportion to $\tau^{1/2}$. This relationship is plotted for the case of aluminum. It is noted that the greatest q_* values depend on the heat conductivity of the substrate and the initial absorptive capacity of the layer. Layer strength improvements are therefore to be sought in the conditions of heat exchange to the substrate. Tests with a 100μ silver layer deposited on polished glass showed the damage threshold for a laser in the free-running mode to be ∿ 4 kj/cm^2 (sic). A reflector of this type is reported in operation for two years without breakdown, as the opaque mirror of a laser resonator operated in both free-running and Q-switched modes.

58. Kulyapin, V. M. Problems of thermal conductivity in phase transitions. Inzhenerno-fizicheskiy zhurnal, no. 3, 1971, 497-504.

An approximate method is developed for solving heat transfer problems in the two-boundary case shown in Figure 1. The model assumes an intense

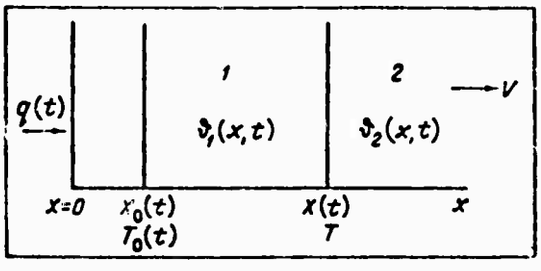

Fig. 1 Model for phase transition problem.

incident flux in the range of $10^7 - 10^{14}$ w/m^2, such as from a focused laser beam, electron beam, etc. Expressions are derived for determining motion of the transition boundaries and for surface temperature variation with time. A comparison of some approximate solutions with experimental data is shown in Tables 1 and 2.

Material	q , w/cm^2	Pulse width, sec	x, mm	
			meas	calc
Duralumin	1.5×10^{10}	3×10^{-7}	2	1.67
Iron	4.2×10^{10}	1.2×10^{-7}	0.7	0.85
Iron	2.3×10^{6}	1.5×10^{-3}	0.6	0.6

Table 1 - Calculated vs. measured values for depth of fused region, x.

Material	t x 10^{-3}, sec	S, cm^2	q_o, w/cm^2	T_o, °K	
				meas	calc
U-8 steel	1.5	10^{-2}	2.4×10^{7}	6400	5400
Kh VG	0.5	3×10^{-4}	2.3×10^{8}	9600	7500
Armco iron	1.5	6×10^{-3}	2.3×10^{6}	4500	4260

Table 2 - Calculated vs. measured values of surface temperature T_o.

59. Lugovskoy, V. B. Calculating surface temperature of a metal target heated by a free-running laser beam. Izv AN UzbSSR, Seriya fiziko-mate maticheskikh nauk, no. 5, 1970, 51-54.

Problems of heat transfer in laser beam-target interactions can in limited cases be solved by standard thermodynamic theory; in the case of a free-running laser, however, complex time variations in power and energy density make the classic approach tedious. Lugovskoy suggests instead an approximate method for computing heat transfer in the target surface region for the free-running laser case. This method arrives at transfer conditions for one pulse and extra-

polates these results by a smoothing operation, over the duration of the applied pulses. Experience has shown that integral heating computed in this manner is reasonably accurate for individual pulse periods on the order of $10^{-5} - 10^{-4}$ sec.

60. Savos'ko, G. Ye. Planar one-dimensional vapor motion for the case of energy absorption in the outer layer of the evaporative material and for beamed energy transfer to a sublimating surface. PMTF, no. 1, 1971, 153-155.

Expressions for vapor motion are derived for the idealized case of intense beamed energy absorption in a cold, motionless absolute black body, resulting in both vaporization and sublimation of the target material. Using a generalized set of integral equations, the author calculates dimensionless parameters of the evaporated material for the assumed case of an iron target. The results show that an intense energy input to the evaporated surface layer is accompanied by appreciable heating of the adjacent surface with resultant sublimation; the sublimating surface in this case will be strongly shielded by the vaporized mass. The secondary beam energy transfer from the vapor region to the sublimating surface is pointed out as one qualitative difference in the analysis of a similar model given earlier by Afanas'yev et al (PMM, no. 6, 1966; ZhETF, v. 52, no. 4, 1967) and Krol' (PMTF, no. 4, 1968).

61. Volosevich, P. P., and Ye. I. Levanov. Effect of thermal conductivity on propagation of laser-generated absorption waves. DAN, v. 194, no. 1, 1970, 49-52.

This paper is a quantitative treatment of the same pressure and absorption "burst" phenomena already described in the article by Vilenskaya and Nemchinov herein (PMTF, no 6, 1969, 3-19), and essentially repeats their analysis. Volosevich extends the problem to a second general case for reduced beam intensities (on the order of $q_o = 10^8$ w/cm^2 or less), in which case a shock wave is not formed in the plasma, and the expansion process is appreciably slowed down. For this "temperature wave" condition the plasma remains quasi-stationary for a relatively long time, which can be an advantage in terms of the shielding it provides for the underlying target surface. Two general cases must therefore be considered, depending on the level of incident flux and temperatures in the burst region, i.e. either a detonation wave or a temperature wave will determine the absorptive behavior of the plasma.

VIII. DEFORMATION

62. Dudukalenko, V. V., and M. B. Romalis. Propagation of shear cracks in residual stress fields. PMTF, no. 3, 1970, 117-119.

A brief theoretical treatment is given to the problem of longitudinal shear crack propagation in a medium subjected to an arbitrary field of internal stresses. From general expressions for stress parameters the authors develop local criteria for crack propagation under cyclic loading conditions, and indicate the applicability of these criteria to fatigue phenomena. The model used assumes propagation in an unbounded x-y plane having an existing internal stress pattern; in this case the latter can be described in terms of helical dislocations whose axes are normal to the x-y plane. Graphical solutions are given, including one defining fatigue limitations.

63. Finkel', V. M., I. S. Guz', I. A. Kutkin, and A. Ya. Volodarskiy. Generation of Rayleigh waves during the development of cracks. FTT, no. 8, 1970, 2300-2305.

Destructive stress tests on plexiglass are described in which Rayleigh waves were observed at the boundaries of cracks propagating on the specimen surface. The wave recording equipment and procedure are described. Spectral analysis of the wave oscillograms, using an M-20 computer, showed that for the tested plexiglass specimens the Rayleigh pulse spectra lay in the 0 to 200 KHz range. An evaluation of spectral energy distribution showed maximum energy concentration in frequencies up to 100 KHz. The analysis also correlates the destructive conditions with Rayleigh wave parameters. Typical oscillograms of Rayleigh waves are included.

64. Gol'dshteyn, R. V., I. N. Ryskov, and R. L. Salganik. Centered transverse crack in an elastic strip. Mekhanika tverdogo tela, no. 4, 1969, 97-104.

An analysis is presented for propagation of a transverse crack in an

elastic material, as indicated in Figure 1. An infinitely long strip of width

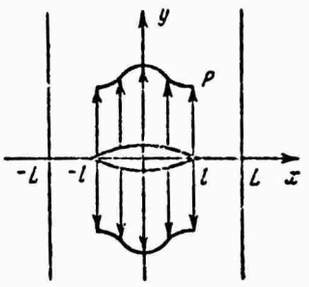

Fig. 1 - Transverse crack propagation model.

2 L is assumed with an initial centered crack of width 2 l. Uniform and symmetrical loading p(x) is applied in the y-direction, as shown. The object was to obtain expressions defining stress concentrations in the vicinity of the crack terminations, for both uniform and concentrated application of p(x). Previous approximate solutions by several other authors are reviewed and criticized. The authors conclude that the problem is best attacked by a method using the Fredholm equation of the second kind, which will provide solutions for any arbitrary kind of applied stress distribution; the analysis given, however, is limited to the symmetrical loading case cited above.

65. Ivanov, A. G., V. A. Sinitsyn, and S. A. Novikov. Scalar effects on dynamic damage to structures. DAN, v. 194, no. 2, 1970, 316-317.

Theoretical and experimental studies are described to determine the effect of scale factors on damage to structures, particularly for the case of explosive stressing. Tests were run on type 22K steel vessels with centrally-located explosive charges; vessel radii R were 5, 15, and 75 cm, with corresponding wall thicknesses of 0.214 R in each case. The limits of the destructive range, i.e., crack formation thresholds, are shown in Figure 1 for theoretical and experimental values. The ordinate $\xi = m/M$, the ratio of charge weight to vessel weight. The results demonstrate the strong dependance of damage behavior on scale factors.

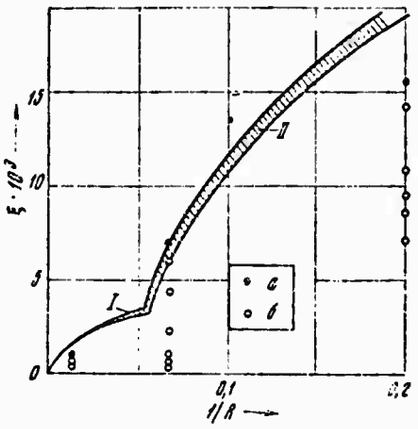

Fig. 1 - Damage threshold to 22 K steel vessels. a - destruction; b - no destruction; I, II - theoretical damage in elastic and plastic ranges.

66. Kamins'kyy, A. O. Kinetics of crack development in viscous-elastic materials. AN UkrSSR. Dopovidi. Seriya A. Fizyko-tekhnichni ta matematychni nauky, no. 9, 1968, 856-860.

An equation describing the steady advancement of the crack ends in a viscoelastic solid is derived, and analytical formulas for determining the propagation of crack points in an infinite viscoelastic strip are discussed as an example. The plane state of stress in a viscoelastic solid weakened by a macroscopic crack is examined in a quasistatic formulation, considering the crack propagation under a constant loading associated with the creep phenomenon. The stress and strain distribution in the viscoelastic solid can be obtained (according to Volterra's principle) from a corresponding elastic solution by replacing the elastic constants in it by time operators; this principle is true also for an increase of the crack's length in a certain time interval, and is used here. The cohesion forces are accounted for by using the surface energy approach, because the effective surface energy is practically independent of the rate of the steady crack point propagation, and does not vary during the whole process of the crack development. An expression for a time related function (depending on the type of crack and load, and on the solid's geometry) which determines the size of an advancing equilibrium crack of length in a viscoelastic medium under constant load, is derived. A sample examination of the development of a crack across infinite strips (of Maxwell and of Kelvin materials) of width 2 L subjected to longitudinal tension is presented, and formulas for determining the instances at which the crack point propagation becomes unsteady (accelerated), and when the crack reaches the critical length, which leads to the fracture of the strip, are given.

67. Kiyalbayev, D. A., and A. I. Chudnovskiy. Destruction in deformed bodies. PMTF, no. 3, 1970, 105-110.

Studies of damage in solids now conclusively have shown that the damage process begins almost instantaneously with load application. The initial stage in this process has a quasisequilibrium character, which permits it to be described in terms of an irreversible thermodynamic process. From a molecular point of view, the damage process develops from structural irregularities, i.e. destruction of the initial order begins, depending on interaction of forces among system elements, as a function of entropy change within the system. This may be arrived at also through the approach suggested by Born for the analogous case of flow and damage. In the present article the authors formulate the conditions for local damage, and give a phenomenological description of the damage process which takes into account the contributing physical and chemical parameters. Specific examples of viscous damage are included, and theoretical and experimental data are compared.

68. Kudryavtsev, P. I. On the stress required for propagation of fatigue cracks. Zavodskaya laboratoriya, no. 11, 1970, 1374-1379.

This is a broad review of the author's and other previous papers on the subject of fatigue crack propagation. Factors of stress concentration, stress cycling rates and material properties are analyzed as functions of crack propagation characteristics. Graphical examples are given showing fatigue crack formation as a function of bending and tension/compression cyclic loading. It is shown that regardless of existing residual stress conditions, fatigue cracks will not begin to appear until the applied stress at the specimen surface reaches some critical value. The treatment is developed in detail for the general cases of smooth surfaces and for notched surfaces, where fatigue cracking is assumed to commence from stress concentrations at the notch.

69. Lepik, Yu. R Propagation of plane plastic waves in a thick plate. PMTF, no. 1, 1971, 100-106.

A theoretical study is described of the propagation and interaction of high-amplitude plane waves in a thick plate, whose free surface is subjected to a monotonically increasing compression load. The case is considered for appreciable plastic deformation; effects of temperature and deformation rate on the mechanical parameters of the medium are neglected. The problem is formulated and solved by means of Lagrange variables. An approximate method

is included for reproducing the structure of the shock wavefronts. The pressure and velocity of a particle at a given location and time are determined by the method of characteristics. A numerical example is given illustrating the proposed approach.

70. Morozov, Ye. M. Relations between energy criteria for destruction and mathematical modeling of deformation phenomena at crack terminations. Prikladnaya matematika i mekhanika, no. 4, 1970, 768-776.

This paper is an extensive critique of recently published work on the theory of crack propagation in plastic and brittle solids. The author cites at length an article by Rayzer (Uspekhi fizicheskii nauk, v. 100, no. 2, 1970) which itself summarizes the state-of-the-art in crack propagation theory, and in the process refutes some work of a number of authors in the field, notably that of G. R. Irwin. Morozov defends Irwin against Rayzer's criticism at length, and concludes in effect that Rayzer is less knowledgeable on the subject than many of those criticized by him.

71. Mikhaylov, A. M. Propagation of shear cracks in LiF single crystals. PMTF, no. 4, 1970, 119-122.

Experimental data from shear crack propagation in LiF single crystals is reviewed and compared to theoretical values for crack formation in quasi-brittle materials. Tests were performed on square rod specimens 4 x 4 x 50 mm^3 in size, with cracks induced in a cleavage plane by forcing a split end apart, as shown in Figure 1. Propagation was forced at constant velocities of 195,

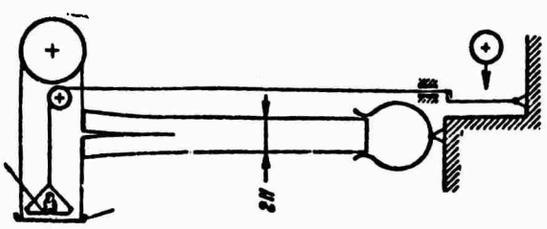

Fig. 1 - Shear crack propagation in LiF.

550 and 2000 mm/sec, and also at an accelerated rate by using gravity force for the cleavage, as indicated in the figure. High speed photos of the crack

frontal point were taken, a sample of which is included. The results confirm a basic proposition in quasibrittle destruction theory, namely that constant energy is expended in crack propagation for the case when the newly exposed area is of constant dimensions.

72. Popov, K. V., and A. P. Kazantsev. On the conditional critical temperature for a given probability of crack generation and propagation for the brittle damage case. FiKhOM, no. 1, 1971, 71-74.

It has been established that for steel in the transition temperature range to the brittle state, crack formation is inhibited by plastic flow. From this it is shown that the probability of crack formation P_x in the brittle state is given by

$$P_x = \exp\left\{-t_1 \nu_1 \exp\left(-\frac{U_1}{kT}\right)\right\}$$

where t_1 is stress application time during crack formation, ν_1 is a frequency multiplier, U_1 is activation energy for plastic flow, T is temperature, and k is Boltzmann's constant. It is emphasized that the subsequent propagation characteristics of the crack depend on the thermal conditions during load application. Thus if plastic relaxation occurs at the crack terminus during stress, then propagation will be viscous, with high energy absorption. If plastic relaxation does not take place, however, propagation proceeds as in the brittle case. In this event the probability for further crack propagation has the same form as the above equation. Graphical data are given relating these factors for type 45 steel.

73. Solov'yev, V. A. Dynamic theory of crack formation in crystal. FTT, no. 9, 1970, 2725-2728.

The theory of crack propagation based on combining of dislocations is analyzed. This postulates a confluence of a dislocation system in the slip plane into one overall dislocation. The probability of this combination is a function of the attractive and repelling forces among dislocations and the mean separation distance between dislocations. The combining action may commence whenever the mean separation distance x approaches a critical value x_o, as for example by applying shear loads in the slip plane. Since a dislocation has mass, it can be accelerated in a stress field to rapidly approach the critical x_o, leading to crack formation. The author analyzes the problem on the foregoing basis, assuming the general case of rapid dislocation movement.

IX. RADIATION DAMAGE

74. Zubov, V. V., V. F. Khokhryakov, and Yu. F. Tuturov. The dielectric properties of polymer materials during pulsed gamma-neutron irradiation. Vy okomolekulyarnyye soyedineniya. Seriya B. Kratkiye soobshcheniya, v. 11, no. 5, 1969, 324-325.

The dielectric properties of polyethlene, poly (tetrafluoroethylene) (oriented and nonoriented), polystyrene and poly (Me methacrylate) were measured in a field of pulsed gamma-neutron irradiation. The measurements indicated that the dielectric loss and dielectric permeability were proportional to irradiation intensity (I). Plots of conductivity vs I confirmed that the dielectric properties of insulators measured during irradiation were dependent on their structure.

75. Muinov, T. M., and A. M. Mavlyanov. Determination of activation energy of thermal decomposition of gamma-irradiated polystyrene. DAN TadzhSSR, v. 13, no. 11, 1970, 13-16.

In a continuing study of the thermal decomposition of irradiated polystyrene (PS), the kinetics of the process were determined by mass spectrometry in both original PS and PS irradiated with a 2×10^8 r dose of gamma-radiation from a Co^{60} source. The stepwise increase in the decomposition rate of the irradiated PS with a similar increase in temperature indicated that a breaking of chemical bonds occurs with liberation of a volatile monomer product. The plots of the calculated activation energy E of the process versus relative weight loss $\Delta W/W$ of both original and irradiated PS indicated a two-phase process. In the first phase, corresponding to a 36 kcal/mole E level, breaking of the weak bonds occurs. The extent of the first phase of thermal decomposition of the irradiated PS was increased to 27—30% in comparison to 8—10% in the original PS. This fact indicated an irradiation promoted increase by a factor of 2.5 to 3 in the quantity of the weak bonds. In the second phase, corresponding to 46 kcal/mole, thermal decomposition proceeds through breaking of stronger bonds of a certain type.

76. Zimakov, I. Ye., V. P. Pletnev, A. M. Chernyshov, N. P. Zhuravlev, V. A. Yanchin, and V. I. Spitsyn. The effect of neutron-irradiation on the characteristics of the hydrogen electrode of a low-temperature fuel cell. Kinetika i kataliz, v. 11, no. 6, 1970, 1583-1584.

A number of hydrogen electrodes with Raney nickel-base catalysts were irradiated with a 2.4×10^{13} neutrons/sq cm x sec flux for 360 and 720 hours. Irradiated and non-irradiated electrodes from the same batch were tested in a hydrogen-oxygen cell with 7 N KOH electrolyte at 90°C and $P_{H2} = 0.6$ atm. The current voltage characteristics show that the initial polarization of the radioactive (Ni^{68}) electrodes was lower than that of the controls. The decrease in polarization was a direct function of irradiation time. Polarization under a 100 mamp/sq cm load increased with time. The potentials of the electrodes irradiated for 360 hrs and 720 hrs were practically equal to the potentials of the controls after 200 and 300 hrs of testing, respectively, under 100 mamp/sq cm load. Thus, initially the hydrogen electrodes are activated by neutrons and their current voltage characteristics are improved, but the improvement does not last under load. The increase in electrochemical activity was tentatively attributed to the formation of structure defects in the crystal lattice of the irradiated catalyst.

X. STATIC HIGH PRESSURE RESEARCH OF SOLIDS

77. Stishov, S. M., V. A. Ivanov, and I. N. Makarenko. Compressibility of sodium at high pressures and temperatures and the Lindemann fusion condition. Zhurnal eksperimental'noy i teoreticheskoy fiziki, v. 60, no. 2, 1971, 665-668.

The volume and compressibility of sodium as a function of pressure and temperature are for the first time measured directly on the fusion curve. The measurements were performed with a piston piezometer. The experimental technique is similar to the one described earlier (DAN SSSR, v. 188, no. 3, 1969, 562-566). The volume and compressibility errors are, respectively, on the order of 0.1% and 2%. Experimental compressibility and volume data are employed for calculating the Debye temperature of solid sodium along the fusion curve. It is shown that the Lindemann parameter, which characterizes the relative displacement of atoms from the equilibrium positions, does not remain constant along the fusion curve.

78. Kabalkina, S. S., M. O. Shcherbakov, and L. F. Vereshchagin. On the polymorphic transition in AgCl at high pressure. Doklady AN SSSR, v. 193, no. 5, 1970, 1015-1018.

High-pressure effects on the crystal structure of AgCl have been investigated by the X-ray diffraction method. A number of diffraction patterns in the pressure range 40 to 115 kbar were obtained. It is found that the diffraction pattern of the AgCl II high pressure phase basically coincides with the data of previous researchers. The AgCl II diffraction pattern data obtained are decoded on the basis of a rhombic cell with the parameters: $a = 6.90$ Å, $b = 5.08$ Å, $c = 4.05$ Å and on the basis of a hexagonal crystal structure ($a = 4.07$ Å, $c = 7.2$ Å). In order to establish the true structure, additional X-ray diffraction patterns for AgCl—NaCl in the pressure range 40–120 kbar were obtained (NaCl being used as an inner pressure standard). From the analysis of results, it is concluded that "rhombic" structure is closer to the experimental reality, although some discrepancies in the diffraction pattern lead to the conclusion that most likely the crystal structure of the AgCl II high pressure phase is a distorted variant of a rhombic structure of the HgO type.

79. Fateyeva, N. S., and L. F. Vereshchagin. Melting pressures of graphite up to 90 kbars. Pis'ma v zhurnal eksperimental'noy i teoreticheski fiziki, v. 13, no. 3, 1971, 157-159.

The investigation reported earlier (DAN SSSR, v. 152, no. 1, 1963; 88, no. 2, 317 and ZhETF, v. 55, no. 4, 1968, 1145) of the graphite melting curve by the optical technique is extended up to 90 kbar. The special chamber employed for this purpose is described in PTE, 1970, no. 3, 222 (see next entry). The melting temperature of a sample was measured by the intensity ratio of two spectral lines $f(T)=I_1(\lambda_1)/I_2(\lambda_2)$. In order to increase the reliability of a measurement, each temperature was measured by two independent intensity ratios: $I_1/I_2=f_1(T)$ and $I_2/I_3=f_2(T)$ with $\lambda_1=420$ mμ, $\lambda_2=622$ mμ, and $\lambda_3=825$ mμ Measurement results are shown in the figure below by a solid line; the dash line represents F. P. Bundy (J. Chem. Phys., 38, 3, 618, 1963) data and the dotted line represents the diamond-graphite equilibrium curve. The melting curve has a temperature maximum of 4900°K at a pressure about 60 kbar.

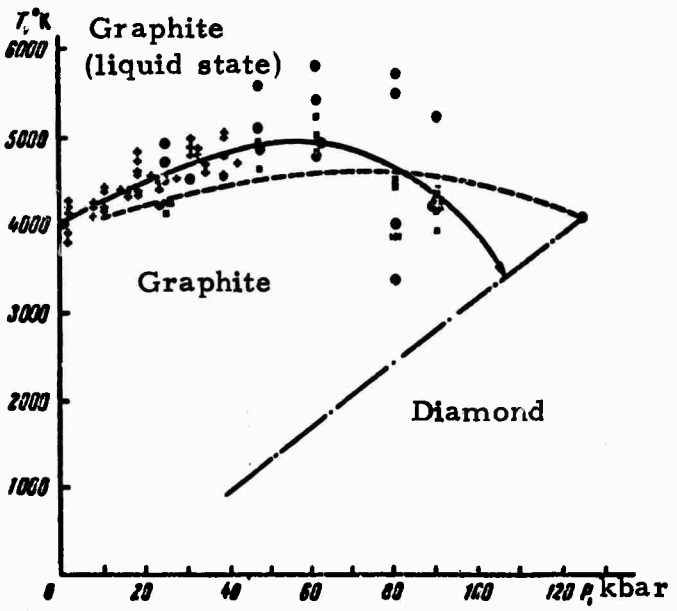

80. Fateyeva, N. S., and L. F. Vereshchagin. A 100 kbar pressure chamber for optical research. Pribory i tekhnika eksperimenta, 1970, no. 3, 222-224.

A steel pressure chamber, shown schematically in the figure below, has been developed for high-pressure research. In the figure, 1 is a gasket, 2 are conical pistons with cylindrical ends 3, entering into the cylindrical portion of bushing 4 in chamber 6. Between the cylindrical portion of piston 3 and the cylindrical opening of bushing 4 (5.0 mm dia) is a 0.5 mm gap, which at higher pressures is filled by the NaCl, the pressure transmitting medium 5. The chamber is equipped with cylindrical windows, extending towards the sides, filled with crystal NaCl. It withstands pressures up to 100 kbar and repeats the accuracy of results (at maximum pressure) within ±6%.

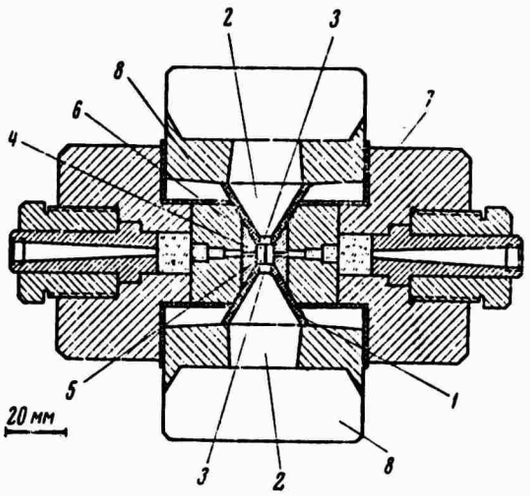

81. L. F. Vereshchagin, Ye. V. Zubova, K. P. Burdina, and G. L. Aparnikov. Behavior of oxides under the combined effect of high pressure and shear stresses. Doklady AN SSSR, v. 196, no. 4, 1971, 817-818.

Behavior of the oxides Al_2O_3, B_2O_3, B_6O, CdO, CoO, CrO_3, Cr_2O_3, CuO, Cu_2O, Dy_2O_3, HgO, In_2O_3, Ga_2O_3, Gd_2O_3, La_2O_3, MgO, Nb_2O_5, NiO, PbO, Sc_2O_3, SiO_2, Sm_2O_3, Ta_2O_5, TiO_2, V_2O_4, V_2O_5, WO_3, UO_3, and Y_2O_3 under pressures on the order of 500,000 kg/cm^2, with simultaneous application of shear stresses, is investigated. High pressures and shear stresses were generated by equipment of the Bridgman anvil type described in detail elsewhere (PTE, 1960, no. 5). Disintegration reactions reported earlier (P. W. Bridgman, Proc. Am. Acad. Arts and Sci., 71, no. 9, (1937)

and Ye. V. Zubova, Dissertation, Mosk. University, 1962) are confirmed, and new similar reactions are observed. It is concluded that the tendency for oxides to disintegrate under the combined effect of shear stresses and high pressure is common and it is limited only by the energy factors. A possible connection is noted between these experiments and creation of native metals in the earth crust where such conditions may exist.

82. Kolobyanina, T. N., S. S. Kabalkina, L. F. Vereshchagin, A. Ya. Michkov, and M. F. Kachan. Polymorphic transitions in the antimony-bismuth system at high pressure. Zhurnal eksperimental'noy i teoreticheskoy fiziki, v. 59, no. 10, 1970, 1146-1155.

Crystal structures and approximate existence boundaries of high pressure phases of the Sb—Bi system are experimentally studied. Investigations were conducted at room temperature employing experimental equipment and technique described earlier (T. N. Kolobyanina et al., ZhETF, v. 55, 1968, 164). A system of Sb_xBi_{1-x} alloys with x varying in steps of 0.1 from 0 to 1 was prepared for this investigation. The samples were mixed with NaCl for the pressure determination. The boundaries of coexistence of phases, I, II, II', and III are determined by two methods: X-ray diffraction and electric resistance measurements. It is established that various phases correspond to the following crystal structures: I — to As-type; II — a primitive cube; II' — monoclinal Bi II type and III — monoclinal Sb III type. Compressibilities of Sb, $Sb_{0.9}Bi_{0.1}$ and $Sb_{0.8}Bi_{0.2}$ are determined by X-ray diffraction measurements at pressures between 0 and 85 kbars. It is concluded that within the pressure range investigated, the Sb—Bi alloys behave as a single homogeneous substance in spite of structural difference at pressures above 25 kbars.

/

83. Kabalkina, S. S., T. N. Kolobyanina, and L. F. Vereshchagin. Investigating the crystalline structure of the high pressure phases of antimony and bismuth. Zhurnal eksperimental'noy i teoreticheskoy fiziki, v. 58, no. 2, 1970, 486-493.

Based on the similarity of the behavior of $A^{IV}B^{VI}$ compounds with group V elements at high and normal pressures, it is assumed that the high pressure phases of Sb III and Bi III will crystallize in a monoclinically distorted structural type. The periods of the elementary cell of Sb III at pressures (p) from 130—160 kbar are: a = 5.56; b = 4.04, c = 4.22 Å, $\beta = 86°$, Z = 4, V = 93.8 $Å^3$.

The periods of monoclinic Bi III at p = 35.5 kbar are: a = 6.05, b = 4.20, c = 4.65 Å, β = 85°21', Z = 4, V = 117.8 Å^3. Two symmetrically independent atoms Sb_1 and Sb_2 are located on planes m of the three-dimensional group C_2h^2 - $P2_1/m$. The assumed structure of Sb III (Bi III) is laminar, the layer consists of two covalently bonded slightly corrugated planes; the interatomic distances correspond to the coordination number seven.

84. Ivanov, V. A., I. N. Makarenko, and S. M. Stishov. Sodium melting at high pressures. Pis'ma v zhurnal eksperimental'noy i teoreticheskoy fiziki, v. 12, no. 1, 1970, 12-15.

The melting of sodium has been studied by the volumetric method at pressures up to 25 kg/cm^2[x 10^3]. Measurements of the sodium volume in the area of the melting curve were made with a piston piezometer similar to one described earlier (DAN SSSR, v. 188, no. 3, 1969, 564-566). The volume value data on solid and liquid sodium along the melting curve are tabulated and illustrated by curves. The nature of the minimum of the curve representing the inner energy ΔU dependence on temperature T is discussed. It is shown that minimum ΔU (T) may be explained as a result of the competition between the respective contributions from the energy changes of interparticle repulsion and attraction, which accompany melting and which depend on the difference in volumes of solid and liquid phases.

85. Voronov, F. F., and S. B. Grigor'yev. Sound velocity in cesium chloride and sodium chloride at pressures up to 100 kbar. Doklady AN SSSR, v. 195, no. 6, 1970, 1310-1312.

Investigations of the propagation velocity of ultrasonic waves in solids at pressures up to 100 kbar, initiated earlier (DAN, v. 182, 1968, 304), are being continued. The experimental setup permitting the use of samples 5—10 mm long and 15 mm in diameter, and the experiment technique is described in the paper cited above. Typical representations of ionic crystals-sodium chloride and cesium chloride are used as research subjects. Measured velocities of longitudinal (V_l) and transverse (V_t) ultrasonic waves in cesium chloride, as functions of pressure, are presented in Figure 1. Similar curves for sodium chloride are presented in Figure 2. The appearance of the curves and their mathematical expressions are discussed.

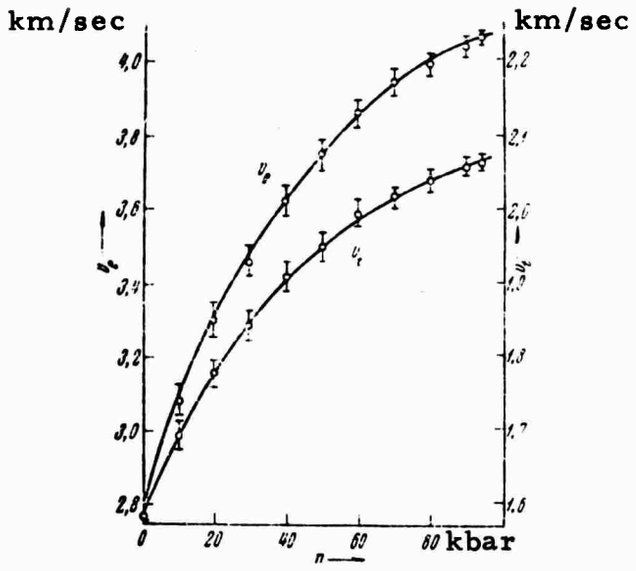

Fig. 1

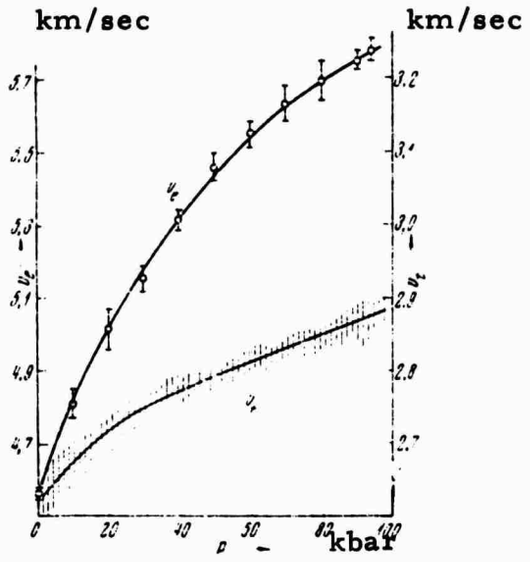

Fig. 2

86. Alekseyev, V. A., V. G. Ovcharenko, Yu. F. Ryzhkov, and A. P. Senchenkov. The equation of state for cesium in the pressure range 20 to 600 atmospheres and in the temperature range 500 to 2500° C. Pis'ma v zhurnal eksperimental'noy i teoreticheskoy fiziki, v. 12, no. 6, 1970, 306-309.

The method employing the γ counting of Cs^{134} (E= 0.606 Mev) has been used to determine the equation of state for cesium in the pressure range 20—600 atm and temperature range 500—2500° C. A measurement cell capable of recording pressure changes is described. The cesium point source was approximated by filling the free space in a measuring tube with a tungsten rod and leaving only a 1—2 mm gap for cesium between the rod and the tube bottom. A tungsten-rhenium thermocouple was employed for temperature measurements. Over 3000 experimental points were measured. The equation of state for cesium is presented as a family of curves and in a tabular form. Parameters of the cesium critical point are determined as follows: T_{cr} = 1760 + 20 °C; P_{cr} = 115 ± 5 atm; ρ_{cr} = 0.4 ± .02 g/cm^3.

87. Bartenev, G. M., I. V. Razumovskaya, and Ye. S. Savin. Theoretical and ultimate strength, and the law of corresponding states. Doklady AN SSSR, v. 192, no. 4, 1970, 775-778.

Concepts of theoretical and ultimate strengths are outlined, and their importance as a standard for future development of highly durable and superstrong materials is stressed. However, they may be of value only if the operating temperatures are taken into account. For this purpose, the temperature dependence of the maximum strength of a homogeneous high-strength structure is studied. The strength satisfies the same conditions of failure (considered as a peculiar sublimation) as the theoretical or ultimate strength at a temperature of $T > 0\,^{\circ}K$. The fluctuation mechanisms responsible for the orgin and development of defects are excluded by assuming that the experiment lasts for a very short time. Further, only the average statistical temperature effects related to the thermal expansion of a rigid body are included. It is shown that the temperature dependence of maximum strength may be expressed in terms of dimensionless arbitrary units, using the law of corresponding states.

XI. SOIL MECHANICS

88. Al'tshuler, L. V., A. V. Balabanov, V. A. Batalov, N. A. Gerashchenko, V. A. Rodionov, V. A. Svidinskiy, and D. M. Tarasov. Confined explosions in liquid and elasto-plastic media. DAN, no. 6, 1970, 1259-1262.

Results of experimental and mathematical studies of confined explosions in water, LnCl solution, moist clay, aluminum, hardened cement with sand mortar, and rock salt are presented. Numerical calculations of elasto-plastic flows were used in the interpretation of results. Experimental observations of the development of the cavity were made by means of pulse x-rays. Charges with a radius of 9 and 17.5 mm were placed in the center of cubic blocks 200 mm on an edge, or in containers with the same diameter. Charge dimensions, initial cavity dimensions, mean density of explosions and corresponding initial pressure are tabulated. The mathematical methods developed can describe with great accuracy a confined explosion in a liquid or elasto-plastic medium, and its effect on the cavity formation process.

89. Mikhalyuk, A. V., and G. I. Chernyy. Experimental study of plastic characteristics of compressed soils under dynamic loading. PMTF, no. 3, 1970, 131-133.

Experimental results are presented graphically of plasticity tests run on a variety of soils under shock compression loading. Soils tested included several types of clay, loam and loess. Specimens were placed in cylinders and compacted to selected degrees by a piston which had an elastic face plate to control load application time. Graphs are given for shear loading as a function of pressure, based on data from strain gauges placed in the specimens. These tests show that increase in load application rate increases the shear load, indicating an increased resistance to load deformation; this was true for all measured soils. The plasticity parameters are thus seen to be functions both of physical soil conditions and of the time characteristic of the load applied to them.

90. Bykovskiy, Yu. A., V. A. Gridin, V. I. Dymovich, Z. I. Matveyeva, and V. N. Nevolin. The feasibility of studying the mass composition of multicomponent rock vaporized by a laser beam. Fizika tverdogo tela, v. 41, no. 2, 1971, 442-443.

A modified time-of-flight mass spectrometer with an Nd^{3+}-activated glass-laser ion source (pulse energy and length--1.5 j and 40 nsec, resp.) was used in an analysis of granite, porphyrite, argillite, and aleurolite. The results of the laser mass spectroscopic analysis were compared with results from spectral analysis and it was determined that the former is more effective in analyzing elements with low atomic weights. Rock with small grain sizes (10—50 μ) were used to determine the relative concentrations of Na, Mg, Al, and Ti. Relative measurement error was 20%, and it is concluded that, for laser-beam flux densities $\geq 10^{10}$ w/cm^2, fractional evaporation is not evident. The results show the laser mass spectrometer as a useful tool for the fast qualitative analysis of multicomponent rock.

91. Tsirul'nikov, A. S., I. A. Rizhenko, A. S. Galitsyn, and Ye. I. Merzlyakov. Method for determining thermophysical properties of rocks at high pressures and temperatures. AN UkrSSR. Dopovydy, no. 11, 1970, 1031-1033.

A solution is presented to the thermal conductivity equation under quasi-stationary thermal conditions, with boundary conditions of the third kind ($\alpha \neq \infty$) using a finite length cylindrical calorimeter. To determine thermophysical properties of rocks under given conditions, when α is known, it is necessary to determine temperature drop between specimen and medium for two points of the specimen. The coefficient α is determined by an experimentally found value $W(r_1, z_1)$ of the specimen-medium system. Iron may be taken as a standard because its thermophysical properties do not depend on the environmental pressure. A diagram is given of the device used in determining thermophysical properties of rocks at geostatic pressures of up to 2500 bars and temperatures up to 620°K.

92. Vovk, A. A., and I. A. Luchko. On the principle of similarity in explosions by cylindrical horizontal cratering charges. AN UkrSSR. Dopovydy. Seriya A. Fiziko-tekhnichny ta matematichny nauki, no. 11, 1970, 1038-1041.

For concentrated cratering charges, the principle of geometrical

similarity applies, according to which the sizes of craters grow in proportion to charge sizes for definite charge values, explosion action index and depth of charge burial. Based on the results obtained at the Institute for Geotechnical Mechanics, AN UkrSSR, by exploding horizontal cratering charges in clay soils at different depths and by using various kinds of explosives, the authors concluded that optimum intervals exist in the explosion action index values, and corresponding intervals of charge seat depths, for which the geometrical similarity principle is satisfied. Formulas for calculating cylindrical charges are presented.

93. Gundarev, K. O. Studying strength characteristics of cohesive soils in the charge explosion zone. AN UkrSSR. Dopovydy, no. 4, 1970, 355-357.

The results of experimental studies of changes in the resistance characteristics of argilloarenaceous soil and the shift in the charge explosion zone are presented. Results show that the specific cohesion of the cohesive soil materials changes ambiguously, i.e. in close proximity to the explosion, the specific cohesion increases relative to the initial cohesion, then decreases as it moves further away from the explosion zone.

94. Mikhalyuk, A. V., A. A. Vovk, I. A. Luchko, and V. A. Plaksiy. On the possibility of controlled change in parameters of explosive pulses in compressible soils. AN UkrSSR. Dopovydy, no. 11, 1970, 1039-1042.

Methods are considered for controlling the shape of an explosive pulse during charge explosions with axial and central symmetries in compressible soils. Changes under dynamic loads of soil mass during the detonation of charges with air pockets are analyzed, and dependencies of wave excitation distribution in detonation of such charges are established. Experimental data on the changes in shape of the charge and depth is presented. The authors conclude that the analyzed methods of controlled explosive excitation can provide increased efficiency for explosions in compressible soils.

XII. ELECTRON BEAMS

95. Zagorodnov, O. G., L. I. Bolotin, I. I. Magda, N. P. Gadetskiy, V. I. Belyayev, and Yu. V. Tkach. Generator of powerful pulsed electron beams. Pribory i tekhnika eksperimenta, 1970, no. 5, 100-102.

A generator producing 30 nsec long 12 ka current pulses at 400 kv is described. Its basic components are a dual shaping line employing distilled water as a dielectric and an electron gun with a multiple needle cathode. The dual shaping line is 500 mm long and consists of three concentric cylinders (100 mm, 150 mm and 214 mm in diameter). The full capacitance of the line was slightly over 10 nf and the leakage resistance was 200 ohms. The line was charged by a voltage pulse generator capable of delivering 350 kv pulses. It is connected to the electron gun by 12 RKP cables in parallel. The cathode of the electron gun contains 86 steel needles with the plane of their points 15 mm from the stainless steel disk-shaped anode. A shielded Rogowski loop around the anode supporting rod serves to measure the current pulses. Its inductance is 0.75 μh, load resistance is 1.68 ohms and the time constant-450 nsec. The entire electron gun assembly is placed into a container filled with transformer oil. Small capacitance of the dual shaping line permits storing up to 0.5 kj and delivering a load of about 10^9 watts. However, the high emission capacity of the cathode exhausts very rapidly and is practically nonexistent after 5—6 pulses.

96. Gridneva, G. N., V. I. Perevodchikov, G. G. Timofeyeva, and K. A. Yumatov. Plasma source of electrons. Pribory i tekhnika eksperimenta, 1969, no. 4, 27-30.

A plasma source of electrons producing a 1.5 a, 30 kv focused electron beam is described. Its design is shown in the figure below, where 1 is the focusing coil, 2 is the accelerating electrode, 3 and 4 are insulators, and 5 is the coil of the electromagnet. The plasma cathode is a modified duoplasmotron, i.e., it contains an incandescent (0.8 mm tungsten) cathode (6) an intermediate electrode, (7) with a 4 mm diameter aperture, and an anode (8) with an aperture of 0.8—1.5 mm. Gap distances are 4 mm between the intermediate electrode and the anode and 5 mm between the anode and the accelerating electrode. In the accelerating electrode, the aperture diameter is 8—12 mm. The working gas is

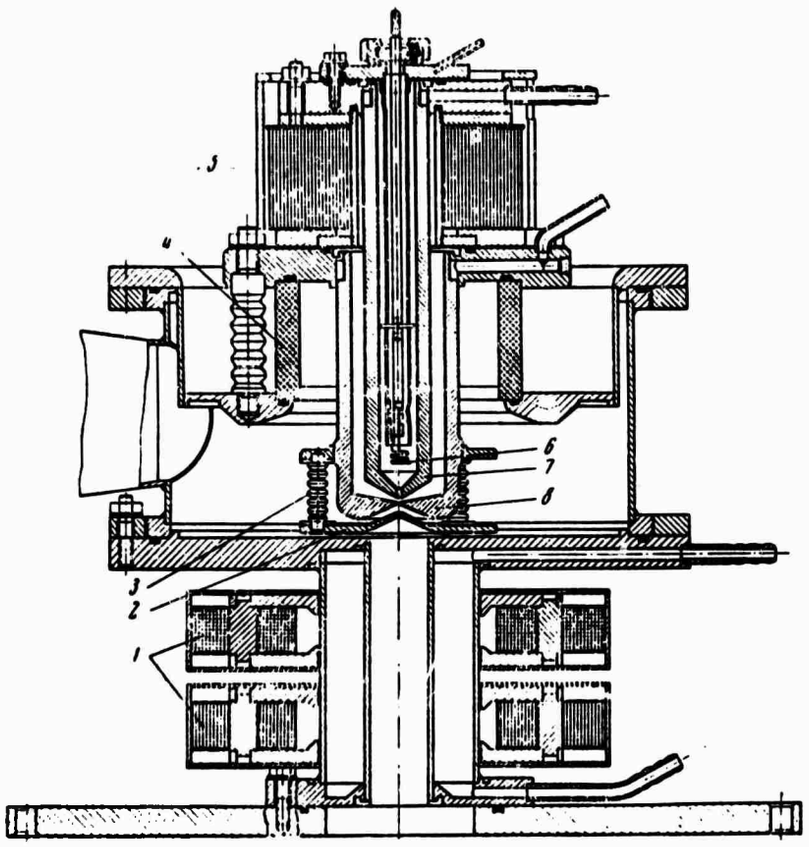

argon at a pressure of $6 \times 10^{-2} - 3 \times 10^{-1}$ torr. The accelerating voltage is up to 30 kv, with an electron current of 0.1 to 1.5 a.

97. Altyntsev, A. T., A. G. Yes'kov, O. A. Zolotovskiy, V. I. Koroteyev, R. Kh. Kurtmullayev, V. L. Masalov, and V. N. Semenov. Thermal explosion in a collisionless plasma under the effect of a relativistic electron beam. Pis'ma v zhurnal eksperimental'noy i teoreticheskoy fiziki, v. 13, no. 4, 1971, 197-201.

The interaction of a relativistic electron beam with plasma has been experimentally investigated. Hydrogen plasma ($n_o \sim 10^{11} - 10^{14}$ cm^{-3}) was generated inside a glass tube (20 cm dia, 300 cm long). The Rius-5 accelerator (developed by Ye. A. Abramyan, IYaF, SO, AN SSSR, and described in DAN SSSR, v. 192, 1970, 76) has been used to produce a 3—4 Mev electron beam (10—15 ka current, $\sim$50 nsec duration). Plasma heating during the beam passage was measured by external diamagnetic probes. The results obtained indicate strong mutual interaction of plasma and penetrating relativistic electrons. In particular, the collisionless plasma acquires, in respect to the relativistic

electron beam, abnormal dissipating properties with a typical scale of $10-10^{-2}$cm (while the classic coulomb mean free path at the experimental conditions is about 10^{13} cm). Thus the phenomenon has the nature of a thermal explosion ($T \sim 10-100$ kev) in a collisionless plasma, followed by secondary relaxation processes, i.e., electron thermal wave and rapid thermal equilization through the entire plasma volume.

98. Ledovskoy, V. P., and G. M. Mladenov. The influence of ionizing phenomena on the interaction of an electron beam with metals. Zhurnal tekhnicheskoy fiziki, v. 40, no. 10, 1970, 2260-2262.

The behavior of a stream of electrons penetrating into a metal is studied. The role of plasma formation in this process is explained, and it is shown that, with increasing power density in a focal point, the ionization of metal vapor leads to a decrease of the beam cross section area, i.e., to the focusing of the beam. The diameter of a plasma filled hollow channel in the liquid phase is an order of magnitude smaller than the beam initial diameter, for most materials.

XIII. HYPERSONIC FLOW PAST BODIES

99. Arutyunyan, G. M. Interaction of a shock wave with a wedge moving at hypersonic velocity. Izvestiya AN SSSR, Mekanika zhidkosti i gaza, 1969, no. 3, 171-177. (1)

100. Arutyunyan, G. M. Applicability limits for a certain precise solution of the problem of shock wave interaction with a wedge moving at hypersonic velocity. Izvestiya AN SSSR, Mekhanika zhidkosti i gaza, 1970, no. 6, 104-107. (2)

The side interaction of the plane shock wave with a wedge moving at hypersonic velocity is theoretically analyzed in (1). It is shown that for certain definite relations between the wedge half-angle (δ) and Mach number of the inflow (M), the problem has an exact analyticai solution. In particular, the solution is presented for the case when a plane shock wave of intensity equal to the attached shock wave is directed parallel to the side of a wedge moving at hypersonic velocity. The relation of δ and M, when the solution is possible, is presented in the figure below, indicating that δ increases with an increase in M and asymptotically approaches some value at a higher M, depending on the ratio of specific heats γ. In (2) the applicability limits of this solution are investigated. It is shown that, in a general case, three types of the existence regions for this solution can be realized, and their existence criteria are derived.

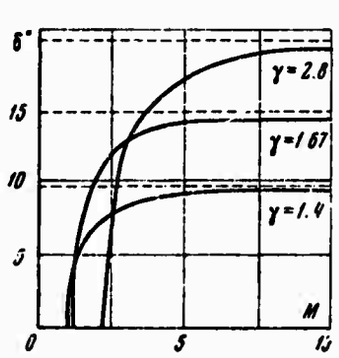

In (1), the counteraction of a plane shock wave with a moving wedge (assuming weakly interacting shocks) is also considered. It is shown that, within the limits of the linearized theory, the solution of this problem may be graphically shown in the M δ plane.

101. Vertushkin, V. K., and Ye. A. Romishevskiy. The role of radiation absorption in front of a shock wave during hypersonic flow around a blunt body. Izvestiya AN SSSR, Mekhanika zhidkosti i gaza, 1970, no. 6, 40-47.

Conditions are derived for the front of a shock wave with the absorption of advanced radiation taken into account. The role of pertinent dimensionless parameters is investigated, and estimates are made of their values for a number of actual cases for blunt bodies entering the dense layers of the Earth's atmosphere. The composition and parameters of the molecular nitrogen stream flowing into the shock wave are calculated, and conclusions are made in respect to general problem formulation for hypersonic flow about a blunt body with radiation taken into account.

For investigation of this case, it is necessary to know how the radiation emitted by the shock wave zone interacts with the cold stream of air flowing in. The importance of accounting for this interaction is indicated by results of observing spacecraft reentry into dense atmospheric layers and by presently available data on strong shock waves. This interaction is associated with the fact that absorption of intense short wave radiation of the shock layer in cold air leads to the photodissociation and photoionization of the air molecules, i.e., to an actual increase of its enthalpy. It is concluded that for the true description of hypersonic flow around blunt bodies which accounts for radiation, it is necessary to solve the combined problem, which considers mutual interaction of the leading radiation in front of the shock wave and gas flow in a shock layer.

102. Breyev, I. M., and Yu. P. Golovachev. Viscous gas flow in a shock layer in the presence of balanced chemical reactions. Zhurnal prikladnoy mekhaniki i tekhnicheskoy fiziki, no. 4, 1970, 150-153.

The authors theoretically consider stationary supersonic air flow around a sphere, with actual physico-chemical processes taken into account. They investigate the flow in a shock layer at the flight velocities of 3 km/sec : $V_\infty \leq 10$ km/sec ($10^4 \leq R_\infty \leq 10^6$), assuming local thermodynamic equilibrium. The flow is described by simplified Navier-Stokes equations, which are solved by the finite-difference method. The case of a cooled body surface is considered and the distribution of gasdynamic parameters for various flow modes is obtained. The distribution of the heat flow and of the friction factor (as a func-

tion of the inflow parameters and sphere radius) as well as the shape and position of the shock wave, are determined. The flow lines and sonic lines are constructed.

103. Alikhanov, S. G., V. G. Belan, G. N. Kuligin, and P. Z. Chebotayev. Plasma expansion in a vacuum and collisionless plasma stream flow around a plate. Zhurnal eksperimental'noy i teoreticheskoy fiziki, v. 59, 1970, no. 6(12), 1961-1966.

The problem of flow of an ultrasonic plasma stream around a plate is reduced to the problem of the expansion of a plasma into a vacuum and is solved numerically for a one-dimensional case by taking into account the Poisson equation. The solution of the problem of expansion of a nonisothermal collisionless plasma into a vacuum is compared with the self-similar solution. The structure of the perturbed zone in the path of a plate located in the stream of a nonisothermal plasma moving with a velocity M = 2 in the absence of a magnetic field is investigated. The density and potential distributions behind the plate are obtained. The results of the experiments and calculations are in good agreement.

104. Diyesperov, V. N., and O. S. Ryzhov. Uniform flow about finite bodies in the transonic velocity range. AN SSSR. Zhurnal vychislitel'noy matematiki i matematicheskoy fiziki, v. 11, no. 1, 1971, 208-221.

Transonic flow about finite bodies by the uniform flow of an ideal gas is examined theoretically. In the vicinity of the sonic line, this flow is assumed to be adequately described by the Karman equation for the disturbance potential. Its solution is sought in a class of self-similar functions as a series in powers of the distance from the body. The term which satisfies the nonlinear equation and describes purely sonic flow has been determined elsewhere before (K. Guderley, H. Joshihara. Quart. Appl. Math., 8, 1951, no. 4, 333-339). The remaining series terms satisfy solutions of linear differential equations. Their study produces systems of eigenfunctions and natural functions, depending on the chosen boundary conditions. Natural functions satisfy the physically correctly stated problem; therefore, they are considered important in transonic gasdynamics and are studied in some detail.

105. Belotserkovskiy, O. M., and Yu. M. Davydov. The nonstationary "large particles" method for gasdynamics problems. AN SSSR. Zhurnal vychislitel'noy matematiki i matematicheskoy fiziki, v. 11, no. 1, 1971, 182-207.

A numerical "large particles" method to solve vortex equations of the inviscid gas motion is developed. It is based on the F. H. Harlow "particle-in-cell" method (Los Alamos Scient. Lab., Report No. LA-2139, 1957) into which the continuity concept is introduced, by means of the law of conservation of mass written for a given cell ("large particle"). This is done preserving the advantages of the Harlow method, i.e., employing both Euler and Lagrange calculating grids and the organization of the calculating process. The numerical flow sheets of the method are investigated in detail, with the basic objective of determining their applicability to aerodynamic problems.

Various difference flow sheets of this method are constructed and their computational stability is investigated by means of their differential approximations. Common numerical algorithms to calculate both the plane and axially symmetrical flows, valid in the smooth flow regions and in the discontinuity regions, are considered.

The problem of incident flow around blunt bodies is solved for a wide range of Mach numbers, from low subsonic to hypersonic velocities including sonic velocities. Numerous calculation results are presented in graph form. An example is shown in the figure below, where lines M = const are constructed for cases of transonic flow $0.6 \leqslant M \leqslant 1.1$ around the end plane. In figure "d", the M profile along the axis of symmetry and the thickness of the shock wave also are shown.

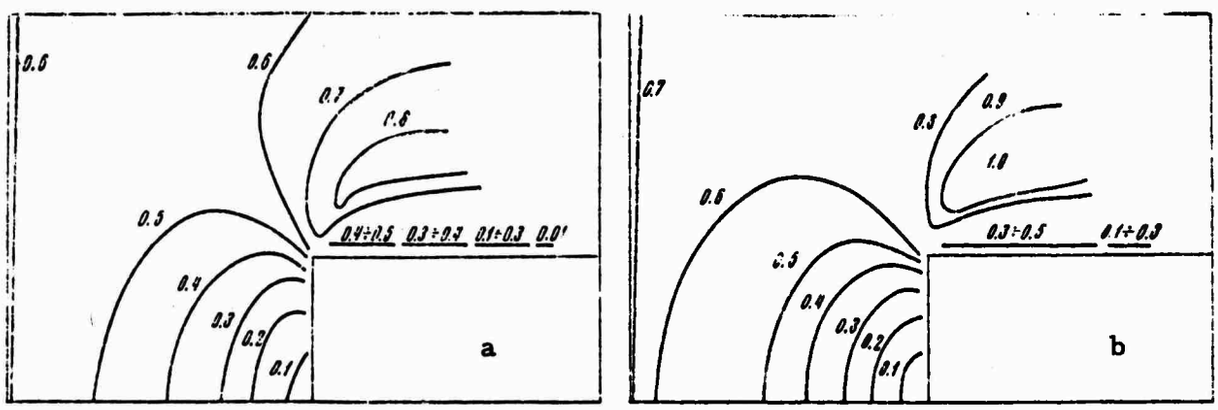

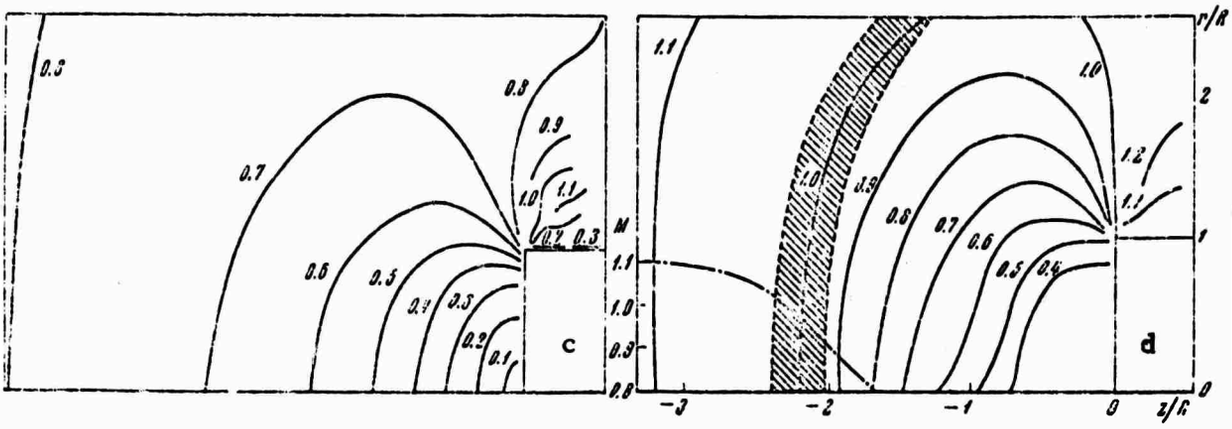

a — $M_\infty = 0.6$; b — $M_\infty = 0.7$; c — $M_\infty = 0.8$; d — $M_\infty = 1.1$

106. Alikhanov, S. G., V. G. Belan, G. N. Kichigin, and P. Z. Chebotayev. Investigation of ion shock waves in a collisionless plasma. Zhurnal eksperimental'noy i teoreticheskoy fiziki, v. 60, 1971, no. 3, 982-992.

The problem of propagation of a stationary shock wave in a collisionless plasma with warm ions ($T_i \neq 0$) in the absence of a magnetic field is solved. The shock wave velocity dependence on potential is found for a temperature ratio $T_e/T_i = 10^1 - 10^3$. The minimal value $T_e/T_i = 5$ for which the waves can exist is found. Results of experiments in propagation of finite-amplitude ion shock waves in a laboratory plasma ($T_e/T_i = 20-50$) are presented. The initial stage of wave formation and dynamics of ion reflection from the wave front are studied. The ion distribution function in a plasma for waves with various amplitudes and velocities is measured. Evolution of a large amplitude wave in conditions close to the experimental ones is studied by carrying out a numerical experiment with a computer-modeled plasma. Results of the theoretical analysis are compared with the experimental data. In all cases considered, the calculations and experiments indicate that the Mach numbers do not exceed 1.6.

107. Perminov, V. D. Axially symmetric bodies with minimum drag in a viscous hypersonic flow. AN SSSR. Izvestiya. Mekhanika zhidkosti i gaza, no. 1, 1971, 90-96.

Axially symmetric bodies of given length, relative thickness, volume and integral heat flow, which present minimum drag to the hypersonic flow of

a viscous gas are studied. The problem is formulated and some results of the numerical solution are presented. Using a modification of Newton's law of fluid friction and assuming that the coefficient of friction is constant, the problem is reduced to minimizing a certain functional relationships described earlier (Hayes, W. D., and R. F. Probstein, Hypersonic Flow Theory, New York, Academic Press, 1959). Exact and numerical solutions of variation problems indicate that friction drag is significant and essential in determining aerodynamic shapes.

Results are presented for the numerical solutions of the following relationships:

(1) shear stress as a function of the shape of the body;
(2) total drag and friction drag as a function of relative thickness of the body;
(3) relative thickness of the body as a function of the shape of the bodies with minimum drag;
(4) total drag minimized and relative thickness of the body as functions of total heat flow;
(5) total drag as a function of total heat flow and relative volume.

These results show that the optimum body is one with a spike on the bow part; that an increase in volume sometimes leads to an initial decrease in total heat flow, depending on the relative thickness of the body; and that the body with minimum drag is characterized by minimum heat flow.

XIV. HYPERSONIC TRAILS

108. Gadion, V. N., V. G. Ivanov, G. I. Mishin, and S. N. Palkin. Measurements of the hypersonic trails conductivity. Zhurnal tekhnicheskoy fiziki, v. 41, no. 2, 1971, 350-357.

The electrodynamic method of conductivity measurements is applied to the investigation of an ionized hypersonic trail. The method is based on the comparison of the measured quantity with the standard one in a symmetric high frequency (4.0 MHz) bridge with two identical coils Z_1 (6 turns, 10μh, and 3 ohms) as its adjacent arms. One of the coils serves as a standard, while the other is a measuring coil which, when placed in the operating section of an aeroballistic range, changes its impedance depending on the conductivity of the ionized hypersonic trail. The unbalance voltage of the bridge is related to this conductivity. Analytical expressions of this relationship and of its transformation into ionization parameters are presented. Experiments were conducted with the plastic models launched from a light-gas gun at velocities of 3000 — 5000 m/sec, and the preliminary experiment results are presented.

It is concluded that suggested method of conductivity measurements may be utilized to study processes in a hypersonic trail.

109. Berezkina, M. K., and M. P. Syshchikova. Relaxation processes in a shock wave in a partially ionized gas. Voprosy fiziki nizkotemperaturnoy plazmy (Problems of the physics of low-temperature plasma; Reports of the second All-Union conference on low-temperature plasma). Minsk, Izd-vo Nauka i tekhnika, 1970, 472-477.

An experiment is reported which studies the structure of the bow wave around a blunt body placed in the supersonic flow of partially ionized xenon and krypton in a shock tube. An optical system is described which permits the simultaneous interferometric measurement of gas density and electron density in front of the bow wave and which also permits shadow photography of the flow around the body. The experiments were conducted at Mach numbers for the front of the initial shock wave between $8 < M_1 < 14$ and in a temperature range at the beginning of the relaxation zone 9000 — 20,000° K. Time variations of the

flow parameters in xenon are shown in the figure below: (a) gas density in the flow, (b) degree of xenon ionization, and (c) interpretation of the (x,t)-scanning of the shadowgraph: curve 1 presents the motion of the top of the shock wave being formed, and curve 2 shows the position of the luminosity front.

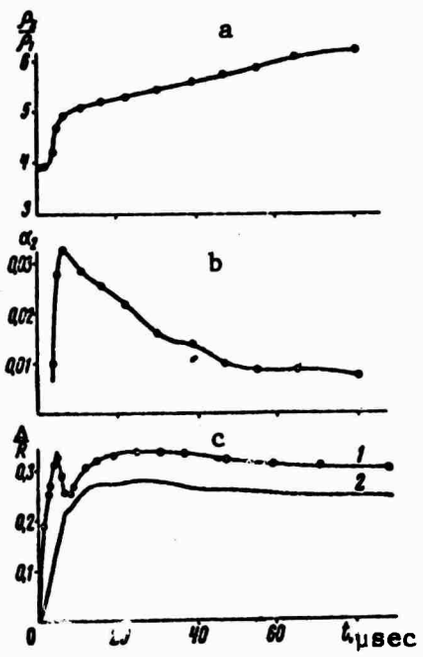

The data obtained for the size of the relaxation zone behind the bow wave for various degrees of ionization of the gas in the free stream are presented in the table below. Here, M_1 is the Mach number, τ_r is relaxation time, $\tau_r P_3^0$ is relaxation time reduced to a pressure of 1 atm, and α_2 and α_3 are the degrees of ionization behind the initial and bow shock waves, respectively.

M_1	τ_r, μsec	T_3^0, °K	$\tau_r \cdot \rho_3^0$, μsec.atm	α_2	α_3
			Xenon		
8,6	2,39	8977	18,7	0,002	0,016
8,83	2,45	9597	17,4	0,004	0,024
8,85	1,91	9671	12,2	0,005	0,026
8,94	2,65	9852	14,6	0,006	0,029
8,98	2,10	9940	12,8	0,006	0,030
9,33	1,56	10560	9,11	0,009	0,040
9,49	1,46	11030	7,62	0,013	0,049
9,79	1,04	11640	5,97	0,017	0,060
9,95	0,55	11950	3,89	0,019	0,064
10,01	0,81	12090	4,18	0,022	0,071
10,14	0,41	12350	2,92	0,023	0,072
10,31	0,48	12690	3,03	0,027	0,081
10,40	0,31	12890	2,70	0,028	0,085
10,45	0,33	13070	2,33	0,030	0,088
10,72	0,28	13550	1,94	0,035	0,099
			Krypton		
10,31	2,24	12800	9,15	0,016	0,057
10,37	1,74	12960	6,48	0,017	0,061
10,44	1,54	13230	6,45	0,019	0,064
10,65	1,26	13710	5,89	0,022	0,072
10,67	1,61	13580	6,19	0,022	0,071
11,02	1,15	14370	4,18	0,029	0,088
11,40	0,94	15130	2,97	0,039	0,106
11,51	0,87	15370	3,09	0,041	0,110
11,63	0,81	15620	2,53	0,044	0,118
11,77	0,83	16000	2,54	0,049	0,126
13,75	0,47	20730	1,50	0,084	0,192

XV. EQUATIONS OF STATE FOR GAS

110. Antanovich, A. A., and M. A. Plotnikov. Apparatus for experimental study of thermodynamic characteristics of gases at pressures to 10–12 kbar and temperatures to 3,000°K. IN: AN SSSR. Teplofizicheskiye svoystva gazov (Thermophysical properties of gases). Moscow, 1970, 156-159.

An apparatus (see Fig. 1) has been developed, in which an inert gas at a high pressure can be maintained indefinitely at a high temperature, using a heating chamber 30 mm in diameter x 150 mm long. Thin-wall cylindrical

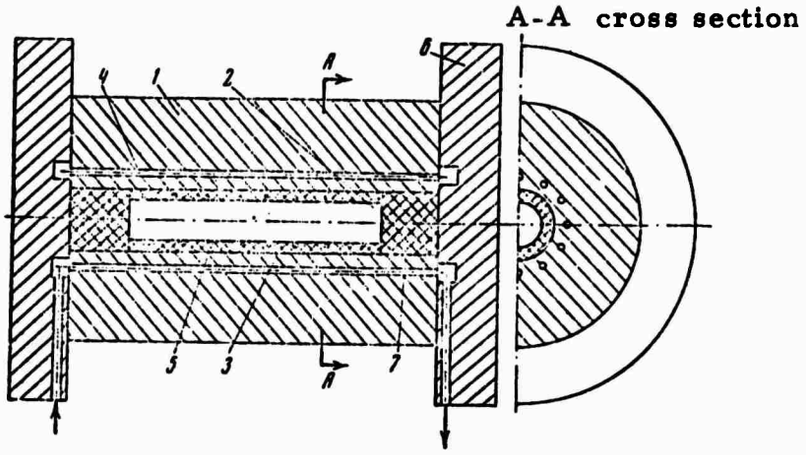

Fig. 1 - Apparatus for high pressure and high-temperature. 1 - cylindrical pressure vessel; 2 - heating chamber; 3 - pyrographite insert; 4 - ducts of water-cooling system; 5 - tungsten coil; 6 - flange; 7 -- heat-insulating stopper.

inserts of pyrolytic graphite were used for heat insulation of the pressure vessel, because of their low thermal conductivity and negligible coefficient of thermal expansion. In a preliminary test, a pyrographite insert with a 2 mm wall thickness and 25 mm diameter did not break in a 2,000° K temperature gradient between the internal and external surfaces. The cold strength

of the vessel also did not decrease significantly in the presence of cooling water ducts. The strength of the heated vessel was considerably increased on account of the nonuniform temperature distribtuion along the cylinder radius. The pressure-induced stress on the internal surface of the cylinder was decreased by 20—25% because of the existence of thermal stresses within the wall material. The electric power supply must be 20—30% greater than theoretical, to compensate for heat losses through the bottom and to accelerate heating of gas up to the operating temperature. Tests of the apparatus showed the reliability and workability of its construction elements up to 6 kbar and 2,000°K or higher. The error in determination of compressibility coefficient of a gas (N or Ar) could be held within 1.5—0.5%, if a tungsten resistance thermometer and a manganin manometer were used inside the heating chamber.

111. Orudzhaliyev, E. D. Sound velocity in carbon dioxide.
IN: AN SSSR. Teplofizicheskiye svoystva gazov (Thermophysical properties of gases). Moscow, 1970, 152-153.

A brief analysis is given in which formulas are derived for calculating specific heats c_p and c_v at constant p and v for CO_2 gas at a given P and T, and known experimental sound velocity a. The formulas for c_p and c_v were derived from $a^2 = -v^2(\partial p/\partial v)_s$ using the equation of state in virial form with the 2nd and 3rd virial coefficients for CO_2 gas.

112. Plotnikov, M. A., A. A. Antanovich, and G. Ya. Savel'yev. Determination of thermodynamic characteristics of real gases at pressures up to 15 kbar and temperatures to 3,000°K.
IN: AN SSSR. Teplofizicheskiye svoystva gazov (Thermophysical properties of gases). Moscow, 1970, 160-164.

A semi-empirical method for calculating the thermodynamic characteristics of gases at pressures up to 15 kbar and in the 700 — 1,200°K temperature range is introduced in view of the absence of any method of determination of these characteristics in the cited temperature range. The method is based on application of the equation of state in virial form with 4—5 virial coefficients. The data obtained by the described method should be in good agreement with those calculated from the Rowlinson equation for the 1,200—3,000°K range. Thus calculated compressibility factor, specific volume V, enthalpy, and entropy of nitrogen at 12 kbar in the 700—1,200°K range differed by a maximun of 0.55% from the corresponding values calculated from the Rowlinson equation, if the selected value for σ is 3.656 Å and the value of the parameter ε (chemical energy) is 91.5°K. The I-S diagram shown for nitrogen, in the ranges of

saturation to 15 kbar and up to 3,000°K, was plotted by the above semi-empirical method and by using data from literature. It shows a sharp rise of isotherms with increase in pressure from about 100 bars.

113. Rabinovich, V. A., L. S. Veksler, and P. T. Slobodyanik. Thermodynamic characteristics of neon, argon, krypton and xenon in the single-phase state. IN: AN SSSR. Teplofizicheskiye svoystva gazov (Thermophysical properties of gases). Moscow, 1970, 153-156.

A method is introduced for calculating properties of thermodynamically similar substances. Using one of the substances as a reference, the experimental virial coefficients B and C of this substance can be substituted for dimensionless virial coefficients B* and C* in the generalized equation of state in virial form: $Z^* = 1 + B^* (T^*)/V^* + C^* (T^*)/V^{*2} + ----$), for gases whose atoms obey the law $\phi = \varepsilon f(\sigma/\eta)$, where ε and σ are individual parameters of the substance. In this case, the reduction parameters can be derived by superposing the curves B*(T*) and C*(T*) of two similar gases. Thus, the equation of state of the reference substance can be used for calculating properties of thermodynamically similar substances. This method has been applied to inert gases; for example, the experimental B(T) of Ne, Ar, Kr, and Xe were completely superposable on the same graph by parallel translation of the origin of coordinates. Using Ar as reference and its experimental B and C data from literature, the equation of state with two virial coefficients was established to describe compressibility of Ar from the triple point to 1,200° K, with an accuracy to 0.1%. The conversion factors k_T and k_V from Ar to Ne, Kr, and Xe were determined by superposed B(T) curves of the four gases. Extrapolation limits of B and C for Kr were presented graphically.

114. Pitayevskaya, L. L., and A. V. Bilevich. Propagation velocity of ultrasound in CO_2 at high pressures, and the applicability of the Raoult law for strongly compressed gases. Doklady AN SSSR, v. 196, no. 1, 1971, 81-83.

The velocity of ultrasound in CO_2 at pressures up to 4.5 kbars and in the temperature range of 25–200°C is measured accurate to 0.3% using the pulse method. Measurements were conducted in the 0.3–5 MHz frequency and no frequency dependence of the sound velocity was found. The curves of the sound velocity dependence on pressure for various temperatures, and the

dependence on temperature based on various pressures are presented. The values obtained are utilized to calculate the ratio of heat capacities $\gamma = C_p/C_v$, which are presented as a function of density for various temperatures. Similar curves are also plotted for the adiabatic compressibility. Finally the Raoult constant for compressed nitrogen, argon and CO_2 is calculated and plotted. In contrast to liquids, this constant has a noticeable temperature dependence, although this dependence is practically linear and this may be useful for possible interpolations.

XVI. EXPLODING WIRES

115. Shumanov, V. S. Measurement of parameters of a plasma formed by electrically-initiated explosion of wires in vacuum. ZhPS, v. 14, no. 2, 1971, 209-211.

Expansion was studied of a dense metallic plasma column formed by explosion in vacuum of metallic wires, mainly copper of different dimensions. The explosion was triggered by the discharge of a capacitor. The plasma expansion was recorded by an SFR high-speed camera, and its velocity was calculated to be from 2.2 to 5 km/sec with wires from 0.1 to 1.1 mm diameter. The energy, momentum, and conductivity of the expanding explosion products were measured in vacuum. The measured parameters were used to estimate the state of the plasma substance; its temperature ($\sim$ 10,000°K), density ($\sim 10^{-15} cm^{-3}$), and single-ionization degree ($\sim$ 100%).

116. Kolesnikov, P. M., V. A. Korotkov, and G. A. Nesvetaylov. Current-voltage characteristics of exploding wires. ZhTF, no. 7, 1970, 1520-1526.

Experimental current-voltage characteristics of Cu, Nichrome, Al, and Ni exploding wires were obtained in air for wires of different diameter and length. The experimental apparatus was composed of pulsed current generator and a system for recording wire potential and discharge current. An increase in diameter of a 55 mm long Cu wire from 0.69 to 1.2 mm caused degeneration of the explosion. Transition to the melting pattern was observed with a 1.75 diameter Cu wire. A peculiar characteristic was obtained immediately after current attained its maximum value. Several characteristic points were noted. The explosion characteristics of 110 mm long wires of different metals were significantly different. The characteristic of the Nichrome wire consisted of straight line segments; the maximum potential for Nichrome was described by an approximate formula. Transient processes in the circuits studied are described by equations in dimensionless form, using the approximations of current-voltage characteristics obtained for Nichrome and Cu wires. Essentially the same experiment is also described in the authors elsewhere (Voprosy fiziki nizkotemperaturnoy plazmy. Minsk, Izd-vo nauka i tekhnika, 1970, 209-213).

XVII. ATMOSPHERIC PHYSICS

117. Basharinov, A. Ye., and Ye. N. Zotova. Spectra of submillimeter transitions between excited electron states of the NO molecule. Optika i spektroskopiya, v. 29, no. 5, 1970, 842-844.

Data which characterize the dependence of the position of the NO molecule terms on the rotational quantum number are calculated for several excited oscillatory levels of the states $C^2\Pi$ and $B^2\Pi$. Values of the interaction parameter H for the states $C^2\Pi$ ($v' = 0, 1, 2, 3, 4$) and $B^2\Pi$ ($v'' = 7, 10, 12, 15, 18$) are presented in the following table.

$C^2\Pi(v') \sim B^2\Pi(v'')$	(v', v'')	1	(0.7)	(1.10)	(2.12)	(3.15)	(4.18)	(5.21)
	H, cm^{-1}		8	55	158	219	49	165
$F^2\Delta(v') \sim B'^2\Delta(v'')$	(v', v'')	1	(0.2)	(1.4)	(2.6)	(3.9)		
	H cm^{-1}		9	67	113	60		
$K^2\Delta(v') \sim B'^2\Delta(v'')$	(v', v'')	1	(0.7)					
	H, cm^{-1}		45					

Possible transitions in the submillimeter and in the longwave portion of the IR spectrum are established.

118. Koppe, V. T., A. G. Koval', B. M. Fizgeer, Ya. M. Fogel', and S. I. Ivanov. Measurement of the effective cross sections and excitation functions for bands of the first negative system of the molecular ion N_2^+ON excitation of nitrogen by fast electrons. Zhurnal eksperimental'noy i teoreticheskoy fiziki, v. 59, no. 6 (12), 1970, 1878-1883.

The effective cross sections for the (0—0), (0—1), (0—2), (0—3), (1—2), (1—3) and (1—4) bands of the first negative system of the N_2^+ ion and the

multiplet lines $\lambda = 5001-5005$ Å in the NII spectrum are measured at energies between 0.5 and 20 keV. Nitrogen was excited by electrons with energies between 0.5 and 20 keV. A detailed description of the experimental setup and measurement technique is presented. Measured values of the effective cross sections of the $10CN_2^+$ bands at an energy of E = 4 keV are presented in the table below.

$v' - v''$	σ, cm^2
0—0	$23{,}6 \cdot 10^{-19}$
0—1	$6{,}8 \cdot 10^{-19}$
0—2	$1{,}3 \cdot 10^{-19}$
0—3	$2{,}8 \cdot 10^{-20}$
1—2	$1{,}07 \cdot 10^{-19}$
1—3	$3{,}6 \cdot 10^{-20}$
1—4	$1{,}01 \cdot 10^{-20}$

In the region of overlapping energies the data obtained are in a good agreement with data published by other authors.

119. Snopko, V. N. "Hot" absorption bands of the Schumann-Runge system of oxygen. Optika i spektroskopiya, v. 29, no. 5, 1970, 835-841.

Photographs of the absorption spectra emerging during the transitions from excited oscillatory levels, the so-called Schumann-Runge system of the oxygen absorption bands in the 1930—2470 Å region, are obtained. A 3-meter-long spectrograph with a diffraction grating (1200 lines/mm on the 150 x 70 mm area) has been used for this purpose (Fig. 1).

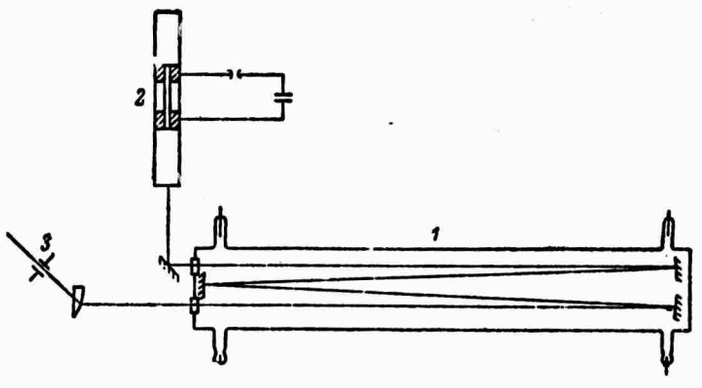

Fig. 1 1 - absorption pipe;
2 - light source
3 - spectrograph slit.

Rotational structure of 14 new molecular bands emerging during absorption from the oscillatory levels $v'' = 5, 6, 7$ of the lower state $X^3\Sigma_g^-$ is analyzed graphically and independently computed with a digital computer. Tables of wave numbers are presented, as are the tables of the zero lines for 32 measured bands, energy differences and rotational constants for oscillatory levels of the lower state $v'' = 3-7$.

120 • Zdunkevich, M. D., Yu. N. Belyayev, and V. B. Leonas. Calculation of the transfer coefficients of dissociating air. Teplofizika vysokikh temperatur, v. 8, no. 6, 1970, 1302-1304.

Values of the collision integrals $Q_{ij}^{(e,s)}$ calculated by K. S. Yun and E. A. Mason (Phys. Fluids, v. 5, no. 4, 1962) and by Yu. N. Belyayev and V. B. Leonas (Fizika goreniya i vzryva, 1967, no. 2) are utilized to calculate transfer coefficients of dissociated air. Results obtained on the basis of the former are presented by solid lines, and by dash lines, based on the latter, and coefficient of viscosity (η) data are presented in Figure 1.

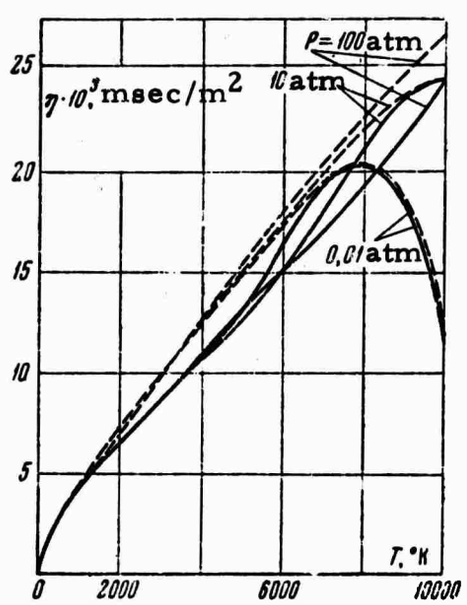

Fig. 1

Values of the thermal conductivity coefficient are given in Figure 2, and variations of $P_r = C_p \eta / \lambda$ as a function of temperature and pressure are presented in Figure 3.

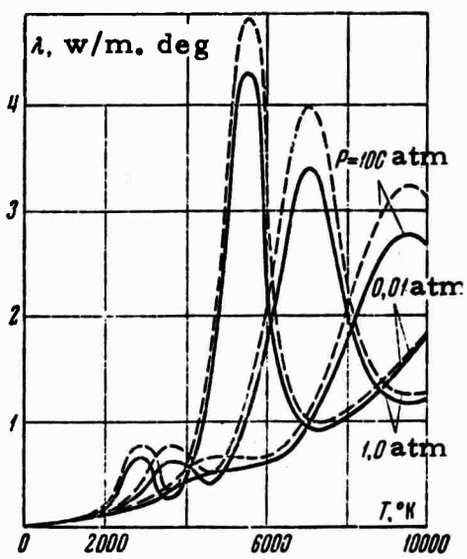

Fig. 2

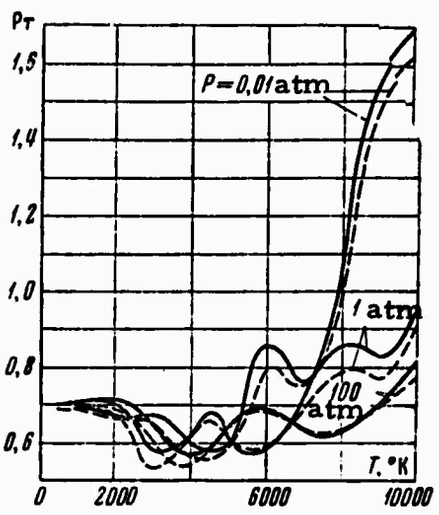

Fig. 3

121. Vlasov, M. N. Distribution of molecular oxygen at the $b^1\Sigma_g^+$ level in the upper atmosphere. Geomagnetizm i aeronomiya, no. 6, 1970, 1043-1047.

An analysis was made of previously proposed mechanisms of formation and destruction of O_2 ($b^1\Sigma_g^+$)molecules during nighttime at different atmospheric heights. The O—O bond is known to be the source of dark emission at $\lambda = 7619$ Å. A comparison was made of the experimental and theoretical height profiles of concentrations of O_2 ($b^1\Sigma_g^+$). It was concluded that at the 90—120 km atmospheric level, dark emission of atmospheric O_2 layers can be well explained by the

following reactions:

(1) $$O + O \rightarrow O_2 + h\nu$$

(2) $$O_2^*(^3\Sigma_g^-)_{v>17} + O_3 \rightarrow 2O_2(^3\Sigma_g^-) + O(^1D)$$

(3) $$O_2(A^3\Sigma_u^+) + O_3 \rightarrow 2O_2(^3\Sigma_g^-) + O(^1D)$$

(4) $$O(^1D) + O_2 \rightarrow O_2(b^1\Sigma_g) + O(3P).$$

The radiation association of O atoms by the reaction (1) is the main source of vibrationally-excited O_2 in the ground electron state, and of the electron-excited O_2 ($A^3E_u^+$). At atmospherics levels below 90 km, the reaction:

$$O + O_3 \rightarrow O_2(b^1\Sigma_g^+) + O_2(^3\Sigma_g^-)$$

is the substantial source of the O_2 ($b^1\Sigma_g^+$) molecules. At levels above 120 km, the O(^{1}D) atoms formed by dissociation recombination react with O_2 by a resonance mechanism (4). The deactivation rate constant of O_2 ($b^1\Sigma$ g) molecules must be relatively low (2×10^{-15} cm^3/sec) to account for the emission below 90 km. Measurement of the vertical distribution of oxygen emission in the upper atmosphere can be used as a new indirect method for studying atomic oxygen concentrations in the 70—120 km atmospheric layer.

XVIII. INSTRUMENTATION AND MEASUREMENT

122. Lisitsyn, Yu. V., V. N. Mineyev, and Ye. Z. Novitskiy. Certain problems in the theory of a polarized sensing element. Zhurnal prikladnoy matematiki i teoreticheskoy fiziki, no. 3, 1970, 56-60.

The following problems are examined: (1) the charge in a polarized sensing element connected to a capacitance load; (2) the relaxation processes in the circuit of a sensing element after the passage of a shock wave; and (3) the polarized current through the sensing element, with two mechanisms of polarization. It is shown that all the required parameters of a shock compressed dielectric can be determined by measurements in the circuits of the short-circuited sensing element and of a capacitance loaded sensing element. The computation of the two polarization mechanisms leads to a solution which qualitatively describes a number of experimental facts. Calculated values for time variation of polarization current density and of the relaxation current are compared with the experimental data.

123. Fominykh, V. I., and O. A. Migun'kov. Detector of intermediate energy neutrons. Atomnaya energiya, v. 30, no. 1, 1971, 59-60.

In the detector described, two plastic hemispheres (114 mm diameter and 12 mm wall thickness) serve as a neutron flux moderator around the low γ-radiation-sensitivity SNM-13 counters (background counting rate 2 pulse/min at γ-radiation 2000 rhm). Its construction is shown in the figure below, where 1 is the spherical moderator, 2 is the SNM-13 counters, and 3 is the cadmium casing. Various energy level neutron sources used to calibrate the detector are described and its sensitivity curves and tables are included in the article.

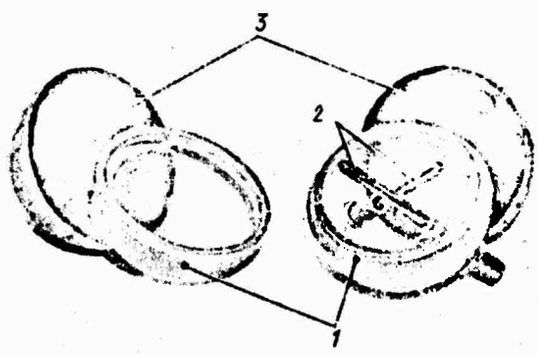

Fig. 1

124. Koval'chuk, B. M., V. V. Kremnev, and G. A. Mesyats. Cascade discharge in a gas and the generation of nano- and subnanosecond large current pulses. Doklady AN SSSR, v. 191, no. 1, 1970, 76-78.

It is shown that if, at the instant when voltage is applied to a gas discharge gap, the cathode has the necessary number of initial electrons, then a large current can be conducted by this gap owing to the development of electron avalanches caused by the initial electrons. For low pulse durations, the discharge channels do not have sufficient time to localize, and the current flows through a cross section equal to the area occupied by the initiating electrons at the cathode. With a rapid current increase, the avalanche commutation can produce pulses of subnanosecond duration, avoid heavy erosion of the electrodes, and reach high frequency of the pulse sequence (density of plasma discharge, i.e., plasma deionization time is small). Expressions are derived for the current amplitude of such a commutator and for the pulse duration. Drawings of two pulse generators are presented.

125. Dubovik, A. S., G. I. Belinskaya, N. M. Sitsinskaya, and V. V. Garnov. High-speed SFR camera for visibleand ultraviolet regions of spectrum in scanning, stereoscopic and spectral photography. Zhurnal nauchnoy i prikladnoy fotografii i kinematografii, v. 15, no. 5, 1970, 346-350.

The present paper describes recently developed modifications to the basic SFR high-speed camera, as follows: (1) SFR-UF--a high-speed moving-image camera for operation in the ultraviolet spectral range beginning at 220 mμ This is an SFR camera with quartz optical elements, having focal lengths of f = 200, 400, and 800 mm with relative aperture 1:15. Its resolution capacity is 18 to 25 lines/mm; (2) SFR-R--a high-speed scanning microscopic camera, with framing rate up to 100,000,000 frames/second on 100 frames (they are equivalent in image quality to conventional frames of 16 mm movie film, and its magnifications are from 1X to 120X with the relative aperture 1:9); (3) SFR-stereo attachment, which produces stereo pairs at 312,000 frames/sec and 1,250,000 frames/second (the stereo optical base can be varied from 200 to 800 mm); (4) SFR spectral attachments: (a) SP-77 attachment using a direct-viewing prism records in the visual spectrum with a dispersion of 100 Å/mm, (b) SP-78 attachment using diffraction grating (600 lines/mm) records spectra with a dispersion of 18 Å/mm (with these attachments the spectra of self-luminous high-speed processes can be investigated with time

resolution down to 2×10^{-8} sec and recording duration of 10^{-5} sec); and (5) SFR-movie spectrograph attachment produces a series of spectra for different spots of the area distributed luminosity of the source. The sequential frequency of spectra is up to 625,000 frames/second. Two such attachments differ by type of prism employed. With the direct-vision prism, the average linear dispersion is 300 Å/mm. With the Rutherford type prism, the recorded dispersion has four values from 25 to 465 Å/mm.

126. Koval'chuk, B. M. and G. A. Mesyats. Large current pulse generator of subnanosecond duration. Priboryi tekhnika eksperimenta, no. 5, 1970, 102-105.

The concept of an avalanche discharge commutator developed earlier (Doklady AN SSSR, v. 191, no. 1, 1970, 76-78) is employed in a pulse generator described in this paper. This pulse generator is capable of delivering current pulses smoothly adjustable from 50 to 1000 a, with a duration of 0.6 nsec at half amplitude and with a repetition frequency up to 10^4 Hz. Diagrams of the generator and pulse shaping circuits are presented, along with performance characteristics and oscillograms. It is expected that the service life of this type of avalanche discharge commutator may exceed 500 hours.

127. Baykov, A. P., A. M. Iskol'dskiy, B. M. Koval'chuk, G. A. Mesyats, Yu. Ye. Nesferikhin, and V. N. Pomerov. A high-power pulse current generator. Priboryi tekhnika eksperimenta 1970, no. 6, 81-82.

The design of the capacitor bank for a pulse current generator is described. It consists of 12 parallel-connected capacitors, 2.5×10^{-6} F each, with an operating voltage of 50 kv (Type KMM2.5/50 modernized capacitors made by IYaF SO AN SSSR). The basic characteristics of the bank are:

Maximum energy	- 40 kj
Operating voltage	- 10-50 kv
Capacitance	- 30×10^{-6} F
Inherent inductance	- $(8\text{-}12) \times 10^{-9}$ h
Natural frequency	- 270 kHz
Active resistance	- 6.5×10^{-3} ohm
Maximum short-circuit current	- 2.5 Ma
Q	- 4.

Several banks of this type may be connected in parallel to provide a stored energy of up to $\sim$ 1 Mj.

XIX. CONFERENCES

128. Panfilov, V. N., S. S. Khlevnoy, and A. A. Deribas. Second All-Union Symposium on Combustion and Explosions. Fizika goreniya i vzryva, v. 6, no. 2, 1970, 256-258.

The Second All-Union Symposium on Combustion and Explosions was held in Yerevan from 25 to 30 October 1969. More than 400 specialists participated. The subjects discussed covered a very wide range. Three sections were set up: chemical kinetics, combustion, and detonation. The subjects discussed in the 114 reports presented included the following: problems of the kinetics of reactions in the gaseous and condensed phases; relaxation processes; the kinetics of reactions in shock waves; the ignition and combustion of gases and condensed systems; heterogenic combustion; investigations of physical phenomena and chemical transformations in shock waves; the detonation of condensed explosives; etc.

Great interest was generated by the plenary reports of A. B. Nalbandyan (Laboratory of Chemical Physics, AN Arm SSR), G. B. Manelis, A. G. Merzhanov, A. N. Dremin (FIKhF AN SSSR) and D. A. Frank-Kamenetskiy (IKhF AN SSSR). In his report, "A new principle for studying the mechanism of slow reactions using electron paramagnetic resonance (EPR) methods", A. B. Nalbandyan examined the possibility of using the EPR method to record the free radicals in the congealed products of slow gas-phase reactions, when the concentrations of radicals in the gas phase are too small to be observed directly. Applying the methods of congealing permits the recording of free radicals and the study of their reactions in these processes as well as the generation of chains in branch chain reactions, the slow oxidation of hydrogen between the second and third limits of ignition, the oxidation of formaldehyde, the photochemical oxidation of hydrocarbons, fluoridation reactions, and reactions of thermal breakdown of a number of compounds.

G. B. Manelis presented new concepts on the mechanism of chemical reactions in solids, based on a zonal model of the propagation of the reaction front.

In the interesting report by A. G. Merzhanov, "Certain new problems in the study of the combustion processes of condensed systems", possibilities were substantiated for using the combustion process to obtain different classes of

inorganic compounds; based on an analysis of experimental data the combustion mechanism was discussed for systems with condensed reaction products, certain problems were formulated for the development of a heterogeneous combustion theory, and possibilities were analyzed for various synthetic and technical problems (the production of stochiometric and nonstochiometric compounds with large yield and objects made from them, as well as the production of non-equilibrium compounds).

D. A. Frank-Kamenetskiy in his report, "Plasma analogies of the combustion theory", raised the important question of the existence of a profound analogy between the heating of a weakly ionized (low-temperature) plasma by an electric field and the heating of a gas by chemical reaction; conditions were analyzed for free plasma propagation and the so-called bound propagation of plasma, which takes place in different kinds of plasmatrons. The latter condition was examined in detail using the example of an electrode-free high-frequency plasmatron. Special attention was paid to the stability (existence) of the heating zone when the flows of injected gas were subcritical; in this case the zone can be assumed to be at the forward edge of the inductor down to as low a flow velocity as desired (this case is not feasible in the usual flame). The theory presented in the report on high-frequency heating of plasma is constructed completely analogous to the thermal theory of combustion and to the use of its ideas.

A. N. Dremin presented a compressive and argumentative report on the latest achievements in studying the phenomena which occur during detonation.

The discussions of the reports and special topics showed that great success recently has been achieved in studying the kinetics and mechanism of the elementary reactions of atoms and free radicals, especially at high temperatures and pressures, and also in studying the kinetics of a number of complex reactions (oxidation of hydrogen and hydrocarbons, fluoridation reactions, etc.)

Sectional reports by V. V. Azatyan (IFKh AN SSSR), K. T. Oganseyan and A. A. Matashyan (Laboratory of Chemical Physics AN Arm SSR), Yu. M. Gershenzon (IKhF AN SSSR) and others were devoted to the detailed discussion of the results of investigating the kinetics and mechanism of radical reactions using the method of EPR. During a visit to the Laboratory of Chemical Physics, AN Arm SSR, directed by A. B. Nalbandyan, the symposium participants were able to become acquainted in detail with the research on the kinetics and mechanisms of gas phase reactions, a considerable part of which is conducted using the EPR method.

A large number of reports were devoted to research on the kinetic laws of thermal dissociation in the condensed phase of a number of real compounds (nitrates, nitroamines, pricrates, azides, etc.). An interesting discussion was generated by the reports of V. A. Koroban (Moscow Chemical and Technological Institute), V. V. Boldyrev (IKhKiG SO AN SSSR), M. S. Sinyakov (Moscow), which were concerned with research on the mechanism of thermal decomposition of ammonia perchlorate.

V. L. Tal'roze presented an interesting report on the development and creation of a laser, operating on a chain reaction with energy branches (the interaction of fluorine and hydrogen). The theoretical and experimental study of the mechanism of this and other reactions, which can be generally covered by the subject of the creation of gas chemical lasers, was discussed by G. A. Kapralovaya and O. M. Sarkisov.

In a great number of reports the theoretical and experimental results were studied for the processes of dissociation, relaxation and recombination in flames and shock waves.

Half of the reports in the section on combustion dealt with problems of the ignition and combustion of condensed systems.

A lively discussion was generated by the report of V. V. Barzykin (FIKhF AN SSSR) on the results of studying the ignition of explosives by a hot dispered flow. In the report of K. G. Shkadinskiy (FIKhF AN SSSR) the regularities of combustion yield in a stationary regime were examined for the case of the combustion of gases and gas compositions by a heated surface. O. Ya. Romanov (Leningrad) reported on the results of experimental research on the ignition and nonstationary combustion of nitroglycerin powder in a semiclosed space.

Theoretical studies of the mechanism of condensed system combustion were discussed by O. I. Leypunskiy (IFhF AN SSSR) and A. K. Filoninko (FIKhF AN SSSR). A. Ye. Fogel'zang (MKhTI) presented results of the experimental study of the effect of the structure of explosives on their combustion velocity. V. M. Mal'tsev discussed spectroscopic research on identifying emission in the flames of a number of condensed systems (hexogen, nitrocellulose, etc.). The report by S. S. Movikov dealt with two new methods of studying nonstationary combustion of condensed systems.

M. A. Gurevich (LPI) gave a critical review of the methods used and the results produced on the ignition and combustion of metallic particles.

L. A. Klyachko (Moscow) analyzed the relationships of ignition and combustion of a combination of metallic particles with a drop of fuel.

In the reports on ignition and combustion of gases, in particular, problems were studied which dealt with the mechanism of methane combustion, with the character of the acoustic action on a turbulent flame, with the effect of electrical magnetic fields on vibrational combustion. Several reports were devoted to methods of calculating the turbulent flare and to the experimental study of the characteristics of ignition and combustion in a turbulent flow, as well as stabilizing the flame behind a poorly streamlined body.

At the section on detonation, L. V. Al'tshuler (IKhF AN SSSR) examined certain laws and features of the behavior of metals, ion crystals and minerals at pressures and temperatures of shock compression. The serious practical value of studying these materials was noted, as well as the real difficulties of studying the region of bound quantum mechanics states. Equations were also presented for the state of the solid and the limit values of the Gruneisen coefficient in the region of degenerated electron gas for relativistic electrons. In the report of S. B. Kormer (IKhF AN SSSR), a review of the work completed by the author was presented on studying the optical properties of dielectrics in the case of shock compression. Data were obtained for the temperature of the material behind the front, for the smoothness and structure of the front, and also for the reflective and absorptive capacities of the compressed material.

Results of investigating the dynamic compressibility, the temperature, the coefficient of absorption of visible light and the electroconductivity of CCl_4, compressed by shock waves of varying intensity, were presented in the report by F. B. Grigor'yev (IKhF AN SSSR).

A. G. Ivanov and V. N. Mineyev (IKhF AN SSSR) examined various theories which describe the polarization mechanism of dielectrics behind the front of a shock wave. They also presented results of studying the effect of polarization in ion crystals, and polar and nonlinear dielectrics. The features of polarization of organic substances (polystyrene and epoxy resins) in shock waves was the subject of the report by Ye. Z. Novitskiy and others (IKhF AN SSSR). The results of research on the polarization in shock waves with varying intensity for chlorobenzene, brombenzene, iodobenzene and nitrobenzene were presented by V. V. Yakushev and A. N. Mikhaylov (FIKhF AN SSSR).

A large group of reports were devoted to presenting results of studying the physico-chemical transformations in various materials, caused by shock waves.

In the report of G. A. Adadurov (FIKhF AN SSSR) on x-ray studies of the properties of monocrystals of molybdenum, copper, and sodium chloride, the possibility was indicated of the transition from the monocrystalline structure to the polycrystalline state under conditions of single compression by a shock wave with high intensity.

R. I. Nigmatulin, S. S. Grigoryan and others (NII mekhaniki MGU) theoretically examined the phenomena which occur in metals during the propagation of plane nonstationary shock waves, and noted the effect on the character of motion and attenuation of the shock wave of phase transitions, the stress deviator and the nonstationary nature of the wave.

S. A. Novikov and I. M. Ainitsina (IKhF AN SSSR) presented results of measurements of the value of the critical stresses shift in relation to the applied pressure for aluminum, copper and lead. The essential role of hardness was noted when the shock-compressed materials expanded.

In the report of A. A. Deribas and others (IGD SO AN SSSR) certain results were presented on studies of welding metals with a shock wave, on studying the shock wave picture which arises when compressing cylindrical bodies with explosives, using x-ray pulse photography.

In the report by A. A. Borisov and others (IKhF AN SSSR) the problem was analyzed in detail of the mechanism of amplifying weak shock waves in the two-phase system "liquid-gas". As the research object, a monodisperse atomization of kerosene in oxygen was selected. The authors successfully explained the amplification of shock waves observed experimentally by using the hypothesis that the main cause of additional energy separation in the zone behind the shock front is the fractionation of liquid drops by means of the rupture of the surface layer of the liquid caused by the gas flow.

129. Kolkunov, N. V. The mechanics and physics of destruction (All-Union Conference held in Moscow). AN SSSR. Vestnik, no. 11, 1970, 135-136.

The Fifth All-Union Conference on Strength and Plasticity, held in Moscow from 22-25 June 1970, was concerned with the mechanics and physics of destruction (destructive processes). More than 700 scientific workers participated who came from 36 cities of the Soviet Union, as well as specialists from Hungary, East Germany, Poland and Czechoslovakia.

Twenty-four scientific reports were read. V. V. Novozhilov reported on the mechanics of brittle destruction which generated great interest because of his broad presentation of the fundamental problems of strength. V. V. Bolotin examined mathematical models of the destruction process of stochastically nonuniform solids. Destruction was treated by him as a random Markov process with a discrete number of states and continuous time. The process of macroscopic crack propagation was simulated. Data were presented on tests of a number of flat specimens under different conditions of load and with varying given initial defects.

V. V. Moskvitin analyzed the qualitative features of the criterion of long-term strength (of the nonlinear Il'yushin criterion type), which is a generalization of the condition of long-term Bailey hardness. A variant for constructing the theory of long-term strength based on the conception of accumulating damage was proposed by V. P. Tamuzh. The report of I. I. Gol'denblat and V. A. Kopnov was concerned with the general theory of the strength criteria of isotropic and anisotropic materials. Along with the basic assumptions which these criteria must satisfy (the convexity of the limit surface, the effectiveness of the limit state, etc.), their different geometric interpretations were examined. In the report by Yu. N. Rabotnov, the creep process was described down to the moment of destruction. The process itself was treated as a viscous flow, which is accompanied by structural changes. A proposal was made to determine the kinetic equations of the development of frangibility by means of a macroexperiment.

In the future, scientists will devote great attention to the problem of brittle and quasibrittle destruction. G. P. Cherepanov presented a report on the linear mechanics of destruction. He touched upon several problems, connected with the development of cracks (adsorption mechanism, electrochemical mechanism, chemico-mechanical effects, etc.). R. L. Salganik showed that the values which characterize the resistance to cracking of materials, when temporal effects exist, do not remain constant. These values were described by a model for which the temporal effects can be accounted for during deformation, as well as the pre-failure phenomenon. S. T. Mileyko discussed experimental observations of the destruction of fibrous materials. He characterized the failure of these materials under conditions of high temperatures, cyclic loads, etc.

A number of reports were concerned with various aspects of fatigue failure in the case of cyclic loads. S. V. Serensen examined the cyclic loading of metal as the deformation of an inhomogeneous polycrystalline conglomerate which is described by a model in the form of a system of components which possess elastic, plastic and viscous properties. V. P. Kogayev developed this

problem in statistical models both with a nonkinetic as well as with a kinetic character. Attempts to join both approaches, in his opinion, facilitate the construction of more complete models of fatigue, which combine the advantages of the models of the character of one and the other. R. M. Shneyderovich analyzed the possibility of creating an intermediate type of failure for elastic-plastic cyclic deformation when the intensity of the quasistatic process connected to the accumulation of unilateral plastic deformations and the intensity of the fatigue process connected with the accumulation of defects have the same order

The features of the operation of materials during severe thermal cycling and thermal fatigue was the subject of the report by G. S. Pisarenko. As the basic criterion of thermal fatigue of a plastically hardening material under thermal cycling loads, which create regular plastic deformations, a proposal was offered to use the value of the summary irreversibly absorbed energy which is consumed in the process of deformation hardening. The regularities of changes in the properties of materials at low temperatures down to 4 °K were traced by P. F. Koshelev. The tendency to brittle failure in this case was analyzed on the basis of the linear mechanics of destruction.

In a group of reports the different aspects of the thermofluctuation theory of destruction was examined. In the report by S. N. Zhurkov and P. I. Betekhtin the destruction of solids was treated as a kinetic process of thermofluctuation of the disruption of the atomic bonds. As a result of experimental study of the dependence of hardness in the case of uniaxial elongation on the time and temperature, the presence of a unit time and temperature connection was established which was checked not only for metallic but for nonmetallic materials. S. N. Zhurkov, V. S. Kuksenko and A. I. Slutsker reported on investigations of the micromechanics of polymer failure caused by thermofluctuation disruptions of separate macromolecules up to the emergence of macrocracks, where the submicrocracks play an important role. V. Ye. Korsukov and V. I. Vettegren' undertook an attempt to study the processes which accompany the growth of major cracks on the molecular level. By shifting the oscillating frequencies of the atoms which enter the composition of the polymer molecules, the real stresses were evaluated at the apex of the major cracks by means of the spectroscopic method. A. M. Leksovskiy and V. R. Regel' reported on experiments to study the kinetics of the growth of major cracks in polymers. The experiments confirmed the thermofluctuation nature of the process. V. I. Vladimirov and A. N. Orlov showed that the generation of cracks at finite temperatures occurs as a result of thermal fluctuations if the local stresses are several times less than the critical ones.

The review report of V. L. Idenbom and A. N. Orlov attracted great attention. The report covered the problem of destruction in the physics of hardness. The role of thermal fluctuations was noted in the kinetics of

destruction as well as the meaning of dislocation accumulations of different types which occur in the generation of microcracks.

Reports of an engineering nature were presented at the conference, which were connected with the solution of several applied problems. I. F. Obraztsov and V. V. Vasil'yev examined problems of the hardness and optimal reinforcement of shells of rotation made of oriented reinforced glass plastics. A. A. Plutalova and G. B. Skripchenko reported on studying the mechanism of destruction of carbon fibers and composition materials based on these fibers. The report by G. P. Cherepanov, A. B. Kaplun and L. P. Karasev was devoted to evaluating the effect of the viscosity of destruction, the dimensions and shape of the defect and the residual stresses on the brittle strength of welded frames.

The reports and their subsequent discussion showed that research on the physics and mechanics of destruction has expanded considerably. As a result our understanding of the nature of failure in solids, and the physical mechanisms of the generation and propagation of cracks has been substantially increased. Success has been achieved in the field of phenomenological theories of accumulating defects and failure under loads and temperatures which vary with time and in the field of stochastic problems of the theory of destruction. More attention must be paid to research on the hardness of composite materials, to developing methods of evaluating the reliability, service life and viability of engineering constructions, and to the study of mechanisms of the development of cracks in relation to other defects of solids.

In the resolution adopted by the conference, plans were laid for a program of further research in this area, as well as organizational measures intended to improve the coordination of this effort being carried out at various institutions.

130. Kiselev, A. B. Thirteenth Scientific and Technical Conference of the All-Union Scientific Research Institute of Electrical Machine Building of the Academy of Sciences SSSR. AN SSSR. Teplofizika vysokikh temperatur, v. 8, no. 6, 1970, 1328-1329.

From 9 to 11 June 1970 in Leningrad the Thirteenth Scientific and Technical Conference of the All-Union Scientific Research Institute of Electrical Machine Building of AN SSSR took place. Reports on low-temperature plasma generators and high-current arcs were covered in a separate section in which about one hundred specialists participated.

In the reports presented in this section, a wide range of problems were examined: the generation of high-power plasma pulses, investigation of the characteristics of stationary plasmatron and electrical current sources, the combustion of arcs and methods of diagnosis.

In the report of B. P. Tsevchenko and F. G. Rutberg (Leningrad) "Investigating high-power pulsed plasma generators", results were presented on the study of a pulsed plasmatron intended for producing high intensity pulse currents, in which hydrogen and its mixtures with metal vapors were used as the working medium. A shock generator served as the energy source.

Maximum average mass temperatures of 10^4°K and pressures of 500 atm. were produced experimentally in a discharge chamber, at a maximum energy input to the arc of 5×10^6 j.

The report of A. N. Berezkin (Leningrad) was devoted to the heating of helium in an electric discharge chamber by means of the spark discharge of a capacitor bank. A description is given of the methods of measuring the amount of energy which is separated out in the active resistor of the discharge chamber in the range of initial pressures of 80 —270 atm and a calculation of the gas parameters was conducted according to the experimentally obtained values for the energy transmitted to the gas in the chamber.

The study of a plasmatron with rising volt-ampere characteristics of the arc was the theme of the report by A. S. An'shakov, M. F. Zhukov, M. I. Sazanov and A. N. Timoshevskiy (Novosibirsk). In the report, results were presented for tests of a single-chamber plasmatron with a cascade output electrode. The relationship of the arc voltage to the determining parameters was found in criterion form.

The communication of A. A. Keselev and F. G. Rutberg was concerned with the experimental use of a three-phase plasmatron device intended for operation for long periods of time.

In the report of L. A. Brichkin, Yu. V. Darinskiy and L. M. Pustyl'nikov (Alma-Ata) the problems of heat exchange in the electrodes of a plasmatron were examined.

S. M. Krizhanskiy and T. V. Krivoborskaya presented calculations of the interaction of the arc column with the longitudinal current of compressed gas.

In a number of reports and papers the methods of diagnosing a dense plasma were discussed.

E. I. Asinovskiy, V. L. Nizovskiy, V. I. Shabashov (IVTAN, Moskva) [IVTAN - Institut vysokikh temperatur AN SSSR] examined the different aspects of studying the transfer properties of a plasma of carbon dioxide and air at atmospheric pressure.

V. S. Borodin, V. F. Gebekov, and V. F. Gindina (Leningrad) discussed a method of increasing the sensitivity of the absorption method when transposing the Fabry-Perot interferometer with a monochromator, and also methods of determining the concentration of the electrons of a dense plasma according to the maximum value for the width of the hydrogen line.

The report of A. A. Koroteyev dealt with the calculation of high-current arc discharges as well as with an evaluation of the parameters of the devices being studied.

I. G. Panevin (Moskva), I. V. Podmoshenskiy, and S. V. Dresvin (Leningrad) and other participants of the conference discussed the special features of the processes which occur in high-power arc devices and also the problems of diagnosing a dense plasma.

V. M. Lashonov (Leningrad) and also Yu. P. Malkov, and Yu. Ye. Filippov (Leningrad) in their reports touched on the problems of arc combustion at high pressure and on the operation of the electrodes.

One of the sessions was devoted to the energy supply of high-power arc devices. This problem was discussed in the reports of L. P. Gnedin, V. G. Novitskiy, F. G. Rutberg (Leningrad), where analysis of the state of the art is presented. E. G. Kasharkiy and F. G. Rutberg (Leningrad) also examined the characteristics of a shock generator during the supply of high-power arcs under pulsed and short term conditions.

In the report of G. A. Sipaylov (Tomsk) the problems of increasing the value of energy given off in the loads were touched upon.

In a number of reports special attention was devoted to methods of increasing the duration of the discharge pulse.

The specialists who participated in this section of the conference discussed the basic problems connected with the generation of low temperature plasma and with high-power arcs and planned several courses of action for future work.

XX. MISCELLANEOUS

131. Aleshkevich, V. A., and A. P. Sukhorukov. Deflection of powerful optical beams by wind in absorbing media. ZhETF Pis'ma, v. 12, no. 2, 1970, 112-115.

A theoretical basis is developed here for the defocusing and deflection of a laser beam in air caused by a crosswind. The analysis refers to earlier experimental reports by Akhmanov et al (Proc. IEEE, QE-4, 1968, 568; also Annotatsiya dokladov. IV Vsesoyuznyy simpozium po nelineynoy optike, Kiyev, 1968, 93) in which beam deflection in the direction of the wind was observed. The model assumes a Gaussian optical beam propagating in the z-direction through an absorptive medium and subjected to a wind of velocity v in the y-direction. Neglecting any axial heat diffusion in the laser beam, one can express the stationary temperature distribution in the plane of the beam by the series

$$T = \frac{\delta P_0 e^{-\delta z}}{4\pi\kappa} \left\{ 2T_y \frac{y}{a} - T_{yy}\left(\frac{y}{a}\right)^2 - T_{xx}\left(\frac{x}{a}\right)^2 + \ldots \right\}$$

where δ is coefficient of absorption, P_0 is initial beam power and a is beam radius. Expansions of the individual members of the series are given in terms of the Macdonald function K_n and the parameter γ which is a linear function of wind velocity. Figure 1 shows the first three terms of the series as functions of γ. A thermal lens effect is thus indicated, in which T_y determines beam deflection while T_{xx} and T_{yy} determine defocusing. The physical significance of this is that the beam will be distorted to an elliptical cross-section at moderate wind velocities, but at high velocities ($\gamma > 10$), again returns to circular. Furthermore, the beam deflection has an absolute maximum at moderate velocities ($\gamma \approx 0.3$) as seen from T_y in Figure 1; deflection

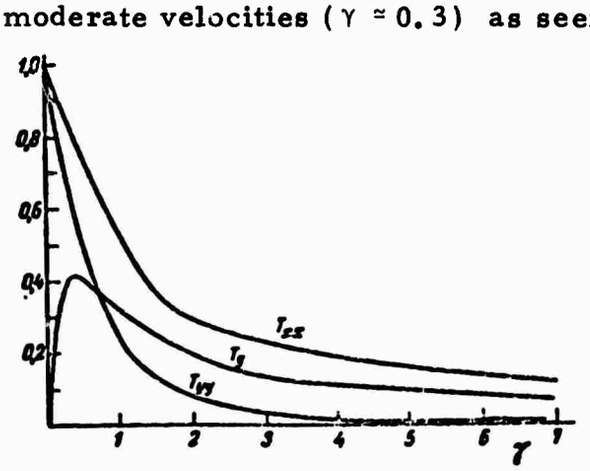

Fig. 1 - Graph of series expansion, $T(\gamma)$

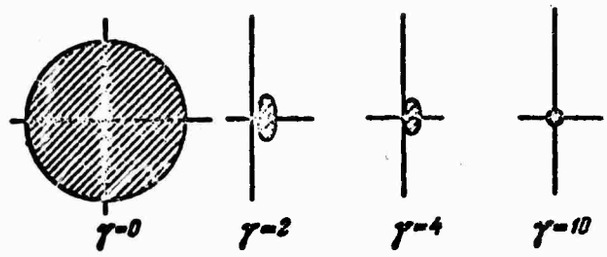

Fig. 2 - Change in laser beam cross-section vs. lateral wind velocity.

is opposite to wind direction. For radiation at 10.6 μ, and a 2 mm radius beam, a "moderate" crosswind velocity ($\gamma = 1$) would be 10 cm/sec. The analysis applies as well to propagation through water; here the analogous flow velocity for $\gamma = 1$ will be 10^{-2} cm/sec.

132. Minin, Ye. A., and E. G. Goncharov. Reflection of optical pulses from a semi-infinite turbid medium. FAiO, no. 11, 1970, 1213-1216.

The theoretical problem of optical backscatter noise is considered for the case of laser propagation in a turbid medium such as water. The authors point out the general lack of data in the problem of backscatter, particularly for the case of nonstationary, narrow-pulse sources. Since analytical solutions of this problem are difficult, even with many simplifying assumptions, the authors use the Monte-Carlo method for noise calculations. Graphical solutions are given, including the effect of pulse smear as a function of propagation parameters.

133. Vel'min, V. A., Yu. A. Medvedev, B. S. Punkevich, and B. M. Stepanov. Probing the region of an exploded mass with a magnetic field. DAN, v. 197, no. 1, 1971, 70-72.

The interaction of external electrical or magnetic fields with an explosion region is of interest in studying field phenomena of explosions.

A technique for magnetic probing of a chemical explosion is accordingly described in which the explosive was placed in a coil excited at 5 MHz, and resultant variation in local conductivity was deduced from the magnetic unbalance following detonation. Type TG TNT was used in 16 g specimens; the sensing coil formed one leg of a bridge. In a cited test, no unbalance was noted up to 16 μ sec following detonation; then with shock wave radius ≈ 16 cm, a smooth variation in bridge balance commences, indicating field disturbance. Averaged data are presented for conductivity variation up to 40 μ s following detonation.

134. Krasnobayev, K. V. Ionization of gas by instantaneously flashing radiation. MZhiG, no. 2, 1970, 14-19.

An analysis is made of ionization of a gas occupying an upper half-space by a radiation emanating from a lower half-space. The gas is assumed to be in a state of gravitational equilibrium at a temperature T_o, and radiation is of Planck intensity at a temperature T_+. The ionization is described by a set of equations in dimensionless form using the radiation model introduced by Clarke and Ferrari (Phys. Fluids, v. 8, no. 12, 1965). The equations were derived for T and $T_+ < 10^4$°K and a gas of a sufficiently low density, e.g. hydrogen, and with a negligible hydrodynamic motion. The equations were solved, using a computer, for ionization degree and T of the gas, and spectral and angular distribution of radiation intensity. Graphs are included showing that the time required for establishing the ionization-recombination balance is density dependent, and is shorter in the higher-density gas layers. At $T_o < T_+$ the radiation intensity near the ionization frequency can be several times higher than Planck intensity. The above cited data could be useful in astrophysics for analysis of nonstationary ionization processes in external mantles of planets or stars.

135. Vel'min, V. A., Yu. A. Medvedev, and B. M. Stepanov. Studies of radiowave propagation through an explosion region. DAN, v. 194, no. 1, 1970, 53-54.

The use of r-f probes to monitor conditions within an explosive region is proposed as a useful diagnostic tool. From the resultant variation in signal diffraction caused by explosion products, some dynamics of the explosion process can be deduced. In the cited experiment the authors passed a 16° wide beam (λ = 8 mm) through the explosion volume generated by type TG TNT charges,

and monitored the detected signal emerging from the explosion. A typical response for a 25 g charge is seen in Figure 1, showing an initial sharp drop

Fig. 1. R-f diffraction in an explosive region. One square = 125μs; $\lambda = 8$ mm.

in transmissibility, followed by a gradually oscillatory rise. Repeated tests show that the number of oscillatory maxima increases with charge size; furthermore, the number of maxima equals the number of Fresnel zones generated by explosive particle diffraction.

136. Popov, Ye. G., A. A. Provalov, and M. A. Tsikulin. Self-shielding of a solid surface from powerful radiation. DAN, v. 194, no. 4, 1970, 805-807.

The authors describe use of solid explosives to generate optical flux which is directed onto a planar target. The basic test objective was to examine the self-shielding generated by ensuing evaporation of the target surface layer. A shaped TNT charge in a mirror-walled shock tube was used, as shown in Fig. 1,

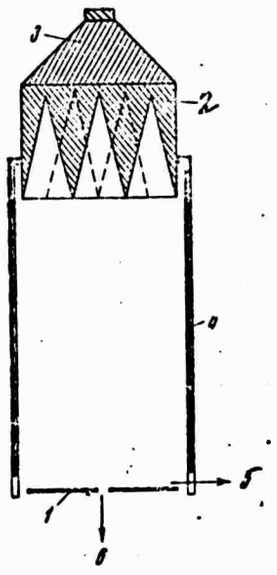

Fig. 1 - Self-shielding experiment.
1 - target with 1-mm center hole;
2 - TG 40/60 explosive (500 g);
3 - shaping lens;
4 - Al tube, d = 84 mm;
5 - photochronograph film

to produce the optical flux. Spectral data show that shock wave temperature on reaching the target was 30,000 °K, corresponding to an impact flux density on the order of 3×10^6 w/cm^2. Actual surface temperatures were considerably lower, down to a few thousand °K, indicating the extent of shielding. Target materials included sulfur, lead, iron, aluminum, graphite, K Cl, HgCl, and asbestos textolite. The tests were conducted both in argon and xenon atmospheres, with the latter yielding the more pronounced absorption effects.

137. Medvedev, Yu. A., B. M. Stepanov, and G. V. Fedorovich. Rapidly-varying excitation of the geomagnetic field by a non-stationary γ-radiation source. Geomagnetizm i aeronomiya, no. 1, 1971, 119-125.

Approximate and rigorous solutions are given for excitation of the geomagnetic field by a gamma radiation source in air. The interaction of γ quanta with the surrounding medium is assumed to generate Compton electrons which have a mean radial motion. Their trajectories are deflected by the geomagnetic field, giving rise to a lateral Compton current, with resultant distortion of the field. Braking of the Compton electrons produces secondary electrons which increase air conductivity and further distorts the magnetic field. The general problem is analyzed, assuming a uniform field and dielectric medium excited by an isotropic point source of gamma radiation. The treatment is based on a stationary and time-invariant γ source, but in principle could be extended to include both time and position variation of the latter.

138. Gudzenko, G. I., and L. A. Shelepin. Feasibility of developing a plasma x-ray laser. IN: Voprosy fiziki nizkotemperaturnoy plazmy. Minsk, Izd-vo nauka i tekhnika, 1970, 478-480.

This paper briefly reviews the known obstacles to creation of an x-ray laser, and suggests a promising approach to achieving this goal. The problem is centered in the fact that the amplification attainable from the inverted state falls sharply with decrease in wavelength, requiring better techniques for short-duration, high-intensity excitation. Recent success in generating ultrashort laser pulses with high power densities, however, may offer a solution to the pumping problem. Thus for a pulse on the order of 10^{-11} sec with $\varepsilon = 10$ j, focused on a cylindrical volume of 5 cm x 10^{-2} cm^2 and having a density of 10^{19} atoms/cm^3, each atom could receive 100 to 1000 ev. This would be

adequate for the extreme ionization required for lasing in the soft x-ray range. The authors admittedly ignore here the problems of resonator and mirror design associated with any practical realization of an x-ray laser.

139. Okun', I. Z. Study of compression waves generated by a pulsed discharge in water. ZhTF, no. 2, 1971, 292-301.

The extremely high shock pressures and temperatures attainable by pulsed electrical discharge under water make this an attractive technique in a variety of studies, including modeling of nuclear explosions. However, difficulties in detailed theoretical analysis of this problem are such that experimental data is generally needed for a given application. The author accordingly has reported a series of underwater electrical explosions using the two configurations of Figure 1 to generate approximately cylindrical and spherical

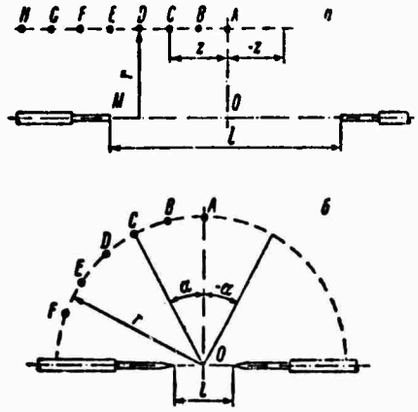

Fig. 1 - Pickup placement for electrical explosion test.
a - l = 32 cm;
b - l = 4, 8 and 12 cm.

compression waves. Most of the description concerns the parameters and placement of the pressure sensors, which were miniature tourmaline piezoelements located as shown in the figure. Tabulated data are included showing discharge electrical parameters as functions of shock wave parameters for both the spherical and cylindrical cases; experimental and theoretical results are also compared.

140. Abramyan, Ye. A., S. B. Vasserman, V. M. Dolgushin, I. A. Morkin, O. P. Pecherskiy, and V. A. Tsukerman. Generator of short flashes of high-intensity hard x-rays. DAN SSSR, v. 192, no. 1, 1970, 76-77.

An x-ray generator has been developed, in which a Tesla transformer was used as the high-voltage source. The generator is enclosed in a steel tank filled with a 50% mixture of nitrogen and sulfur hexafluoride at 14 kg/sq. cm. A capacitor charged to 28 kv delivers electric pulses to the cathode of the x-ray tube through the transformer and a conductor when the conductor potential reaches a maximum of 7 Mv. An x-ray dose of 10 r was recorded at 100 cm from the anode during a single flash of 50 nsec, which was sufficient for taking an x-ray picture of a 160 mm thick lead specimen. The dose rate was 2×10^{11} r/sec near the exit window of the tube. The maximum lead thickness which can be x-rayed with 8 kj of stored energy is comparable to that accessible to x-rays produced by an earlier machine with 200 kj of stored energy. The described generator may be used for taking x-ray pictures of rapid processes, for studying radiation stability of the materials, etc.

141. Kosarev, Ye. L., V. G. Zatsepin, and A. V. Mitrofanov. Fundamental characteristics of radio emission in the decimeter range from streak lightning. ZhTF, no. 2, 1971, 315-322.

R-f emission from streak lightning in the 100—1300 MHz range have been studied experimentally to verify the hypothesis of P. L. Kapitsa on the electromagnetic nature of ball lightning. Oscillograms of r-f from streak lightning were recorded by a series of UHF pickups, each tuned to a specified frequency; sensitivity of the pickups was 10^{-17} w in the 1 MHz band at a signal to noise ratio of approximately 1. About 200 simultaneous recordings were made at frequencies of 100, 400, 700 and 900 MHz. The longest signal of 10 msec duration was recorded at 700 MHz. The signals from 200 μsec to 5 msec duration were detected at 1.6 km and ∿ 100 m from the lightning source, respectively.

A log normal amplitude dependence of the observed UHF signals was obtained for 400, 700 and 900 MHz signals. The statistical spectral distribution of radiation intensity of streak lightning, with 60 and 90% confidence, confirmed an earlier conclusion of Kosarev et al (ZhTF, no. 11, 1968, 1831) that the mechanism of emission in the decimeter range is different from the usual

dipole radiation. Magnetic bremsstrahlung of the electrons in the lightning-induced magnetic field is one of the possible mechanisms of UHF generation. Experimental time-dependence of the UHF pulses was in good agreement with a Cauchy distribution.

142. Geras'kin, A. S., V. N. Korchagin, and S. A. Lovlya. Experimental study of an explosion in a waveguide. DAN SSSR, v. 195, no. 2, 1970, 325-328.

Pressure P, specific impulse I and specific energy E were measured in waves generated both inside and outside an encased oil well or a water pool by small explosive charges. The design of the casing was varied to determine its effect upon the wave parameters. Statistics of the experimental data show that the parameters of a shock wave propagating outside the casing, acting as a waveguide, are maximal near the explosion origin, and decrease along the waveguide and in the radial direction. The detonation wave propagating inside the waveguide exhibited a mildly sloping rise and decrease in pressure as a function of time. The P, I, and E in a detonation wave generated by an electric detonator increased by a factor of 1.8, 1.25, and 2, respectively, in a waveguide whose wall thickness was increased from 4 to 8 mm. The same parameters inside a waveguide of 114 mm diameter and 8 mm wall thickness were 7.5, 28, and 270, respectively, times greater than in free water at the same distance from the charge. An increase in the waveguide diameter resulted in a decrease in parameters of the wave propagating through the liquid inside the waveguide. Perforations in the waveguide had a similar effect. A symmetrical wave with P rising gradually to a maximum then decreasing in the same manner was recorded inside the waveguide in the explosion of heavier charge (13 g PETN/m instead of 1.5 g TNT).

143. Korotkov, V. A., and G. A. Nesvetaylov. The shape of a compression pulse in an electric wire explosion in water. FGiV, v. 6, no. 2, 1970, 250-252.

Exploding wire tests in water are described, in which the effects of wire diameter and metal on characteristics of the pressure wave in water were studied; these are compared to the technical difficulties experienced in controlling amplitude, duration, and reproducibility of a pulse generated by a spark discharge. The experimental parameters of the discharge contour were kept constant, and pressure was measured at 0.6 m from the exploding wire. Oscillograms of pressure and discharge current in the explosions of 25 mm long copper wires and in those initiated by a spark discharge with a 25 mm gap show that the shape of the compression pulse in water greatly depends on wire diameter. An approximately rectangular pulse was obtained with wire of 0.08 mm diameter; use of diameters above 16 mm resulted in pulse degeneration and conversion to a shock wave. The maximum shock wave amplitude

was observed at d = 0.40 mm, which is considered as optimum for the selected length. The compression waveform at d = 0.55 mm did not have the shape of a shock wave and its amplitude was decreased. It was concluded that the shape of a compression pulse in the acoustic range in water can be varied within wide limits by varying the diameter of the explosive wire. Characteristics of the shock wave in acoustic range were not substantially altered by using Al, Ni, or nichrome wires instead of Cu wire.

144. Ioffe, A. I., N. A. Mel'nikov, K. A. Naugol'nykh, and V. A. Upadyshev. Shock wave from optical breakdown in water. PMTF, no. 3, 1970, 125-127.

Shock waves were induced by focusing in water light pulses from a Q-switched ruby laser. Pulse energy was varied from 0.06 to 2 j and pulse duration was about 20 nsec. Apparatus is described for photographic recording of pressure impulses and simultaneous measurement of the pulse energy E' before entering the liquid cell and E'' after passing through the cell. Breakdown in water was observed at E' > 0.06 j with single-spike laser pulses. The spark resulting from breakdown at E' < 0.2 j was split into separate spots of 100 μ magnitude. The shape of the spark at higher pulse energies indicated that breakdown occurs in front of as well as in the focal region. A difference was noted in the shape of the spark generated by a two-spike laser pulse. Duration of pressure impulses was of the order of several hundred nsec and increased with increase in the focused energy. The average propagation velocity of the impulses at a distance of several cm was close to sonic. The recorded pressure impulse of 100 atm at a distance of 17 mm and E' = 0.6 j was found to be of the same order of magnitude as that calculated (150 atm), by using an approximate formula which describes a high-strength point explosion. An even better agreement was noted between the theoretical (550 atm) and experimental (500 atm) values of pressure impulses at a 0.3 cm distance from breakdown point and ∿0.1 j optical pulse energy.

145. Buzukov, A. A., and V. S. Teslenko. Pressure at the shock wavefront in the area near a laser spark breakdown in water. PMTF, no. 3, 1970, 123-124.

An experiment is described in which a ruby laser beam with 0.5 j power output and 50 nsec duration was focused in a drop of water suspended at the end of a dropper. Explosion of the drop was recorded by a SFR-IM high-speed photorecording camera. Velocity U of water dispersion was measured in a

direction perpendicular to the beam axis, from recordings of the dispersion process. Laser-induced pressure P in the shock wavefront was determined at distances R = 0.4 to 3 mm from the focal point, in directions normal to the beam axis. P at various distances from the center of breakdown was calculated from the formula

$$U = \frac{2 P \cos \alpha}{\rho c}$$

where ρ is density of the liquid, c is sound velocity in the liquid, and α is the angle of incidence of the shock wave. The plots of P versus R were in agreement with the author's earlier P measurement data (PMTF, no. 5, 1969). A photo sequence of an exploding drop is included.

146. Kozachenko, L. S., and B. D. Khristoforov. Shock waves in a shallow water basin. PMTF, no. 4, 1970, 165-171.

The pressure profile p (t), duration τ, and specific impulse I of an explosive shock wave were measured in a water basin with an air-saturated sand bottom, 87 m long, 20 m wide, and 3 m deep. The shock waves were generated by the underwater detonation of a spherical TNT charge placed at relative depths H = 1 to 11 charge radii R_0. The measurements were made by pressure pickups located at a relative distance R = 30, 60, 90, and 120 from the blast center at a depth h and for relative depths H_* of the basin = 1, 2, 4, and 12. The experimental p (t) profiles were substantially affected by variations of H, R, and H_*. In a basin with $H_* = 12$. the frontal pressure induced by a blast near the water surface or the bottom is greatly affected by the distance between the charge and the water boundaries, and the boundary effect increases with the increase in R. In a basin of $H_* = 2$ or 4, the maximum pressure p from the blast and the maximum τ and I of the shock wave, are independent of H, as recorded at the mid-depth of the basin. At $H_* = 12$, the maximum τ and I were observed at $H_* = 6$; they decreased with decrease in distance from either the pickup or the charge to the boundary surfaces. Calculations showed that the interaction of a shock wave with the bottom is determined by the characteristics of the bottom: the parameters of a shock wave were formulated for a three-phase ground as functions of the density of its components and sound velocity in the ground. Calculated shock wave parameters were found to be in satisfactory agreement with the experimental data.

147. Buzukov, A. A., and V. S. Teslenko. Initial rise velocity of a water cupola in underwater blast of spherical charges and blasting cords. FGiV, v. 6, no. 2, 1970, 253-255.

The initial rise velocities u_1 and u_2 were measured in underwater blasts of respectively a 50:50 spherical charge of TNT and Hexogen, and lengths of a commercial blasting cord of 12 g/m (DSh-A) and 13 g/m (DSh-B) of PETN. The TNT-Hexogen charges were suspended at relative depths $H_1 = 0.3$ to 1.9, while the blasting cords were stretched horizontally on brackets at a relative depth $H_2 = 0.05$ to 0.008. Experimental detonations of TNT-Hexogen charges weighing 7 to 40 g and of the blasting cord were carried out in a 6 m^3 laboratory basin; tests with TNT-Hexogen charges weighing from 40 to 205 g, were done in an open air basin at depths greater than 3 m. The rise of the water cupola was recorded by the ZL-1 and SKS-1M high-speed (to 3000 frames/sec) movie cameras with a 100 μsec exposure. The rise height of the cupola as a function of time was measured with a maximum 7% error. Empirical relations for displaced water velocity are given as functions of charge parameters; in some cases, calculated velocity values were up to 1.6 times higher than the experimental data. Presumably, this discrepancy is connected with the complex pattern of pressure decrease behind the shock wavefront.